



universität
wien

MASTERARBEIT

Titel der Masterarbeit

„Autonomous Parvovirus Interaction with the Innate
Immune System“

Verfasser

Bernhard Englinger Bakk.rer.nat.

angestrebter akademischer Grad

Master of Science (MSc)

Wien, 2013

Studienkennzahl lt. Studienblatt: A 066 834

Studienrichtung lt. Studienblatt: Masterstudium Molekulare Biologie

Betreuerin / Betreuer: ao. Univ.-Prof. Mag. Dr. Johann Rotheneder

I would like to thank

Dr. Jürg Nüesch, for his kind willingness to accept me in his group and for his devotional supervision and help during my labwork and writing process and who could bring me a bit closer to understanding the concept of science,

Dr. Johann Rotheneder, for his uncomplicated supervision and evaluation of my thesis at my home university,

Dr. Séverine Bär and Claudia Plotzky for their helpful instructions and patient support in the lab,

Dr. Jean Rommelaere and the entire department of tumor virology of DKFZ for this great working experience, which was as easy-going as it was productive,

my parents, each delicious culinary care package of whom brought a touch of home to me,

Philip Grossen, my great companion, whom i hope to get another chance to beat at our merciless bike races up the königstuhl,

Ruth, Matsi and Hanni, whose sunday evening dinners were equally professional as was their advice in scientific questions,

Rafi, for exciting and inspiring evening discussions- at the bar and in the wall,

you, Anna, for all those countless fruitful discussions, motivating evening lab sessions, reinforcing advice, alleviating support and for your ear, that was always open when the toddler felt like grumbling,

you all, for elevating this period to the phase of a lifetime in bewitching Heidelberg, which I will never forget.

Table of Contents

1. Introduction	1
1.1 Principles of oncolytic virotherapy	3
1.2 Parvoviruses in oncolytic virotherapy	5
1.3 The genome and its transcripts	9
1.4 Parvoviral proteins and their functions in permissibility	14
1.5 Parvovirus life cycle	18
1.6 Innate immune recognition of viruses	20
2. Aim	29
3. Materials	30
3.1 Bacteria	30
3.2 Media and additives for bacterial cultures	30
3.3 Cell lines	30
3.4 Media and additives for cell culture	31
3.5 Wild Type Viruses	31
3.6 Single- and combined mutant viruses	31
3.7 Enzymes	32
3.8 Restriction Enzymes	32
3.9 Primers	33
3.10 DNA probes	35
3.11 Loading dyes, DNA- and protein markers	35
3.12 Antibodies	35
3.13 Chemicals	36
3.14 Buffers and reagents	37
3.15 Kits	38
3.16 Laboratory consumables	38
3.17 Equipment	39
4. Methods	41
4.1 Cell biological methods	41
4.1.1 Cultivation of cells	41
4.1.2 Isolation of mouse embryonic fibroblasts (MEFs)	41
4.2 Molecular biological and microbiological methods	41
4.2.1 Recovery of viral genomic DNA by Polymerase Chain Reaction (PCR)	42
4.2.2 Molecular cloning	42
4.2.3 Generation of mutant virus variants by site-directed mutagenesis	45
4.3 Production of infectious particles	47
4.4 Amplification of viral stocks	48
4.5 Purification of viral stocks by CsCl- gradient ultracentrifugation	48
4.6 Determination of viral titers	49
4.7 Determination of protein expression levels by sodium-dodecylsulfate Polyacrylamide gelelectrophoresis (SDS-PAGE) and Western Blot analysis	51
4.8 Nuclear- cytoplasmic fractionation of western blot samples	52
4.9 Biochemical fractionation	53
4.10 Semi-quantitative determination of gene expression on transcriptional level by RNA isolation and reverse-transcription PCR	53
4.11 Determination of viral DNA replication by southern blot analysis	54
4.12 Immunofluorescence	55
4.13 Cell cycle arrest by double synchronisation	56
5. Results	57

5.1 Generation of MVM virus stocks propagating in freshly prepared mouse embryonic fibroblast cells (MEF).....	57
5.2 Viral DNA amplification in A9 fibroblast cell line and freshly isolated MEFs	60
5.3 Viral protein synthesis	61
5.4 Antiviral activities induced by MVM infections of MEFs	66
5.5 Potential MVM sensor and counteracting targets of MEF-induced anti-viral activities	71
5.5.1 Host cell sensor.....	71
5.5.2 Interference of MVM with the mRNA- processing machinery	73
5.6 Genetic characterization of MVM _{CR}	79
5.7 MVMp recombinants	84
6. Discussion.....	88
6.1 Genetic characterization of MVM _{CR}	89
6.2 Infectivity of MVMp and MVM _{CR} in MEFs	94
6.3 Susceptibility of MEFs towards MVM _{CR}	96
7. Summary.....	103
8. Zusammenfassung	106
9. References.....	109

Table of Figures

Figure 1. Genome map of MVMp.....	11
Figure 2. The NS1- protein.....	15
Figure 3. Life cycle of MVM.....	20
Figure 4. Intracellular antiviral recognition network.....	22
Figure 5. Type- I IFN response.....	26
Figure 6. Viral mechanisms to counteract cellular antiviral responses.....	28
Figure 7. Titration of ssDNA in viral stocks.....	58
Figure 8. Titration of infectious particles in viral stocks.....	59
Figure 9. Replication efficiency of MVM _{CR} and MVMp.....	60
Figure 10. Analysis of NS1 expression by immunofluorescence microscopy...	62
Figure 11. Analysis of viral non- structural proteins in synchronized MEFs by immunofluorescence microscopy.....	64
Figure 12. Kinetics of MVM _{CR} and MVMp viral protein expression in MEFs and A9 cells.....	65
Figure 13. Growth kinetics of infected and mock- treated MEFs.....	67
Figure 14. Dynamics of antiviral innate immune activity in MEFs and A9 cells.....	68
Figure 15. NFkB- activation in MEFs.....	70
Figure 16. Induction and subcellular distribution of SGTA.....	72
Figure 17. Analysis of upregulation and localization of RNA- processing factors in infected MEFs and A9 cells by confocal immunofluorescence microscopy..	74
Figure 18. Induction and subcellular distribution of CPSF6.....	78
Figure 19. Genetic characterization of MVM _{CR}	79
Figure 20. Localization of base alterations in MVMp in comparison to MVM _{CR}	80
Figure 21. Alterations in the non- structural gene region.....	82
Figure 22. Exact genetic loci of identified base alterations and their resulting amino acid changes.....	83
Figure 23. Site- directed mutagenesis of MVMp.....	85
Figure 24. Replication efficiency of MVMp mutants.....	86
Figure 25. <i>In vivo</i> phosphorylation of NS2 in MVMp- and in MVM _{CR} - infected MEFs.....	94

1. Introduction

The principle of oncolytic virotherapy of cancer is characterized by the ability of certain viruses to selectively replicate in- and to kill neoplastic tissue while leaving untransformed cells unharmed, as well as to trigger a host anti-tumor immune response. This is based on the fact that malignantly transformed cells show diverse perturbations of regulatory mechanisms such as deregulated cell cycle progression or insensitivity against anti- proliferative stimuli and by this often provide favourable conditions for viral replication.

Healthy tissue is endowed with a number of cellular factors dedicated to sense viral pathogenic structures exposed in various cellular compartments upon infection. Sensing this triggers a first-line innate immune response, signaling infected- and surrounding non- infected cells in an autocrine and in paracrine manner, respectively, to enter a latent anti-viral state by shutting off macromolecular synthesis and activating the means to destroy viral intruders. This is characterized by the inhibition of gene expression and by the degradation of viral (and also cellular) gene transcripts and proteins. In case the invader cannot be eradicated, infected cells trigger death-inducing pathways and enter apoptosis in order to keep spreading of progeny virions into the surrounding tissue at bay (Pichlmair and Reis e Sousa, 2007; Fuertes et al., 2012). By genetic instability, transformed cells often acquire mutations that impair innate immunity. For tumors, this can provide important advantages as they might escape or be insensitive towards host anti- tumor immune stimuli. Importantly, the lost ability of cancer cells to efficiently mount an innate anti-viral immune response is another important factor adding to the observation that some viruses preferentially infect and kill tumor cells, commonly referred to as them being so-called oncotropic viruses. (Naik and Russell, 2009).

Amongst all groups of potential oncolytic viruses, autonomous parvoviruses are considered excellent candidates for virotherapy of cancer, owing to their natural oncotropism and comparably low pathogenicity in humans (Cornelis et al.

2006). Accompanied by numerous *in vitro* observations, this was shown by *in vivo* studies, in which rats were made subject to syngenic glioma engraftment (Geletneky et al., unpublished). Administration of rat parvovirus H1 (H1-PV) resulted in a complete regression of the tumors. Furthermore, treatment of tumors, established by xenotransplantation of human cervical carcinoma cells into immunocompromised mice also led to major regression of those neoplastic lesions (Dupressoir et al., 1989). These and many other studies provided proof of principle for the parvoviral oncosuppressive potential and paved the way for the currently ongoing phase I/IIa clinical trial comprising patients suffering from glioblastoma multiforme (Geletneky et al., 2012).

Despite promising results in various cancer entities, parvoviral therapy seems to be in need of further improvement. While an impaired ability of transformed cells to counteract viral infection is one important prerequisite for successful oncolytic virotherapy, inherent- or spontaneously acquired mechanisms of viral agents to counteract an innate immune response not only in neoplastic- but also in healthy tissues depict an important safety concern in the potential application of respective viruses as therapeutic agents and constitute a potential threat to the treated organism. As to date these parvoviral mechanisms, suppressing an innate immune response are poorly understood on a molecular level, it is of great importance to understand this interplay in order to improve parvoviral cancer treatment.

The prototype strain of Minute Virus of Mice (MVMp), a close relative of H1-PV, was also shown to have oncoprotective effects in various experimental models (Rommelaere and Cornelis, 1991). The mouse fibroblast cell line A9 is the natural host of MVMp and it is fully permissive to infection, whereas Mouse Embryonic Fibroblasts (MEFs), its primary, untransformed counterparts were shown to be non-permissive for this virus. Importantly, the parental strain of MVMp, referred to as the Crawford strain (MVM_{CR}), was originally isolated from primary MEFs, in which it was reported to have the ability to replicate. As MEFs were shown in principle to be fully capable of mounting an innate immune response, it can be hypothesized that MVM_{CR} disposes of means to antagonize

or circumvent this response, rendering those cells permissive to productive infection (Grekova et al., 2010).

As for MVM_{CR} there exists no information on the viral DNA sequence, the aim of this study was to recover this original specimen to make it subject to genetic characterization. This information should then be used to compare the newly obtained genomic sequence with that of MVMp in order to identify alterations in the genetic code of MVMp, possibly having occurred during its adaptation process to A9 fibroblasts. This should provide a basis to pinpoint potential mechanisms of MVM_{CR}'s ability to propagate in MEFs, concentrating on the putative counteraction of a first-line innate immune reaction, which is possibly ascribed to an NFkB- mediated type-I interferon response, the induction of which will be a major focus of this study. Understanding the interplay between oncolytic viruses and the host innate immune system will help optimize the targeting of candidate therapeutic viral agents to neoplastic tissue in order to make viruses safer in respect to a potential application in human patients.

1.1 Principles of oncolytic virotherapy

Within the last decades, enormous advances have been made in the field of oncologic therapy. As knowledge of the biology of cancer has grown very rapidly and complex pathologic mechanisms of this highly heterogeneous disease have been dissected on a genetic and cell biological level, new treatment strategies have evolved to complement standard surgical- and chemotherapeutic intervention as well as radiation therapy. One such approach- targeted cancer therapy- aims to target and inhibit specific cellular oncogenes, which are responsible for malignant transformation and often found to be exclusively- or in great excess- present in cancer cells. This is achieved by administering antibodies or small synthetic molecules, which should find their way through the organism to primary tumor sites or metastases without harming healthy tissues (Zhukov and Tjulandin, 2007). Another strategy attempts to boost anti-tumor immunity by various agonists, supporting the patient's intrinsic

immune system to counteract neoplastic lesions (Finkelstein and Fishman, 2012). These and other strategies have resulted in benefits for patients suffering from various cancer types, not only in terms of overall survival, but also concerning the tolerance of these novel treatment modalities, as they are often accompanied by milder adverse effects due to more specific modes of action, compared to first generation cancer therapy (Valdivieso et al., 2012).

However, for many cancer entities there is still a severe lack of reasonable treatment options and novel therapies often fail due to frequent development of resistance towards the administered drugs. The often observed heterogeneity of tumors even of the same type accounts for the fact that not all patients suffering from a certain cancer type will ultimately respond to respective drugs. So, for many malignant tumors, prognosis all too often remains poor and overall survival could not be elevated substantially. Therefore, the development of other strategies will be necessary to fight this challenging disease.

Oncolytic virotherapy is an emerging treatment modality, which has the aim to use viruses as tools for selective infection and killing of tumor cells without having pathologic effects on healthy tissue (Russell and Peng, 2007). This „lysis“ of tumors should on one hand be attributed to direct viral cytotoxicity, and on the other hand should this destruction of malignant tissue have an immunotherapeutic effect by releasing tumor- associated antigens, thereby stimulating an anti-tumor immune response (Naik et al., 2012).

Some viruses, such as autonomous parvoviruses or reoviruses preferentially replicate in transformed cells. This seems to be rather attributed to tumor biological reasons, since, by resisting translational suppression or pro-apoptotic stimuli, tumors often have lost the ability to limit a virus infection. Other virus species, such as measles, adenovirus, vaccinia and herpes simplex virus can be engineered to specifically target cancer cells. This is achieved in various ways. For example, manipulating surface proteins to bind to receptors that are unique to cancer cells depicts one way to redirect virions to malignant tissue (Cattaneo et al., 2008). This approach can be combined with arming oncolytic viruses with transgenes encoding cytotoxic proteins under the control of tumor-

specific promoters to enhance target cell killing (Russell et al., 2012; Nettelbeck, 2008; Kaufmann and Nettelbeck, 2012).

This therapeutic approach is expected to bring along benefits compared to conventional- but also to other novel therapies mentioned above. As low- to inexistent pathogenicity towards healthy tissue has been shown in various preclinical studies and in clinical trials, oncolytic virotherapy promises to have the potential to reduce adverse effects as compared to numerous other drugs (Russell et al., 2012). Furthermore, the multimodal manner by which viruses take over the deregulated molecular cell machinery of transformed cells, which ultimately causes their death, depicts an advantage over the limited action potential of most therapeutic molecules, which majorily hit only a single or few cellular targets (Nüesch et al., 2012; Cornelis et al., 2006). This makes the development of resistance against the treatment more improbable.

Nevertheless, despite promising preclinical results, oncolytic virotherapy faces various problems when it comes to clinical efficacy. Diverse issues, such as optimization of delivery to neoplastic lesions, enhancement of productive growth and intratumoral spread, triggering of an anti-tumor response as well as avoidance of rapid and deleterious viral depletion by neutralizing antibodies will have to be further addressed in order to develop applicable and possibly curative virotherapeutics. (Russell et al., 2012; Fuertes et al., 2012)

1.2 Parvoviruses in oncolytic virotherapy

The family of *Parvoviridae* (lat. *parvus*= small) comprises a number of isometric, non- enveloped DNA viruses containing linear, single- stranded genomes with an approximate length of 4-6kb. The family is classified into several subfamilies, which themselves are again subdivided into various genera, amongst others into dependoviruses and autonomous parvoviruses, which show a broad host range in vertebrates. The former group, of which adeno-associated viruses (AAVs) are prominent members, is dependent upon adenovirus co-infection in order to replicate (Tattersall, 2006). Due to their intrinsic replication deficiency

and their good tolerability towards genetic manipulation, these viruses are ubiquitously assayed for their potential to be used in the field of gene therapy (Carter, 2006). In contrast, members of the genus autonomous parvovirus are not in need of the presence of such a helper, but- when encountering a permissive target cell- are capable of effective infection and propagation therein (Tattersall, 2006).

Due to their minute size of 18-28nm, autonomous parvoviruses are among the structurally simplest viruses known. Each virion contains a protein shell, consisting of two to four structural protein (VP) species, present in variable ratios. Each spherical capsid is built up by 60 copies of these structural proteins and accomodates a single copy of its respective genome (Chapman and Agbandje-McKenna, 2006). This guarantees a maximum of possible genetic information in a most confined space. Their genome length of about 5.1kb does not allow for a great multitude of encoded genetic information, so both posttranscriptional- and posttranslational modification strategies are employed to increase diversity of viral gene products (Cotmore and Tattersall, 2006). Upon infection of permissive cells, expression of a small set of multifunctional structural- and non-structural proteins is sufficient to drive the viral life cycle and to result in progeny virion production. Yet, despite the fact that the non-structural proteins are able to modulate the cellular replication- and protein expression machinery in a complex and multimodal manner, parvoviruses are strictly dependent on a proliferative state of their host cells (Bashir et al., 2000; Nüesch et al., 2012, Lachmann et al., 2008). This is illustrated by several facts: Neither do infectious virions dispose of proteins autonomously promoting replication, nor does their genome encode such factors, so parvoviruses are fully dependent on the host cell replication- and protein synthesis machinery. Furthermore, their early promoters were shown to be targets of mitogenic signaling stimuli such as E2F, c-Myc and MAPK- mediated activation of ATF/CREB transcription factors (Nüesch, 2006; Cornelis et al., 2006).

Since their detection in the late 1950', parvoviruses were frequently isolated from tumor cells as contaminants in tumor virus research which created the

initial notion of them being etiological agents of cancer development (Siegl, 1984; Toolan, 1990). Contradicting these expectations, a positive correlation between parvovirus infection and tumorigenesis could never be shown. On the contrary, following studies revealed that these agents were in some cases able to interfere with tumor development, a process commonly referred to as oncosuppression (Rommelaere and Cornelis, 1991). This is at least partly due to their nowadays well-described and above- mentioned S-phase dependency, which favours their replication in highly proliferative tissues while leaving resting- or slowly dividing cells unharmed (Bashir et al., 2000; Tattersall, 1972). Members of the genus parvovirus, to which this observation applies are therefore sometimes termed ,viruses in search of a disease'. Therefore, besides revealing the basic molecular biology of these viruses, they were from that time on assayed for their potential to target and kill cancerous cells.

Within the research field of parvovirus- associated oncolytic virotherapy, the rodent parvovirus H1 (H1-PV) has attracted special attention, because it shows natural oncotropism. This is characterized by selective killing of various transformed cell types *in vitro* as well as by various preclinical studies, which showed inhibition of tumor progression or- in some cases- even complete tumor regression in both syngenic- and xenograft models *in vivo* (Geletneky et al., 2010; Raykov et al., 2004; Rommelaere and Cornelis, 1991; Faisst et al., 1998). However, the exact molecular mechanisms by which oncotropic parvoviruses preferentially exert their cytopathic effects in tumor cells while not being virulent towards normal proliferating cells are not fully understood and are yet to be unraveled.

Minute Virus of Mice (MVM), of which several strains are described is a close relative of the rat virus H1-PV. The fibrotropic prototype strain MVMp has been studied extensively. It is considered largely apathogenic in mice- its natural host organism- as well as in humans and it has also been shown to be endowed with oncolytic properties (Cornelis et al., 2006). However, the term ,prototype' might be somewhat intriguing, since MVMp is a derivative of an original species, isolated by Crawford in 1966 as a contaminant in studies of mouse

adenoviruses (Crawford, 1966). This original isolate was reported to be capable of productive infection of primary, untransformed mouse embryonic fibroblasts (MEFs). Initial attempts to study this virus within its natural host turned out to be elaborate and poorly reproducible owing to variable infectivity and rather slow replication rate of this cell type when cultivated *in vitro*. In order to create a system in which it was more feasible to characterize the properties of this virus on both genetic and functional levels, Tattersall, by serial passaging, adapted the original isolate to A9, a transformed mouse fibroblast cell line (Tattersall, 1972). This enabled adequate characterization of the adapted strain, which was from then on called the prototype strain of MVM, MVMp, and for many years, the original isolate took a back seat.

During this adaptation process to A9 cells, MVMp lost its ability to cause productive infection in MEFs- their natural counterparts. The causative mechanisms of this observation are not known, yet, Harris and coworkers observed a type-I interferon induction upon inoculation of mice (Harris et al., 1974). In *in vitro* studies, Grekova et al. showed that suppression of MVMp in MEFs is at least partially attributed to a type-I interferon- mediated innate immune response in those cells. This paper states that recognition of the virus by an unknown cellular sensor triggers NF κ B signaling, resulting in macromolecular synthesis shut-off, degradation of cellular (and viral) transcripts and production of IFN- β . By this, cells enter a latent anti-viral state, which is characterized by suppression of viral DNA replication and gene expression and thus results in an abortive infection. In A9 cells this anti-viral response could not be observed upon infection with MVMp (Grekova et al., 2010). This is not surprising, since it is commonly accepted that transformed cell types are often defective in fully functional innate immunity, rendering them susceptible to a greater variety of invaders, which- in an untransformed environment- would be suppressed (Pitha, 2000).

However, as mentioned above, the parental strain of MVMp, MVM_{CR} is capable of productively infecting not only A9, but also MEFs (Crawford, 1966; Tattersall, 1972). This might suggest that MEFs have an intrinsic deficiency in responding

to intruding viral agents. It is therefore feasible that MVM_{CR}, before having been adapted to A9, might have disposed of means to counteract or circumvent this first-line innate immune response. Possibly due to lower selective pressure during passaging in A9, MVM_{CR} probably acquired genetic modifications that made it lose its infectivity for MEFs.

As to date information on the genome sequence of this original isolate is not available, identifying those putative genetic alterations was a major subject of this study. Looking at the above mentioned observation in a chronologically inverse way, this is of interest in respect to cancer therapy, since obviously it is possible that slight changes in the genome of candidate oncolytic viruses may result in a shift of host tropism in which the virus might spontaneously acquire the ability to productively infect not only its target tumor, but also healthy cells. This depicts a potential safety risk to treated patients in parvovirotherapy. Therefore it will be important to define the potential interaction points of MVM_{CR} with the host innate immune system. Learning more about this interplay might also serve as a basis to identify new tumor markers, making it possible to better understand and to optimize parvovirus- mediated tumor cell killing. Furthermore, new findings in this area could potentially be extrapolated to H1-PV- based therapy, which is at the current stage being tested on a clinical level.

1.3 The genome and its transcripts

The genome of MVM is approximately 5.1kb long and consists of a linear, single- stranded DNA chromosome, which on either end is flanked by short terminal palindromes, folding back on themselves to create imperfect duplex telomeres (see figure 1). This partial base- pairing results in typical secondary hairpin structures, termed inverted terminal repeats (ITRs). In the case of MVM, during the packaging process of newly generated virions the viral genome is inserted vectorially into preformed capsids in a 3'- 5'- manner by the helicase activity of the major non- structural protein NS1. Due to its secondary structures, the 5'- end is often not translocated entirely into to capsid, leaving a

remaining tail of approximately 20 nucleotides with a covalently attached NS1 protein exposed on the surface, where it is prone to nucleolytic cleavage in the extracellular space or in the endosomal compartment during entry into a target cell. Yet, the absence of the 5'- end does not seem to impair infectivity. (Cotmore and Tattersall, 2006)

In MVM, the great majority of packaged viral genomes are of negative sense. This leads to the gene map of this virus being characterized in a 3'-5'-orientation. Therefore, by convention and as a matter of simplification, the 3'-end of the negative strand is termed left end and the 5'- terminus is defined as the right end, respectively. The right-end hairpin is assumed to have a cruciform structure, consisting of 248 nucleotides and it is approximately twice the size of the Y- shaped left-end ITR. Both ends are crucial for viability, as they contain specific protein- binding sites and consensus sequences, necessary for multiple mechanisms such as DNA replication and packaging. Furthermore, the terminal, complementary back- folding serves as a self- priming mechanism to enable the recruitment of cellular DNA-Polymerase complex to initiate DNA amplification. Deletions in these regions are often lethal for the virus. (Cotmore and Tattersall, 2006)

As the space for genetic information on parvoviral genomes is very confined, these viruses have evolved a complex pattern of alternative splicing, polyadenylation and utilization of multiple, overlapping reading frames to maximize this encoded information. Furthermore, ,ambisense' densoviruses, another group of parvoviruses further enrich their coding capacity by encoding additional genetic information in the opposite direction on the complementary strand. MVM, however, is a ,monosense' virus, encoding its entire gene products in one reading direction. (Cotmore and Tattersall, 2006; Qiu et al., 2006)

The total genome of MVM is ordered into 100 map units and sequences exhibiting specific functions are sorted into this scheme according to their approximate locations. The two promoters of MVM, for example, are located at map units 4 and 38, respectively, rendering them the names P4 and P38,

respectively. The parvoviral genome encodes two major genes. Under the control of the P4 promoter and initiating transcription approximately at nucleotide 200, the first major gene occupies

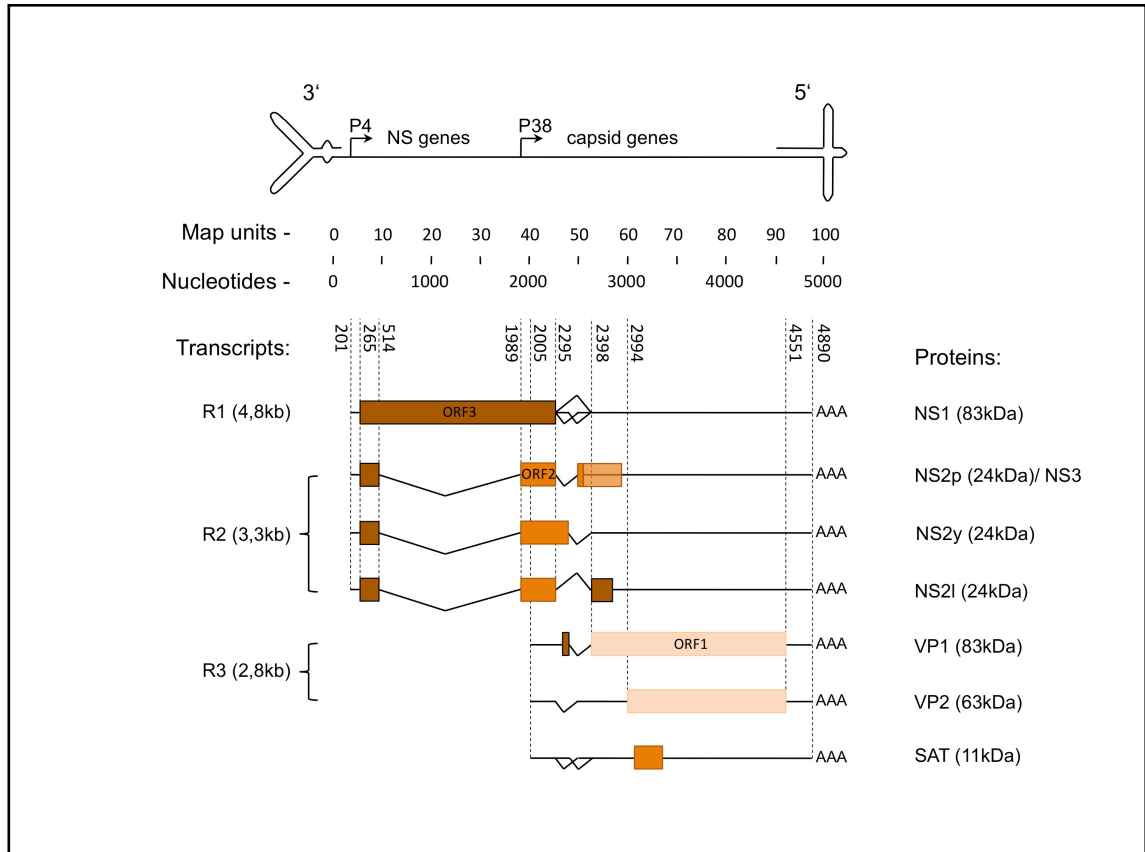


Figure 1. Genome map of MVMP. A negative- sensed, single- stranded chromosome is depicted. P4- and P38- promoters are indicated at their respective positions at map units 4 and 38, respectively. Primary transcripts of these promoters, encoding structural- and non- structural proteins, are marked as R1, R2 and R3, respectively. Differential open reading frames are indicated by alternate colouring of respective exons. Viral pre-mRNAs all share the same C-terminus. The MVMP genome encodes the major non- structural protein NS1, three isoforms of NS2, NS2p, -y and -I, respectively, as well as the structural proteins VP1, VP2 and SAT (not shown).

the left half of the coding sequence, encoding the non- structural proteins. The second gene at the right half of the genome is under the control of the P38 promoter and it encodes the structural proteins, of which the approximate transcription initiation site is around nucleotide 2005. All of the generated RNAs are polyadenylated at the far right end of the genome at position 4890, making

them span virtually the whole genome, starting from their respective transcription initiation sites. Transcription of these genes gives rise to two nascent pre-mRNAs, which are subject to alternative splicing to produce three major transcripts, termed R1, R2 which encode the non- structural proteins 1 and -2, respectively, and R3, which encodes the capsid proteins. RNA production is subject to temporal phasing. P4 promoter products R1 and R2 are produced prior to P38- controlled R3 transcripts. The reason for this lies in the fact that the P4 promoter as well as its upstream enhancing elements exhibit binding domains for cellular transcription factors such as E2F or cyclic AMP response element (CRE). For activation of the P38 promoter, binding of the NS1 gene product of the P4 promoter is necessary, which enhances its activity a 100- fold. (Qiu et al., 2006)

The first major transcript encodes the non- structural protein NS1, which exerts multiple regulatory functions during the infectious cycle. As mentioned above, this pre-mRNA spans almost the entire genome length, having its initial transcription site at nucleotide 201, whereas its polyadenylation signal is located at position 4890, respectively. The pre-mRNA exhibits a single open reading frame (ORF), starting downstream of the transcription initiation site at nucleotide 265 and terminating at nucleotide 2295, yielding the 83kDa protein product. Downstream, adjacent to this ORF, the transcript is spliced by excision of the so- called 'small intron', which is necessary for mRNA export and which is shared by all primary transcripts. (Qiu et al., 2006)

From the same pre-mRNA, the second major transcript R2 is formed. It encodes the NS2 protein. It is generated by engagement of the spliceosomal machinery to splice- sites within the NS1- specific ORF, which results in the excision of the so-called 'large intron', spanning between nucleotides 514 to 1989, respectively. This leads to a frame shift, defining the NS2- specific exon between position 1989 and the small splice. The excision of the large splice connects this exon with the other exon, lying upstream between 260 and 514, which is shared by NS1 and NS2. This leads to the fact that these two proteins exhibit the same N-terminus, but due to the loss of a major portion of NS1 and

the reading frame- shift in the NS2- specific exon, the C-terminus of NS2 is distinct from that of NS1, yielding a protein with the size of approximately 24kDa. Furthermore, the small intron of NS2 pre-mRNA can be alternatively spliced by two disparate splice donors and –acceptors, respectively. This adds additional short ORFs downstream of the 3'- splice acceptors, creating three NS2 isoforms, termed NS2-P, NS2-Y and NS2-L, respectively. An amber read-through of the NS2-P isoforms can lead to an elongated open reading frame, encoding the non- structural protein NS3. The relative ratio, at which NS1/NS2 mRNAs are generated depends largely on how efficiently the cellular splicing machinery detects the 3'- large splice acceptor. Slight variations within this region can result in major shifts of this ratio, resulting in enhanced generation of respective mRNAs that are favoured by this change of excision pattern. This can have a drastic effect on host cell tropism, as illustrated by the lymphotropic strain of MVM, MVMi. This virus preferentially replicates in lymphoid cell lines, whereas it is not able to propagate in fibroblasts. MVMp and MVMi exhibit disparate large- splice acceptors, characterized by a single base alteration at position 1970, changing an A residue in MVMp to a G residue in the lymphotropic strain. The A residue favours splice- site recognition of MVMp in fibroblasts, whereas the G residue of MVMi seems to restrict it. In lymphoid cells, the opposite is observed. This variation accounts for the fact that the two variants are processed with differential efficiencies in the two respective cell types, rendering the viruses infectious for one- but not for the respective other cell type. Thus, the relative amounts of parvoviral non- structural proteins are an important aspect in cell tropism and seem to vary between different cell types. (Qiu et al., 2006)

The third major transcript R3 is produced by the P38 promoter and it encodes the structural proteins VP1 and VP2, which constitute the viral capsid. The primary transcript spans from the transcription initiation site around nucleotide 2005 until the common polyadenylation site at residue 4890. Alternative excision of the small splice leads to two different coding regions of partially disparate reading frames. The shorter splice variant of VP2 is generated predominantly, resulting in a protein ratio between VP1 and VP2 of

approximately 1:5. VP1 mRNA encodes an 83kDa protein, whereas the truncated form of VP2 is relatively smaller, having a molecular weight of 63kDa. Alternative splicing near the 5'- terminus causes the two proteins to have distinct N- termini, whereas they share a common C- terminal domain. (Qiu et al., 2006) An additional open reading frame was identified a few bases downstream of the start codon of VP2, generating a transcript for the short protein SAT.

Taken together, the genome of MVMP is complex and it contains multiple regulatory elements for both replication- and transcription processes. The self-priming terminal hairpins are crucial for DNA amplification. Efficient viral propagation is dependent upon temporal phasing of gene expression and upon fine- tuned processing of primary transcripts, which defines not only the identities of resulting protein products but also their relative quantities to each other. (Cotmore and Tattersall, 2006)

1.4 Parvoviral proteins and their functions in permissibility

To enable efficient replication in permissive host cells, the limited coding capacity of autonomous parvoviruses is compensated for by a multifunctionality of some of their protein products.

The seemingly most important parvoviral protein is NS1 (see figure 2). This protein, which shows predominantly nuclear localization during infection, is endowed with mediating numerous virus- host interactions during the entire viral replication cycle (Nüesch et al., 1998). This is depicted by its multiple distinct functional domains, spanning over its whole amino acid sequence. To exert these functions, which comprise roles in viral DNA amplification and gene expression as well as in mediating direct cytotoxicity and viral spread, NS1 disposes of ATPase activity, a homo- oligomerization- and a DNA- binding site, helicase activity, a promoter trans- regulation motif and a domain capable of interacting with other proteins (Nüesch, 2006). NS1 shows various serine and threonine residues which are prone to phosphorylation. These sites are targets

for multiple cellular kinases. Modifications of the NS1 protein by these kinases further broadens its activity spectrum. This contributes to a timely and spacial regulation of NS1, depending on which exact subcellular compartments it is located in during the different stages of the parvoviral infectious cycle. (Corbau et al., 1999; Nüesch and Rommeaere, 2006)

Another important function of NS1 is its ability to act as a scaffold, hijacking cellular factors and bringing together proteins that- under normal circumstances would not interact. This profound intrusion into these cellular interaction patterns is, for instance, depicted by the ability of NS1 to bind to the serine/threonine protein kinase casein kinase (CK) –II α , resulting in phosphorylation of unusual targets such as the actin- cytoskeletal network or tropomyosin, which partly accounts for NS1' direct cytotoxic activities. (Nüesch and Rommelaere, 2007; Nüesch and Rommelaere, 2006; Nüesch et al., 2008)

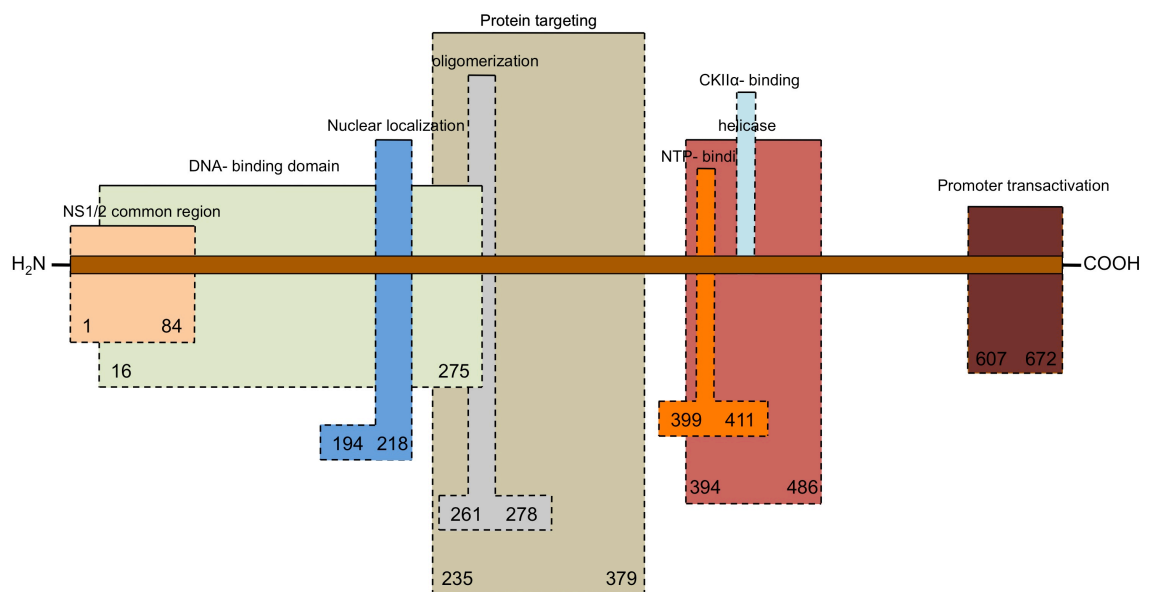


Figure 2. The NS1- protein. The major non- structural protein of MVM comprises 672 amino acids and exerts multiple functions in the parvoviral infectious cycle, including, amongst others, promoter trans- regulation, interaction with cellular proteins as well as mediation of cytotoxicity. Functional domains and their respective locations within the polypeptide sequence are indicated.

Potential interaction partners mediating innate immunity

Small glutamin-rich tetratricopeptide (SGTA) (see chapter 1.6) stands for a cellular 35kDa protein that has been shown to exert various functions, such as the involvement in the cell cycle. It has also been reported to interact with parvoviral NS1 and to be recruited into subnuclear APAR bodies (see life cycle) in the course of viral DNA replication (Cziepluch et al., 2000; Cziepluch et al., 1998). The function of SGTA in this respect is yet unknown, however, the structural similarities it shares with IFIT proteins (see chapter 1.6) might also suggest a role in intracellular, immunogenic recognition of viral nucleic acid structures. As this protein was observed to accumulate in APAR bodies during parvovirus infection, it remains to be shown whether it also exerts functions during parvoviral replication cycles other than in the nucleus.

The NS1 protein might also interfere with cell integrity at yet a different level. Normal cellular processing of primary gene transcripts includes splicing of pre-mRNA as well as the addition of a methyl-guanosine cap at the 5'- terminus and polyadenylation at the 3'- end, preceding the export of mRNAs to perinuclear ribosomes. Recruitment of the splicing machinery is mediated by binding of heterologous nuclear ribonucleoproteins (hnRNPs) or other small nuclear ribonucleoproteins (snRNPs) to respective splice sites (Berg et al., 2007). One of these nucleoproteins is hnRNP-Q (Kabat et al., 2009). DEAD-box polypeptide (DDX) 18 (see chapter 1.6) belongs to a family of RNA helicases and is- like hnRNP-Q, also putatively implicated in RNA modification and delivery to ribosomes (Dubaele and Chène, 2007; Schmid and Linder, 1992). Subsequently to the completion of splicing events, further maturation steps are conducted, characterized, as mentioned, by capping and polyA- tail synthesis. Cleavage and polyadenylation specificity factor (CPSF) subtype 6 forms part of a multiprotein complex, necessary for the latter maturation step (Dettwiler et al., 2004). This complex mediates cleavage of the pre-mRNAs at their respective polyadenylation sites to enable subsequent polyadenylation by polyA-polymerase (PAP). Matured mRNAs leave the nucleus incorporated in large ribonucleoprotein- complexes, which direct them through nuclear- pore

complexes to ribosomal subunits and thus to render them amenable to translation. Without the conjunction of these proteins, mRNAs lack proper orientation towards the ribosomes and are prone to rapid degradation by cytosolic RNases. NS1 has been reported to bind to hnRNP-Q (Harris et al., 1999), CPSF6 and DDX18, respectively (Nüesch, unpublished). However, if this interaction plays a specific role, additionally to the above mentioned ability of NS1 to hijack cellular kinases to change their activity profile, in the parvovirus life cycle remains to be shown.

The role of the second non-structural protein of autonomous parvoviruses, NS2, is not fully understood. It was, however, reported to be required for productive infection of permissive host cells (Naeger et al., 1993; Eichwald et al., 2002). NS2- negative forms of MVM were shown to be impaired in several processes, including DNA amplification, translation and capsid assembly. As seen for NS1, all three isoforms of NS2, NS2p, -y and -l, respectively, were shown to have the ability to interact with cellular proteins. One of these targets is chromosome region maintenance protein (CRM) 1, a nuclear export factor. In a work by Bodendorf and coworkers, which revealed this interaction, this protein was hypothesized to account for efficient re- export of NS2- which, due to its small size may diffuse freely into the nucleus- into the cytoplasm. Furthermore, the question was raised whether the NS2-CRM1 complex might be an export- factor of parvoviral mRNAs, favouring their export over that of the cellular transcripts. (Bodendorf et al., 1999)

An important observation was made by Choi and coworkers, which revealed that the ratio between NS1 and NS2 proteins seems to play an important role in host range of MVM (Choi et al., 2005) (see chapter 1.3). They found that substitution of a single nucleotide within the large splice acceptor of MVMi was likely to improve removal of the respective intron in fibroblasts, which led to a balance- shift of the NS1/NS2 ratio in favour of the latter in those cells. This resulted in its accumulation and was hypothesized to be the causative agent for the observed adaptation of the lymphotropic strain of MVM in fibroblasts. Importantly, Choi et al. additionally observed that mutating NS2, in order to

enhance its interaction with CRM1 also led to an increased fitness of MVMi in fibroblasts. What the exact mechanisms of NS2 in connection to the parvoviral life cycle are on a molecular level remains to be shown.

As mentioned in chapter 1.2, viral capsids are composed of the structural proteins VP1 and VP2, respectively, which contribute to the protein- shell at a ratio of about 1:5. The surface morphology of this shell is characterized by an icosahedral assembly, yielding 12 five- fold symmetry axes. On each of these axes, there are cylindrical projections, elevated from encircling canyons. In the center of each protrusion, there is a small pore which projects from the outer surface of the virion into the inner core. Through these pores, VP2 N-termini can be exposed. These have been hypothesized to play certain roles in the parvoviral infectious cycle, either early during entry-, or later during egress processes. (Hueffer and Parrish, 2003; López-Bueno et al., 2006)

1.5 Parvovirus life cycle

The infectious cycle of MVM begins at the surface its host cell, where it attaches to glycoproteins, using sialic acid as binding site (Allaume et al., 2012; Lopez-Bueno et al., 2006). This triggers endocytosis of the viral particles through clathrin-coated pits. Internalized virions are then routed into late endosomes (see figure 3). Cytoplasmic trafficking of those vesicles towards the nucleus is accomplished by active transport along the microtubular network. Acidification of the endosomal compartment leads to conformational changes of the capsid, which is an important step for the endosomal release of the viral particles and results in their perinuclear accumulation. (Cotmore and Tattersall, 2007)

Steric modification of the capsid proteins during the trafficking process probably accounts for the exposure of sequences that enable the transport of viral particles across the nuclear envelope, most likely passing through nuclear pore complexes (Weitzman, 2006). In case the target cell is in a non- proliferating state, viral particles may remain assembled, latently waiting for the cell to enter S-phase. As soon as the G₁/S- checkpoint is passed, particles are

disassembled, a process in which viral genomes are likely to be extracted by DNA polymerase which binds to the 5'- ends of the viral genome, exposed through capsid pores. Upon release of the viral (single- stranded) genome, a double- stranded DNA intermediate is generated, using the terminal hairpins as primers. This process is cyclin A- dependent, which partly accounts for the S-phase dependency of this virus (Bashir et al., 2000). As for MVM, genomes are packaged practically exclusively as negative- sense strands, this step is necessary to create transcription templates to allow for expression of viral proteins. This process, which largely depends on cellular mitogenic stimuli, is commonly accomplished following initial genome replication. The reason for the necessity of viral DNA amplification preceding gene expression lies in the fact that the latter cannot be initiated before a positive- sense transcription template is formed. Nevertheless, non- structural proteins are also key recognition factors of viral origins of replication, located within the terminal repeat regions, which further enhances viral replication. Viral DNA is amplified upon the recruiting of the cellular replication machinery to distinct nuclear foci, subnuclear replication factories, termed autonomous parvovirus replication (APAR)- bodies, employing a complex cascade of amplification-, cleavage- and religation reactions, referred to as the rolling- hairpin strategy. In parallel, newly synthesized capsid proteins are translocated into the nucleus and form nascent capsids, which are subsequently loaded with viral single- stranded DNA in an NS1- dependent manner. (Cotmore and Tattersall, 2006; Weitzman, 2006; Cziepluch, et al., 2000)

By an unknown mechanism, assembled particles translocate from the nucleus to the endoplasmic reticulum. Viral egress and release into the extracellular space is achieved by transport in exocytic vesicles through the Golgi apparatus, delivering progeny virions to the plasma membrane (Weitzman, 2006; Bär et al., 2008). In case viral replication has perturbed cellular mechanisms in excess- or in case it has consumed cellular energy to such an extent that the infected cell is no longer able to maintain its physiological integrity, it may result in necrotic death, shedding the newly produced virus in a vesicle- independent manner. (Rommelaere et al., 2010; Weitzman, 2006)

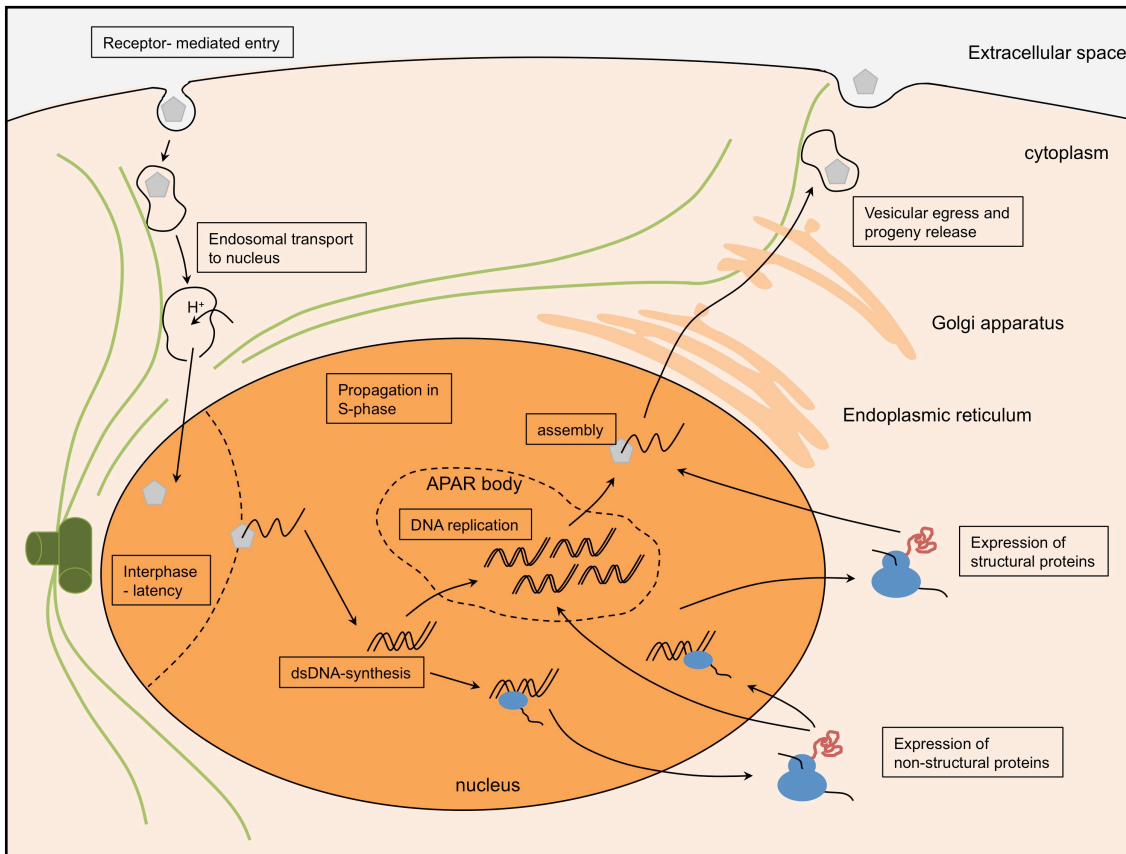


Figure 3. Life cycle of MVM. MVM particles enter cells via receptor- mediated endocytosis and are translocated to the nucleus in endosomes by active transport along microtubules. Particles enter the nucleus through nuclear pore complexes. Conversion of uncoated, negative- stranded ssDNA to a double- stranded transcription intermediate during cellular S- phase initiates viral protein expression and DNA amplification. Non- structural proteins are necessary for efficient viral replication. Newly produced non- structural proteins accumulate in the nucleus to form capsids, which are subsequently loaded with viral genomes. Assembled progeny particles exit the nucleus and are released from the host cell by vesicular egress.

1.6 Innate immune recognition of viruses

Mammalian cells dispose of a great multitude of ways to counteract viral infection. Apart from lymphocyte- mediated mechanisms, which employ cytotoxic T-cells, natural killer (NK) cells and the production of neutralizing antibodies, there is another layer of defense, acting independently of those professional immune cells. This layer comprises cell- intrinsic mechanisms, which constitute an important first- line innate immune response to keep viral

infection at bay, and which are shared by all metazoan cell types. These mechanisms are defined by a resin of sensors, which are able to detect the presence of viral structures within multiple cellular compartments (see figure 4). As different virus species exert greatly diverging entering-, replication- and exit strategies, the measures of respective host cells to counteract infection are equally diverse. These measures are crucial for an organism to fight such invading pathogens and usually result in their very efficient eradication. Central to these processes is the induction of type I interferons (IFNs), especially of IFN- β , which is a key mediator of cellular antiviral activity. Mounting a first- line innate immune response against viruses includes two consecutive steps. The first one is defined by the recognition of a viral agent in an infected cell, signaling for the induction of (amongst others) IFN- β expression. This recognition can be of varying nature. Either, viruses trigger an antiviral response directly upon entry, or at later stages through specific replication intermediates. The second step comprises IFN- β - mediated autocrine and paracrine induction of a huge set of antiviral genes, whose protein products work in concert to create an intracellular environment impeding viral replication. (Pichlmair and Reis e Sousa, 2007; Fuertes et al., 2012)

The primary recognition of viruses can take place in variable cellular compartments, depending on the route the incoming virions take to access their respective preferred locations to replicate. Basically, it can be stated that the major viral structures (pathogen- associated molecular patterns, PAMPs)- recognized by the cellular sensors are their nucleic acid components. However, in the case of virus counteraction, it can be delicate for the cell to distinguish between a possibly virulent invader and cell- intrinsic structures. This is due to the fact that all viruses are produced by cells and thus, up to a certain extent, share molecular patterns with their respective hosts. Hence, a major reason of how an infected cell is able to discriminate virus from self seems to lie in the abnormal localization of their nucleic acid components. Similarly, exact molecular make-ups of those nucleic acids may vary slightly from those of the host. One example for this is 5'- triphosphate RNA, created during replaction of RNA viruses such as influenza. Such termini are usually not present in cells as

mRNAs contain methyl-guanosine caps and as tRNA- and rRNA- termini are usually obscured by ribosomal proteins. Thus, the presence of 5'- triphosphate-bearing RNAs serve as a recognition factor for cellular defense sensors. (Pichlmair and Reis e Sousa, 2007; Haller et al., 2005)

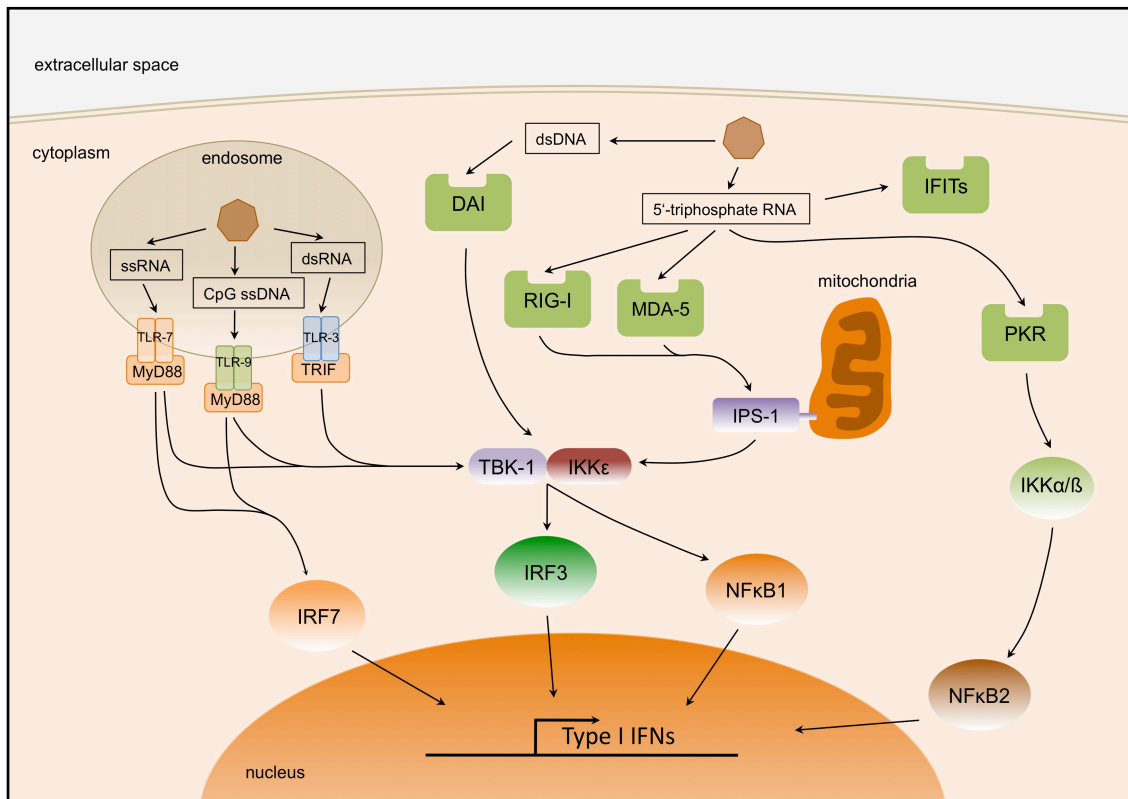


Figure 4. Intracellular antiviral recognition network. Viral patterns, above all specific features of their nucleic acid components are sensed throughout various subcellular compartments. Pattern recognition receptors include TLRs, located in the endosome, sensors, such as RIG-I, MDA-5, DAI, PKR as well as IFIT- proteins, surveying the cytoplasm for viral presence. Endosomal recognition, through autophagy, can additionally include viral structures present in the cytoplasm. Activation of those sensors triggers NFκB- and IRF- mediated signaling to promote type-I IFN expression.

In various stages of an infectious cycle, viral structures are commonly exposed in the cytosol. This can be observed for example during viral entry or during replication processes, which direct viral RNA or DNA out of membrane-enclosed intracellular compartments. There are various cytosolic factors, capable of detecting such incoming, non- self structures. Retinoic acid-inducible gene 1 (RIG-I) belongs to the family of RIG-I-like receptors (RLRs). It contains a conserved DEAD- (abbreviation for Asp-Glu-Ala-Asp) box motif,

which is able to bind 5'- triphosphate double- stranded RNA (dsRNA) and a Caspase- recruiting domain (CARD) with which it is able to interact with downstream signaling partners. Another RLR is Melanoma Differentiation-Associated protein (MDA) 5. Both proteins are RNA helicases, which, upon binding of RNA structures, signal to the nucleus for expression of IFN- β . This is accomplished by activation of the mitochondria- associated downstream adapter interferon- β promoter stimulator (IPS) -1, which is shared by both RIG-I and MDA5. IPS-1 promotes activation of TANK-binding kinase (TBK) -1 and I κ B kinase (IKK) ϵ , which, upon heterodimerization phosphorylate the transcription factor interferon- regulatory factor (IRF) 3. Activated IRF3 homodimerizes and translocates to the nucleus, where it binds to IFN- β - gene regulatory elements to promote its transcription. RIG-I and MDA5 are distinctive by binding different RNA patterns, but to a certain extent, they also show functional redundancy. Another group of anti-viral proteins comprises the interferon-induced proteins with tetratricopeptide repeats (IFITs). These proteins contain a tetratricopeptide repeat (TPR) region, a structure composed of tandem repeats of a pair of antiparallel α - helices, arranged as a helix-turn-helix motif. TPRs show similarities towards the target- binding leucine- rich repeat domains of Toll-like receptors (TLRs). TPR motifs are commonly regarded as protein-protein interaction sites. However, IFITs have been reported also to bind 5'-triphosphate RNA with high specificity and to be strongly induced by IFN- β . This observation established their role in sequestering genomic RNA to inhibit further viral replication. Importantly, IFITs were also shown to interact with the cellular RNA- processing- and translation machinery, providing a potential direct link between recognition of non-self nucleic acids to the inhibition of protein synthesis, important for suppression of viral replication. (Rehwinkel et al., 2010; Pichlmair et al., 2011; Pichlmair et al., 2009; Pichlmair and Reis e Sousa, 2007)

Apart from the necessity for a 5'- triphosphate and the double- strandedness, RNA secondary structures seem to play an additional role in the responsiveness of the two factors, as intrastrand hybridization of ssRNA has been shown to be a contributor of RIG-I activation. However, RIG-I and MDA5 also seem to play partially redundant roles in recognizing viral nucleic acids.

Another RLR, laboratory of genetics and physiology (LGP) -2, seems to have an inhibitory effect on the anti- viral activity of RIG-I and MDA-5. This was suggested upon the observation that LGP-2- negative mice show enhanced IFN- β production upon infection with RNA- viruses (Venkataraman et al., 2007). An additional way, by which cytosolic dsRNA can be detected, is via the serine and threonine protein kinase R (PKR). In an IRF3- independent manner, binding of PKR also results in induction of IFN expression by employing IKK α and - β . This activates the transcription factor nuclear factor κ B (NF κ B) 2, which also binds to the IFN- β - promoter. Another nucleic acid species, which is normally not present in the cytosol is dsDNA. This species can be sensed by DNA-dependent activator of IRFs (DAI), which activates the IRF3 transcription factor via TBK-1/IKK ϵ in an IPS-1- independent manner. (Pichlmair and Reis e Sousa, 2007; Haller et al., 2005)

A common way of viruses to enter their target cells is via receptor- mediated endocytosis, directing them into endosomal compartments, where they might expose their genomes. These endosomes are far from being devoid of microbotic sensors. In fact, their membranes are interspersed with PRRs, most importantly with TLRs, which survey endosomes for viral presence and of which each member shows specificity towards disparate viral patterns. Of this family of receptors, three should be mentioned here. TLR3 shows expression in a wide variety of cell types and it was identified as a receptor for dsRNA. Via the adapter protein TRIF, it signals to TBK-1/IKK ϵ , linking the endosomal recognition of pathogens to that of the cytosol, which promotes IRF3- mediated induction of type I IFN expression. The other two important viral receptors in endosomes are TLR7 and -9, respectively. TLR9 recognizes unmethylated CpG- DNA motifs, whereas TLR7 was reported to bind to genomic ssRNA. Both PRRs use the same adaptor protein for downstream signaling, MyD88, which is distinct from that of TLR3. Upon receptor engagement, MyD88, via IKK α , promotes activation of the transcription factor IRF7, which- as IRF3 does- translocates to the nucleus to activate IFN- β transcription. Alternatively, phosphorylation of TBK-1/IKK ϵ can bridge TLR7/9 signaling to the NF κ B1 transcription factor, which homodimerizes and binds to the IFN- β promoter to

complement its induction in addition to the IRF transcription factors. Unlike TLR3, cell type distribution of TLR7 and -9 is rather restricted, showing their highest expression in cells of the lymphoid lineage, but however, these pathways are to some extent also operative in other cell types. It should be stated that recognition of viral pathogens by the mentioned TLRs is not restricted to incoming viral structures during entry procedures, but can also include cytosolic replication intermediates, taken up into endosomes by autophagic processes, as shown by Lee et al., 2007. Autophagocytosis provides a bridge between the anti-viral surveillance of cytosolic- and endosomal compartments, broadening the possibilities for TLRs to detect the presence of viruses in a cell. Together, these cytosolic- and endosomal receptors have the ability to recognize a broad range of viral patterns. This enables the efficient initiation of counteracting mechanisms to eradicate these intruders. (Fuentes et al., 2012; Pichlmair and Reis e Sousa, 2007)

After recognition of a viral intruder, the hallmark of the second crucial step, taken to counteract infection is characterized by the release of IFN- β from infected cells, which results in an autocrine- and paracrine stimulation of a great number of interferon responsive genes (ISGs), which induce a latent antiviral state in order to impair viral replication (see figure 5). This serves as an amplification loop of antiviral responses in cells, which are already infected and warns surrounding uninfected tissue about the presence of a pathogen.

Upon binding of IFN- β to its cognate receptor (IFNAR), a JAK-STAT signaling pathway is triggered. Conformational change of IFNAR causes Janus Kinase (JAK) -1, bound to its cytosolic terminus to autophosphorylate itself and to concomitantly activate the latent transcription factors signal transducers and activators of transcription (STATs). These transcription factors, most importantly STAT1 and -2 dimerize and translocate to the nucleus, where they bind to interferon- stimulated response elements (ISRE) within the promoters of several hundred ISGs to activate their transcription. Expression of these genes results in the accumulation of proteins that act on multiple levels to abort infection or- if a respective cell is not yet infected- to be prepared in case a virus enters. For

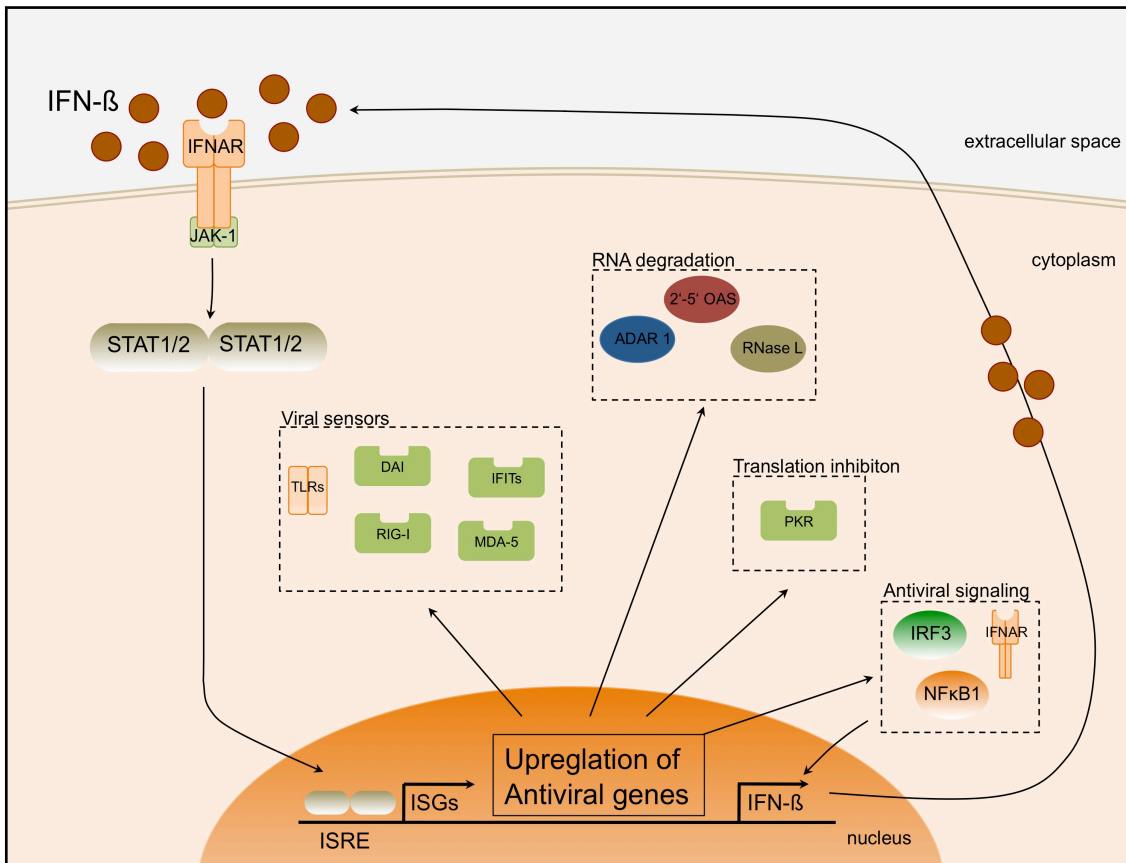


Figure 5. Type- I IFN response. Autocrine and paracrine signaling of IFN-β, mediates a Jak/Stat- dependent activation of hundreds of interferon- stimulated genes (ISGs). These encode proteins dedicated to intracellular virus- sensing, antiviral signaling and macromolecular synthesis shut- off, which, taken together, initiate a latent antiviral state in order to impair viral growth and –spread.

example, the entire set of the surveillance machinery, including RLRs, DAI, IFITs, TLRs as well as their downstream signaling effectors are upregulated, providing a positive feedback loop in order to make for a more efficient recognition of invaders. Antiviral measures also comprise a shut- off of the cellular macromolecular synthesis machinery. On a translational level, this is characterized by an activation of PKR, which itself is also upregulated upon IFN-β signaling. PKR phosphorylates the eucaryotic translation initiation factor 2α (eIF2α), rendering it incapable of binding to the ribosomal initiation complex and thus halting protein synthesis. This shut-off goes hand-in-hand with radical RNA degradation (including cellular RNAs). This is mediated by the upregulation of 2'-5' oligoadenylate synthetase (2'-5' OAS), which in turn activates RNase L to promote fragmentation of gene transcripts. Additionally,

adenosine deaminase acting on RNA (ADAR) -1 modifies viral replication intermediates by deaminating RNA. Amongst others, these measures usually result in abortive infection by efficient eradication of viral pathogens. In case cellular counteraction mechanisms are no longer tolerable, this state might result in induction of apoptosis and elimination of the infected cell from the organism. (Fuertes et al., 2012; Pichlmair and Reis e Sousa, 2007)

Bearing in mind these exquisitely specific means of a cell to fight viruses, it is perspicuous that these agents have evolved a multitude of ways to evade or counteract these mechanisms (see figure 6). A significant amount of these strategies target the IFN system and they can downregulate its activation on multiple levels. For example, NS1 of influenza A sequesters dsRNA molecules to hide them from IFN- induction. V proteins of paramyxoviruses block MDA5 activation and promote degradation of STAT1. Specific HCV proteins inhibit RIG-I and, as ssRNA Ebola virus (EBOV) does, negatively interfere with TLR3 signaling. Human herpes virus 8 (HHV-8) produces dominant- negative IRF homologues to block interferon induction. Herpes simplex virus (HSV) 1, through its γ 34,5 protein prevents phosphorylation of eIF2 α by PKR and thus interferes with translation inhibition. Poxviruses produce soluble IFNAR analogues, „viroceptors“ which sequester secreted IFNs from their cellular counterparts to inhibit autocrine- and paracrine signaling. This illustrates that downregulation of the cellular antiviral immune response takes place on multiple levels. As described, an IFN response acts in a cascade- like manner, amplifying responses at every downstream step. Thus, inhibition of IFN signaling at early stages also affects distant effectors of the circuit, which results in an amplification of the inhibitory effects. This has important consequences not only for infected-, but also for surrounding cells, which are no longer able to establish an anti-viral state. (Haller et al., 2005; Pichlmair and Reis e Sousa, 2007)

In respect to parvoviruses, a lot is yet to be unraveled concerning the mechanisms underlying cellular antiviral activities. In the case of AAV, Zhu and coworkers showed that these viruses can induce IFN signaling in a TLR9-

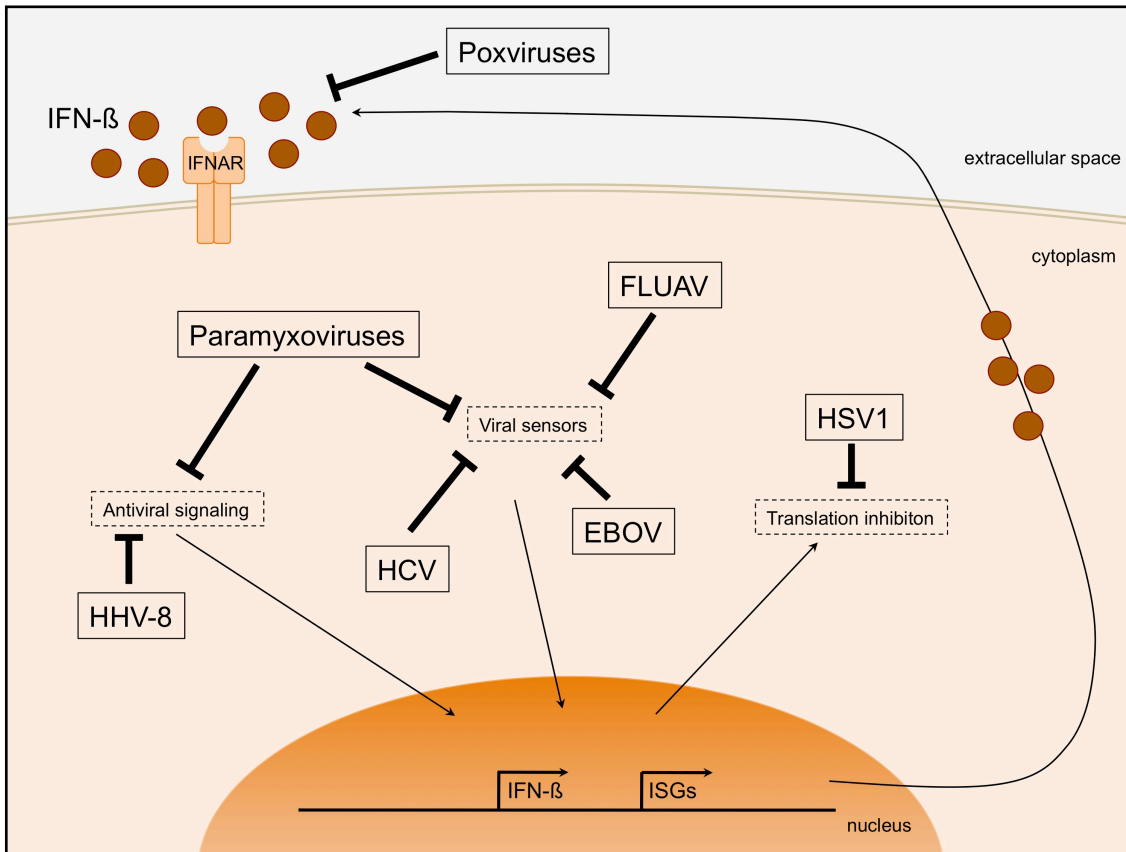


Figure 6. Viral mechanisms to counteract cellular antiviral responses. Ability of viruses to interfere with the host- cell immunity comprises multiple distinct levels. Amongst others, viral sensing, IFN- β - mediated antiviral signaling as well as proper functioning of ISG- encoded proteins can be impaired. For abbreviations see text.

dependent manner (Zhu et al., 2009). Recognition of these particles was also attributed to their partial self- complementarity (Jayandharan et al., 2011; Rogers et al., 2011). In 2010, Grekova and coworkers described an IFN induction in MEFs. In their paper, they could show an activation of IFN- receptor signaling and an upregulation of antiviral proteins, such as PKR or 2'-5' OAS (Grekova et al., 2010). Similarly, Ventoso et al. 2010 showed that MVMp infection results in an activation of PKR, which greatly restricts viral replication (Ventoso et al., 2010). However, to which exact cellular sensor this activation is attributable remains elusive.

2. Aim

This study aims at characterizing potential novel molecular mechanisms, by which parvoviruses interact with the host cellular machinery to enable their replication in primary cells. For this, an original isolate of MVM, dating back to 1968, will be used. It is hypothesized that this virus- in contrast to MVMp- disposes of means to evade or counteract an innate antiviral immune response, thereby broadening its host spectrum to achieve a productive infection in mouse embryonic fibroblast (MEF) cells.

To this end, the original isolate of MVM will be recovered and assayed for replication competence in MEFs. It will be attempted to characterize potential differences in antiviral responses between MVM_{CR} and MVMp. Furthermore, formerly identified interaction partners of the MVM NS1 protein will be assayed for potential roles in MEF permissibility towards MVM_{CR}. Particular focus is given to the mRNA- processing factors CPSF6, DDX18, hnRNP Q, as well SGTA, since a possible functioning for the MVM replication cycle is still elusive so far.

Finally, the study aims to identify differences in the genomic sequence between MVMp and its progenitor MCM_{CR}. This information will be used to generate recombinant MVM_{CR}-like infectious-clone DNA on the base of pDB-MVMp. These clones should then serve to characterize the MVM functions allowing growth in MEFs and potentially to characterize the interplay of MVM with the host innate immune response.

3. Materials

3.1 Bacteria

Name	Description	Company
<i>E. coli</i> DH5 α	heat shock competent	laboratory stock
<i>E. coli</i> SurE	heat shock competent	laboratory stock
<i>E. coli</i> XL1 Blue	heat shock competent	laboratory stock

3.2 Media and additives for bacterial cultures

Name	Description	Company
Agar		Sigma-Aldrich
Ampicillin Technologies	25mg tablets	Agilent
Isopropyl β -D-1-Thiogalactopyranoside (IPTG)	100mM aqueous solution	US Biological
Luria Broth (LB)		laboratory stock
5-bromo-4-chloro-indolyl- β -D-galactopyranoside (Xgal)	20mg/ml in Dimethylformamid (DMF)	US Biological

3.3 Cell lines

Name	Description	Company
293T	Human Embryonic Kidney	laboratory stock
A9	Mouse fibroblasts	laboratory stock
NBK	Human Newborn Kidney	laboratory stock

MEF	Mouse Embryonic Fibroblast	laboratory stock
-----	----------------------------	------------------

3.4 Media and additives for cell culture

Name	Description	Company
Dulbecco's Modified Eagle Medium (DMEM)		Sigma-Aldrich
Dulbecco's Modified Eagle Medium (DMEM) w/o isoleucine		Sigma-Aldrich
Fetal Calf Serum (FCS)		PAA Laboratories
2x Minimum Essential Medium (2x MEM)		Gibco
L-Glutamin	200mM in 0,85% NaCl	Gibco
Penicillin/Streptomycin	100µg/ml + 10U/ml	Gibco
Trypsin-EDTA	0,25%	Gibco

3.5 Wild Type Viruses

Name	Company
Minute Virus of Mice, Prototype (MVMp)	laboratory stock
Minute Virus of Mice, Crawford Isolate (MVMcr68)	laboratory stock

3.6 Single- and combined mutant viruses

Name	Description	Company
MVMp Δ1967+ Δ1970	non-coding alterations	this work
MVMp ΔT1984C	aa substitution L575S (NS1)	this work
MVMp ΔA2258C	aa substitution S666R (NS1) + N174P (NS2)	this work
MVMp ΔT3274C	aa substitution L160S (VP2)	this work
MVMp ΔT3621C	aa substitution S276P (VP2)	this work
MVMp Δ1967+ Δ1970+		

Δ T1984C	NS-encoding alterations	this work
MVMp Δ 1967+ Δ 1970+		
Δ T1984C+ Δ A2258C	NS-encoding alterations	this work
MVMp Δ T1984C+		
Δ A2258C	NS-encoding alterations	this work
MVMp Δ T3274C+		
Δ T3621C	capsid-encoding alterations	this work

3.7 Enzymes

Name	Description	Company
Klenow Polymerase	1U/ μ l	GE Healthcare
Taq Polymerase	5U/ μ l	Clontech
Pfu Polymerase	2.5U/ μ l	Stratagene
Phosphatase, alkaline	1U/ μ l	Roche
Proteinase K	20mg/ml	laboratory stock
T4 DNA Ligase	400U/ μ l	New England Biolabs
DNase I	1U/ μ l	Roche
DpnI	10U/ μ l	Stratagene

3.8 Restriction Enzymes

Name	Company
AfeI (Eco47III)	New England Biolabs
AhaIII	Invitrogen
BglI	New England Biolabs
BglII	New England Biolabs
BstEII	New England Biolabs
EcoRI	New England Biolabs

EheI (NarI)	New England Biolabs
HindIII	New England Biolabs
PmeI	New England Biolabs
SnaBI	New England Biolabs
Xba	Roche
XhoI	Roche

3.9 Primers

PCR primers

Name	5'-3' sequence
120fw	AGCGGTTTCAGGGAGTTTAAA
1320fw	ACCAACTTTTCACTGCCTGA
1650fw	ATTCGCATTGATCAAAAAGG
2100rev	TGCTCCAAGGCTCTAAAGCC
2780fw	TAAACGCACTAGACCACCTG
2970rev	GCCGTCACCCAAGAATCTAT
3600rev	AGTACCTGTGGCAAATTCGT
4005fw	TTCAGGTAGAGACACCAAAG
4140rev	GCTGTAAAACATTTGAAA
4890rev	TTTATTATTTTTTTGGTCCT

Primers for sequencing analysis

Name	5'-3' sequence
MVMp #1984	5'-CTGGTGA CTTTGGTTTGG-3'
MVMp #2258	5'-TTGGAGCACACCAAATAC-3'
MVMp #3274	5'-ATGAGCAAATTTGGACAC-3'
MVMp #3621	5'-ATCTTTCAGTGACCTACG-3'

Primers for site-directed mutagenesis

Name	5'-3' sequence
MVMp #1984fw	5'-GCCAACTCCTATAAATTCAGTTCGGCACGCTC-3'
MVMp #1984rev	5'-CGGTTGAGGATATTTAAGTGATCCAAGCCGTGCGAG-3'
MVMp #2258fw	5'-GTTGAAGAAAGACTTCCGCGAGCCGCTGAACTT-3'
MVMp #2258rev	5'-CAACTTCTTTCTGAAGGCGCTCGGCGACTTGAA-3'
MVMp #3274fw	5'-CTGTTACAGAGCAAGACTCAGGAGGTCAAGCTATA-3'
MVMp #3274rev	5'-GACAATGTCTCGTTCTGAGTCCTCCAGTTCGATAT-3'
MVMp #3621fw	5'-CTTACTACTTTGACACAAATCCAGTTAACTCACACACACG-3'
MVMp #3621rev	5'-GAATGATGAAACTGTGTTTAGGTCAATTTGAGTGTGTGTGC-3'

Primers for qRT-PCR

Name	5'-3' sequence
MVMp NS1fw	5'-GCGCGGCAGAATTCAAAC-3'
MVMp NS1rev	5'-CCACCTGGTTGAGCCATCAT-3'
Probe:	5'-6-FAM-ATGCAGCCAGACAGTTA-MGB-3'

Primers for RT-PCR

Name	5'-3' sequence
GAPDHfw	5'-ACCACAGTCCATGCCATCAC-3'
GAPDHrev	5'-TCCACCACCCTGTTGCTGTA-3'
PKRfw	5'-GGCCTTGTC AATAGCTTTGC-3'
PKRrev	5'-GGGCTCTTTAACAGCTTCTG-3'
IFN- β fw	5'-CCCTATGGAGATGACGGAGA-3'
IFN- β rev	5'-CTGTCTGCTGGTGGAGTTCA-3'
OASfw	5'-GTGCTCCTCCGCTGTAAGAC-3'
OASrev	5'-ACAGAACCTCCCAACAGGTG-3'
TLR9fw	5'-CCTGCACTTCTCTTGCCACA-3'

TLR9rev	5'-TCCATGAAGAGAACGCGCAG-3'
NS1fw	5'-CGAGGAGCGGAAACTACTTG-3'
NS1rev	5'-TACATGGCAGTGCCAGCCTT-3'

3.10 DNA probes

Name	Description	Company
NS1	MVMp NS1 coding region	laboratory stock
Salmon Sperm DNA	10mg/ml	laboratory stock

3.11 Loading dyes, DNA- and protein markers

Name	Description	Company
6x DNA Loading Dye	DNA loading dye	Thermo Scientific
10x Fast Digest green buffer	DNA loading dye	Fermentas
λ DNA/EcoRI+HindIII	DNA marker	Fermentas
Spectra BR Protein Ladder	Protein marker	Thermo Scientific

3.12 Antibodies

Name	Source	Company
<u>Primary antibodies</u>		
α-capsid	rabbit	laboratory stock
α-CPSF6	goat	Santa Cruz Biotechnology
α-eIF2α	goat	Santa Cruz Biotechnology
α-pelF2α	rabbit	Cell Signaling Technology
α-DDX18	goat	Santa Cruz Biotechnology
α-NS1C	rabbit	laboratory stock

α -NS2	rabbit	laboratory stock
α -p50	rabbit	Santa Cruz Biotechnology
α -p52	mouse	Santa Cruz Biotechnology
α -p65	rabbit	Millipore
α -PKR	mouse	Santa Cruz Biotechnology
α -SGT	rabbit	laboratory stock
α -pSTAT1	rabbit	Cell Signaling Technology
α -pSTAT2	rabbit	Cell Signaling Technology
α -STAT1	mouse	Santa Cruz Biotechnology
α -STAT2	rabbit	Santa Cruz Biotechnology
α -Tubulin	rabbit	Santa Cruz Biotechnology

Secondary antibodies

Goat anti-rabbit/mouse IgG, HRP-linked	Cellsignal
Rabbit anti-goat IgG, HRP-linked	Cellsignal
Alexa Fluor 488/594/647 rabbit anti-rabbit IgG	Invitrogen
Alexa Fluor 488/594/647 donkey anti-mouse IgG	Invitrogen
Alexa Fluor 488/594/647 donkey anti-rabbit IgG	Invitrogen

3.13 Chemicals

<u>Name</u>	<u>Company</u>
Agar	Sigma-Aldrich
Agarose	Invitrogen
Ammonium persulfate (APS)	Sigma-Aldrich
Bromodeoxyuridine (BrdU)	Sigma-Aldrich
4',6-Diamidin-2-phenylindol (DAPI)	laboratory stock
Dimethyl sulfoxide (DMSO)	Sigma-Aldrich
Elvanol (Polyvinyl alcohol)	Alfa Chemicals

Ethanol	Sigma-Aldrich
Ethidium bromide (10mg/ml)	Roth
Ethylendiaminetetraacetate (EDTA)	Sigma-Aldrich
Formaldehyde	Sigma-Aldrich
Para-Formaldehyde	Sigma-Aldrich
Glycerol	Sigma-Aldrich
Hydrochloric Acid (HCl)	Sigma-Aldrich
Isopropanol	Sigma-Aldrich
Phalloidin-Rhodamin	Sigma-Aldrich
Sodium-dodecyl-sulfate (SDS)	Sigma-Aldrich
Sodium Hydroxide (NaOH)	Sigma-Aldrich
Sodium chloride (NaCl)	Sigma-Aldrich
Tetramethylethylenediamine (Temed)	Sigma-Aldrich
Trishydroxymethylaminomethane (Tris)	Sigma-Aldrich
Triton-X100	Sigma-Aldrich

3.14 Buffers and reagents

Name	composition
BSA	
1x PBS	0,14M NaCl, 2,7mM KCl, 2mM KH ₂ PO ₄ , 10mM Na ₂ HPO ₄
1x Tris-Glycine buffer	25mMTris, 0.192M glycine
2x HBSS	50mM Hepes, 1.5mM Na ₂ HPO ₄ , 0.28M NaCl, 10mM KCl, 12mM D+Glucose
4% PFA	4% para-Formaldehyde in 1x PBS
20x SSC	3M NaCl, 0.3M Trisodiumcitrate-dihydrate, pH7
100x Denhardt's solution	2% BSA, 2% Ficoh 400, 2% Polyvinylpyrrolidone
Denaturation buffer	1.5M NaCl, 0.5M NaOH

Depurination buffer	0.25M HCl?
Lämmli buffer	4% SDS, 20% Glycerol, 10% 2-mercaptoethanol, 0.004% bromphenol blue, 0.125M Tris HCl
LB medium	1% bacto-tryptone, 0.5% bacto-yeast extract, 0.5% NaCl
Neutralization buffer	0.5M Tris-HCl (pH7), 3M NaCl
TE buffer	10mM Tris-HCl (pH8), 1mM EDTA
Wash buffer I	2x SSC, 0.1% SDS
Wash buffer II	0.2x SSC, 0.1% SDS
Casein solution	2% casein in 10% BSA
Milk	10% dry milk in PBS
Tris-HCl	10mM, pH 8.5

3.15 Kits

Name	Company
Amershan Megaprime DNA Labeling System	GE Healthcare
Advantage-HF 2 PCR Kit	Clontech
Plasmid Miniprep Kit	Qiagen
Plasmid Maxiprep Kit	Qiagen
QIAquick Gel Extraktion Kit	Qiagen
QuantiTect Reverse Transcription Kit	Qiagen
NE-PER Nuclear and Cytoplasmic Extraction Reagents	Thermo Scientific
RNeasy Mini Kit	Qiagen
Single Step Mutagenesis Kit	Stratagene
TaqMan Universal PCR Master Mix	Applied Biosystems
TA Cloning Kit, pCR2.1	Invitrogen

3.16 Laboratory consumables

Name	Description	Company
Cell culture dishes	6/15cm	Greiner Bio-One/Nunc
Cell culture flasks	75cm ²	Greiner Bio-One/Nunc
Cell lifters		Costar
Chemiluminescence sensitive films		GE Healthcare
Falcon tubes	15/50ml	Greiner Bio-One
Needles	0.4x20mm	Braun
Nylon membrane	Hybond-N	GE Healthcare
Parafilm		Pechiney
Pasteur pipettes	230mm	WU Mainz
PCR tubes	200µl	Biozym
Petri dishes	10cm	Greiner Bio-One
Pipettes, disposable	2/5/10/25ml	Falcon
Pipette Tips	10/200/1000µl	Greiner Bio-One
Reaction tubes	1.5/2ml	Eppendorf
Syringes	1ml, 2ml	Henke Sass Wolf
Whatman paper	3mm	Schleicher & Schüll
X-Ray films	BioMax	Kodak

3.17 Equipment

Name	Description	Company
Balance	BL 1500 S	Sartorius
Blotting Chamber	Trans-Blot SD	Bio-Rad
Centrifuge (table top)	Centrifuge 5415 C	Eppendorf
Centrifuge (Falcon tubes)	CK3800	Hermle
Confocal fluorescence microscope		Leica
Fluorescence microscope		Leica
Geiger Counter	Typ LB 1210 B	Berthold
Incubator		Thermo Scientific

Laminar flow chamber		Labotect
Microwave oven		Severine
Milli-Q ultrapure water unit	Biocel A10	Millipore
NanoDrop 2000		Thermo Scientific
PCR thermo cycler	GeneAmp PCR system 9700	PE Applied Biosciences
pH-meter	Calimatic (electrode 81-02)	Knick
Pipettes	2/20/200/1000µl	Gilson
Pipettor, mobile	Pipetboy acu	Integra Biosciences
Shaker	Polymax 1040	Heidolph
Thermo mixer		Eppendorf
Ultracentrifuge		Beckmann
UV crosslinker	UV Stratalinker 1800	Stratagene/Agilent
Vortex mixer	VF2	IKA Labortechnik
X-ray film cassette		Rego
X-ray film processor	E.O.S	AGFA

4. Methods

4.1 Cell biological methods

4.1.1 Cultivation of cells

Cells were grown in sterile 75cm² culture flasks in Dulbecco's Modified Eagle's Medium (DMEM), supplemented with 10% heat-inactivated fetal bovine serum (FCS), 2mM L-glutamine, 100µg/ml penicillin and 10U/ml streptomycin (DMEM⁺). To maintain adequate confluency, transformed cell lines were first briefly washed, detached with 0.25% Trypsin/EDTA solution and subsequently reduced to appropriate densities every 3-6 days. Primary cells were reduced every 7 days and obtained fresh medium every 3-4 days. For experiments, cells were detached and seeded in culture dishes at densities of 5x10³ cells per spot (spot slide), 2x10⁵ cells per 6-well dish, 5x10⁵ cells per 6cm culture dish and 5x10⁶ cells per 15cm culture dish, respectively. After seeding, cells were incubated at 37°C, 5% CO₂ to adhere to the culture dish surface for further experimentation.

4.1.2 Isolation of mouse embryonic fibroblasts (MEFs)

To obtain primary MEFs, pregnant C57BL/6 mice were sacrificed on day 18 postconception. Embryos were extracted from the uteri and transferred into sterile culture dishes. Embryonic tissue was digested with 0.25% Trypsin/EDTA and homogenized mechanically. Supernatant containing single cells was collected, briefly centrifuged to separate non-homogenizable debris and seeded in 15cm culture dishes at a density of 5x10⁶ cells per dish. 24-48h after seeding, medium containing non-adherent- and dead cells was discarded and replaced by fresh DMEM⁺. Subsequently, cells were used for experiments or cultured at above mentioned conditions to a maximum of five passages before reaching senescence and crisis.

4.2 Molecular biological and microbiological methods

4.2.1 Recovery of viral genomic DNA by Polymerase Chain Reaction (PCR)

In order to amplify viral DNA for subsequent sequencing analysis, infectious particles from viral stocks were first digested by proteinase K overnight at 46°C and remaining viral capsids were mechanically disrupted by shear-stress. For amplification of viral DNA, an Advantage-HF 2 PCR kit was used and PCR was performed according to the manufacturer's instructions. 5 primer pairs (see materials) were used, yielding partially overlapping fragments between nucleotides 120-2100, 1320-2970, 1650-3600, 2780-4140 and 4005-4890, respectively. For the first three fragments, an annealing temperature of 52°C was chosen, primers of the last two fragments were annealed at 54°C. Fragments were amplified by *Taq*-Polymerase from 100ng of template DNA in 32 consecutive cycles of template denaturation at 94°C for 1 minute, annealing at the indicated temperatures for 1,5 minutes and extension at 72°C for 1,5 minutes. Resulting PCR products were separated by agarose gel electrophoresis, corresponding bands were extracted and stored at -20°C until further use.

4.2.2 Molecular cloning

Preparative agarose gel electrophoresis

To isolate DNA fragments obtained by PCR or by preceding restriction endonuclease digestion, preparative agarose gel electrophoresis was performed. Depending on the molecular weight of fragments to be separated, ultra-pure agarose was dissolved in SharpE buffer by microwave heating at a concentration of 0.8%- 1.5%. Before gels were poured, 5µl of ethidium bromide (20µg) were added and mixed to enable visualization of bands after electrophoretic separation. Samples were mixed with 6x loading dye and loaded into gel slots. As a reference for nucleic acid separation, 5µl of λ /EcoRI+HindIII marker was added to one slot. Electrophoresis was run at 120V for 45 minutes.

Gel extraction

To recover fragments from agarose gels, respective bands were detected upon low dose UV irradiation (wavelength 366nm) and were isolated with a scalpel.

Subsequently, DNA was extracted from gels using a QIAquick Gel Extraction Kit, following the manufacturer's instructions. To increase sample concentration, elution of sample DNA was divided into two consecutive centrifugation steps, first of which employed 50µl- and second of which employed 30µl of EB buffer, respectively.

DNA ligation of PCR fragments

PCR fragments containing A- overhangs produced by *Taq*- Polymerase, obtained in chapter 2.1 were ligated directly into pCR2.1 vector containing complementary T- overhangs. Ligation was performed according to manufacturer's instructions (TA Cloning Kit). Briefly, 50ng of vector DNA (pCR2.1) was mixed with 200ng of respective PCR fragments (insert) and ligated at 12°C overnight in the presence of 5U of T4 DNA ligase.

Transformation of ligated plasmid DNA by heat shock

To amplify vectors containing the desired inserts, various strains of chemically competent *E.coli* were transformed. After thawing on ice, bacteria were incubated with ligation mixtures for another 20 minutes on ice to let the DNA come into close proximity of the cell surface. To induce uptake of vector DNA, bacterial cell membranes were transiently permeabilized by heat-shocking at 42°C for 30 seconds and put back on ice for 2 minutes. 900µl LB medium were added and the mix was incubated at 37°C for 1 hour under constant shaking. Subsequently, bacterial suspensions were streaked out on 2% LB-agar plates containing 100µg/ml ampicillin and incubated overnight at 37°C. pCR2.1 vector contained an *amp^r* gene. To allow for selective growth of positively transformed bacterial cells, agar was supplemented with 100µg/ml ampicillin. To distinguish vectors carrying the respective inserts from „empty“ backbones, a „blue/white screening“ was performed. Before streaking out the bacteria, plates were pretreated with X-Gal, an artificial substrate of β - galactosidase and with IPTG, an inducer of the lac operon. pCR2.1 carries the lacZ gene, encoding β - galactosidase. This enzyme converts X-Gal into a blue chromophor. Vectors containing the desired inserts exhibit a disrupted lacZ gene, thus rendering

bacterial colonies carrying these vectors incapable of converting X-Gal into its coloured product and thus making colonies appear as white spots on the plate. These are distinguishable from blue colonies carrying „empty“ backbones. After 1 hour of inoculation on the shaker, bacteria were centrifuged at 300g for 1 minute. 800µl of supernatant were discarded, pellet was resuspended, streaked out on agar plates and bacteria were inoculated overnight at 37°C.

Amplification of transformed colonies

4ml LB medium containing 100µg/ml ampicillin were inoculated with single colonies of positively transformed bacterial cells, picked from overnight culture and incubated 12 hours or overnight at 37°C under constant shaking.

Isolation of plasmid DNA from bacterial cultures

To isolate and amplify plasmid DNA from bacterial cultures, plasmid Miniprep was performed following manufacturer's instructions (Quiagen Plasmid Mini Kit). Plasmid DNA was eluted with 80µl 10mM Tris-HCl and stored at -20°C until further use. DNA concentration was determined by spectrophotometric measurement at a peak absorbance wavelength of 260nm.

To produce plasmid stocks, 400ml LB medium were inoculated with bacteria from glycerol stocks containing the desired vector and were amplified overnight under constant shaking at 37°C. Plasmid DNA from these suspensions was then isolated by a Plasmid Maxi Kit according to the manufacturer's instructions, was resuspended in 1ml TE buffer and stored at -20°C.

Restriction digest of isolated plasmids

Before being submitted to sequencing analysis, correctness of the inserts was verified by restriction endonuclease digestion. Resulting fragments were separated by analytical agarose gel electrophoresis. Samples yielding putatively correct band patterns were submitted to sequencing analysis. Standard M13 primers binding within the multiple cloning site of pCR2.1 or primers designed to bind within the respective fragments were used for sequencing analysis.

Production of glycerol stocks

To produce stocks of bacteria carrying desired plasmids, 2ml of the overnight cultures were centrifuged for 1 minute at 850g, supernatant was discarded, pellets were resuspended in LB medium containing 15% Glycerol and were stored at -80°C.

4.2.3 Generation of mutant virus variants by site-directed mutagenesis

To introduce site-specific mutations into viral genomes to produce variants differing from wild-type in single- or combined base substitutions, site-directed mutagenesis was applied in two distinct manners.

Chimeric PCR

This method employed two consecutive PCR steps. The first step included two parallel amplification reactions, introducing the wanted base alterations. To accomplish this, a set of complementary inward primers, containing the respective alterations and binding to the sequences to be mutated had been designed (see materials). Additionally, pairs of 5'- and 3'- outward primers had been designed (see materials). To set up the first PCR step, two separate reactions were prepared, containing 100nmol of either 5'- forward- and 3'- inward- mutant primers or 5'- inward- mutant- and 3'- outward- primers each (see materials). 10ng of expression vector pDB-MVMp per reaction served as DNA template and 5µl of DMSO were added to a final reaction volume of 50µl. Reactions were carried out according to the manufacturer's instructions (Clontech Advantage-HF 2 PCR Kit), employing 30 repetitive cycles of denaturation for 1 minute at 95°C, annealing for 1 minute at 61°C and extension for 2.5 at 68°C, creating one „left“ and one „right“ fragment for each mutation to be introduced. PCR products were separated by running through a 0.8% agarose gel and respective fragments were isolated and extracted. For the second PCR step, 10ng of respective „left“ and „right“ fragments each served as templates and were amplified by adding respective 5'- forward- and 3'- reverse outward primers, again using Clontech Advantage-HF 2 PCR Kit. Same reaction conditions as in the first PCR step were employed, yielding the desired

full-length mutant fragments. These were again separated by running through a 0.8% agarose gel, isolated, extracted and- if not used immediately- stored at -20°C. To amplify fragments, they were inserted into vector pCR2.1, competent SurE bacteria were transformed with ligated plasmids, which, after amplification were isolated.

Cloning of mutated fragments into pDB-MVMp expression vector

To transfer fragments containing desired mutations from vector pCR2.1 into expression vector pDB containing the MVMp genome, plasmids were digested by specific pairs of restriction endonucleases. To achieve this, 1µg of DNA was mixed with 1U of restriction enzymes each and incubated for 1.5 hours at 37°C. To increase substrate specificity, 2µl of BSA were added to the reaction. Intramolecular religation of backbone DNA was prevented through 5'-dephosphorylation by alkaline phosphatase. To achieve this, respective samples were incubated with 1U of enzyme for 30 minutes at 37°C, followed by thermal inactivation at 60°C for 10 minutes. Another 1U of enzyme was added and the procedure was repeated once. Samples were separated by agarose gel electrophoresis and respective DNA bands were extracted. Mutated, pCR2.1-derived fragments served as inserts, being ligated into viral genome-containing expression vector pDB, which served as vector backbone. Ligation, amplification and isolation of resulting plasmids was performed as shown in chapter 2.2.

Single- step site-directed mutagenesis

To insert point mutations alternatively to chimeric PCR, QuickChange Site-Directed Mutagenesis Kit was used, consisting of a single PCR step. For this method, the same mutant primers, complementary to opposite strands were used as in 2.3.1 and 10ng of expression vector pDB-MVMp per 50µl- reaction served as DNA template. All steps were carried out following the manufacturer's instructions. In a temperature cycling reaction consisting of 16 cycles of 30 seconds of denaturation at 95°C, of 1 minute of annealing at 61°C and of an 8 minutes' extension time at 68°C, primers were incorporated into newly

synthesized DNA, generating whole mutant plasmids. Subsequently, samples were digested with 1U of *Dpn I* endonuclease for 1h at 37°C to degrade methylated- and hemimethylated parental plasmid DNA template. To amplify newly generated mutant plasmids, XL-1 Blue bacteria were transformed with 5µl of respective products. Transformation was carried out as described in chapter 2.2.4. 900µl of SOC medium were added after heatshock. As plasmids, successfully taken up by bacteria and enabling their growth through expression of the Amp^r gene automatically contained the sought-after PCR fragment, no prior treatment of agar plates with IPTG and XGal for blue/white screening was necessary. After successful transformation, colonies were processed as shown in 2.2 and isolated plasmid DNA was stored at -20°C until further use.

4.3 Production of infectious particles

To produce infectious virus particles from expression vectors carrying the viral genomes, 293T cells were transfected with these vectors by the means of CaCl₂- transfection. Cells were seeded in twenty to forty 15cm petri dishes at a density of 5x10⁶ cells per dish and were incubated at 37°C, 5% CO₂ for 24 hours. The next day, transfectant was prepared, mixing 112.5µl of 2.5M CaCl₂ with 1125µl H₂O and 15µg of respective plasmid DNA per dish. This solution was transferred dropwise into 1125µl of 2x HBSS per dish and incubated for 20 minutes at room temperature to allow calciumphosphate and DNA to form complexes and precipitate. Per dish, 2.25ml of the precipitate was then added dropwise to the cells. Dishes were shaken gently to homogeneously distribute DNA complexes for efficient endocytosis. Cells were incubated at 37°C for 7 days. To harvest newly generated virus, cells were detached by scraping with a cell lifter into the medium. Dishes were washed once with 10ml PBS and the suspension was centrifuged at 1200g for 5 minutes. Supernatant was taken off and pellets were resuspended in VTE buffer (0.5ml per dish). To extract virions from cells, plasma membranes were disrupted by 5 consecutive cycles of freezing at -80°C for 45 minutes and thawing at 37°C for 15 minutes. Subsequently, cellular debris was briefly pelleted (1200g, 5min), the

supernatant containing released virus was transferred into a fresh falcon tube and stored at -80°C until further use.

4.4 Amplification of viral stocks

To produce new virus from existing, infectious particle- containing stocks, NBK cells were seeded in twenty to forty 15cm petri dishes at a density of 5×10^6 cells per dish and incubated at 37°C for 24 hours. The next day, 5ml virus suspension per dish was prepared by mixing unsupplemented DMEM with viral stock at an MOI of 1. The medium was removed, cells were overlaid with virus suspension and were incubated for 1 hour at 37°C, 5% CO₂ under regular shaking to guarantee efficient infection. 15ml of DMEM⁺ per dish were added and cells were incubated at 37°C, 5% CO₂ for 7 days. As described in 2.4, cells were detached, disrupted by consecutive freeze-thawing to release intracellular virions, suspension was centrifuged to remove cellular debris and the resulting viral stock was stored at -80°C.

4.5 Purification of viral stocks by CsCl- gradient ultracentrifugation

To separate viral particles from cellular debris in suspensions obtained in virus production, particles were purified by CsCl- density gradient ultracentrifugation.

To prepare the density gradient, 5ml CsCl (1.4g/cm^3 in VTE buffer) were pipetted into a centrifuge tube and carefully overlaid with 1ml of 1M saccharose (in VTE buffer). 5ml of respective virus suspensions were slowly pipetted onto the saccharose. Tubes were centrifuged at 241.000g for 24 hours at 12°C. The next day, 200µl fractions of the gradient (lower phase) were decanted into 1.5ml tubes under sterile. Suspension densities were measured by the means of optical refractometry. Fractions showing a density between 1.3702- and 1.3758g/cm^3 were considered to contain viral particles and were pooled. Empty capsids were pooled from fractions within densities ranging from 1.3683- to 1.3692g/cm^3 . CsCl was removed from purified virus suspensions by dialysis in selectively permeable molecular porous membranes in 2l of VTE buffer

overnight at 12°C under gentle agitation. The next days, virus suspensions were transferred into fresh tubes under sterile conditions and stored at 4°C.

4.6 Determination of viral titers

To determine viral titers in stock solutions, several techniques were applied in order to make possible an administration of different viruses at comparable multiplicities of infection (MOIs) in experiments.

Plaque assay

To determine concentrations of fully infectious particles in viral stocks, plaque assay was performed. NBK cells were seeded in 6cm petri dishes at a density of 5×10^5 cells per dish and were incubated 24 hours, 37°C, 5% CO₂. The next day, serial dilutions with concentrations ranging from 10^{-5} to 10^{-10} of original viral stocks were produced with DMEM without FCS. Medium was removed, cells were overlaid with 400µl of respective virus suspensions and incubated for 1 hour at 37°C and shaken gently every 10 minutes. Cells were overlaid with 8ml semisolid medium composed of 6.2 parts of 2x Minimum Essential Medium (2xMEM) with 3.8 parts of 2% agar. Virus suspension was sucked off and cells were covered with 8ml overlaying solution. Cells were incubated for 6 days at 37°C. To stain cells, a solution consisting of 15 parts of 2xPBS, 2 parts of Neutralred (0.33%) and 15 parts of 2% agar were mixed and added at a volume of 3ml per dish. Cells were incubated for another 24 hours at 37°C, 5% CO₂. Agar was removed from the dishes and cells were fixed with 4% formaldehyde for 15 minutes. To obtain viral titers, infectious centres defined as plaques were counted, multiplied by 2.5 and by the respective dilution factor, to obtain the amount of virions in the stock solutions, defined as plaque- forming units per ml (PFU/ml).

Southern Blot

To determine viral titers of unknown stocks, represented by their total amounts of viral genomes present in the solutions, they were compared to stocks of

known concentrations. To achieve this, serial dilutions of the stock solutions were produced and made subject to proteolytic digest by proteinase K overnight at 46°C. To achieve this, respective volumes of virus suspensions were filled up with 1µl proteinase K and proteinase K- buffer to a total volume of 50µl. The next day, samples were homogenized using needle and syringe. Subsequently, relative amounts of viral DNA present in the samples were determined by agarose gel electrophoresis and southern blot analysis. Resulting signal intensities were compared semiquantitatively to those of known titers and multiplied or divided by the respective factors to obtain the concentrations of the analyzed stocks, considered as viral particles per ml.

Genomic titration by quantitative real-time PCR

To obtain a quantitative measurement of the amounts of total viral genomes present in stock solutions regardless of the existence of fully infectious particles, quantitative real-time PCR was performed. This was done to characterize the capability of viral genomes to produce infectious particles in host cells during transfection experiments and was assessed by comparing ratios between amounts of viral genomes and plaque-forming units, determined by plaque assay.

In order to prepare samples for PCR, non-viral- or unpackaged viral DNA present in the stocks was degraded. 50µl of respective stocks were treated with benzonase for 30 minutes at 37°C in the presence of 5µM MgCl₂. Viral capsids were subsequently denatured by taking 10µl of the digested suspension, adding 3 volumes of 1M NaOH and incubating the mix at 56°C for another 30 minutes. Subsequently, the suspension was neutralized by adding 40mM HCl to a total of 1ml. qRT-PCR was performed according to the manufacturer's instructions. Briefly, 6.7µl of sample DNA was added to a total amount of 20µl per reaction in a 96-well plate, containing 1x Taqman Master Mix (10µl), TaqMan probe, forward- and reverse primers at an amount of 6.5nmol each (see materials). Plates were sealed with adhesive transparent cover and centrifuged at 2600g for 5 minutes. PCR program was run at a profile of an initial cycle at 50°C for 2 minutes and at 95°C for 10 minutes, followed by 40 cycles, each consisting of

15 seconds at 95°C and of 1 minute at 60°C. Increase of fluorescence intensity, obtained by an increased activation of fluorophore by the 5'-3' exonuclease activity of Taq Polymerase is proportional to the incorporation of Taqman probe and thus to the rate of amplification of newly synthesized DNA from the template. Upon completion of the reaction, the initial amount of present template DNA was determined by comparing the detected gain of fluorescence to that of a known standard. To determine the concentration of viral genomes in the stock solution, this amount was multiplied by a factor of 135000 accounting for the serial steps of dilution done to prepare the PCR reaction.

4.7 Determination of protein expression levels by sodium-dodecylsulfate Polyacrylamide gelelectrophoresis (SDS-PAGE) and Western Blot analysis

To analyze the expression levels of specific viral and cellular proteins, SDS-PAGE and Western Blot analysis were performed. Cells were seeded in 15cm petri dishes at a density of 5×10^6 cells per dish and were incubated for 24 hours. Viral dilutions were prepared in unsupplemented DMEM, media was removed, cells were overlaid with 5ml of virus suspensions per dish. After 2 hours of incubation, 15ml of DMEM⁺ were added to each dish. Cells were detached by scraping in- and washing with 10ml of PBS. For Western Blot analysis, cells were pelleted at 1200g for 5 minutes and the supernatant was removed. Pellets were resuspended in 300µl of CoIP buffer and put on ice for 30 minutes to disrupt cells and centrifuged at 20.000g for 10 minutes to obtain whole cell lysates. Protein- containing supernatants were transferred into new tubes, supplemented with 100µl of Lämmli buffer and- if not used immediately- frozen at -80°C. For SDS-PAGE, 10%- and 12% polyacrylamide gels, respectively, were prepared according to molecular weights of sought-after proteins. In order to make migration velocity of proteins depend solely on their respective molecular weights, 0.2% SDS was added to the gels. Polymerization of acrylamide was triggered by adding ammonium persulfate (APS) and tetramethylethylenediamine (Temed) were added immediately before pouring. To break potential quaternary structures of peptides, samples were put to 95°C

for 7 minutes in the presence of 2-mercaptoethanol before being loaded onto the gels at a volume of 20µl per slot. 5µl of prestained Spectra BR Protein Ladder was used to serve as a reference of protein separation during electrophoresis and as a verification of successful subsequent Western transfer. SDS-PAGE was carried out at 120V for 3 hours. Electrophoresis chambers were disassembled and gels were transferred into a semi-dry blotting chamber. Blotting sandwich was assembled according to the manufacturer's instructions and proteins were blotted onto a nitrocellulose membrane at 25V for 1.5 hours. To block unspecific epitopes, membranes were incubated in 10% dry milk (in PBS) for 1 hour under constant shaking. In case phospho-peptides were to be detected, membranes were blocked in 2% casein (in 10% BSA in Rinse buffer). Primary antibody solutions were prepared at adequate dilutions in 10% dry milk or 2% casein, respectively and membranes were incubated overnight at 4°C under gentle agitation. The next day, membranes were washed 3x20 minutes with PBS. Horseradish peroxidase- (HRP-) coupled secondary antibodies were added, membranes were incubated for 1 hour under constant shaking and washed again 3x20 minutes. Chemiluminescent HRP- substrate was added for 1 minute and membranes were developed after adequate exposure times.

4.8 Nuclear- cytoplasmic fractionation of western blot samples

To analyze, subcellular distribution and nuclear accumulation of specific target proteins by SDS-PAGE and Western Blot analysis, nuclear- cytoplasmic fractionation of treated cells was performed following the manufacturer's instructions (NE-PER Nuclear and Cytoplasmic Extraction Reagents kit). Briefly, cell membranes were disrupted and samples were centrifuged. The supernatant, containing cytoplasmic contents was collected. The pellet, consisting of intact nuclei was then lysed to yield the nuclear contents in the supernatant after an additional centrifugation step. Cytoplasmic- and nuclear extracts were stored at -20°C until being made subject to SDS-PAGE and Western blot analysis as described in 2.8.

4.9 Biochemical fractionation

Cells were seeded at a density of 5×10^6 cells per 15cm petri dish (two dishes per sample), incubated for 24h at 37°C, 5% CO₂ and infected –or not- with MVMp or MVMcr. 2 hours p.i., medium was changed. At indicated time points (see results), cells were detached mechanically, pelleted at 500g for 5min, resuspended in 300µl Hypobuffer and homogenized mechanically with a douncer and needle and syringe. Homogenate was centrifuged at 800g for 5min at 4°C (A). Resulting Pellet was resuspended in 300µl Hypobuffer with 1% Triton and protease inhibitor cocktail (Hypobuffer⁺), incubated 30min on ice and centrifuged at 150000g for 1h at 4°C. The supernatant yielded nuclear membrane- associated proteins (nM), the resulting pellet was resuspended in 300µl Hypobuffer⁺ and yielded nuclear scaffold- associated proteins (insoluble scaffold, iS). The supernatant obtained in A was centrifuged at 150000g for 1h at 4°C. Resulting supernatant yielded the cytoplasmic protein fraction (C). The pellet was resuspended in 300µl Hypobuffer⁺, incubated on ice for 30min and centrifuged at 150000g for 1h at 4°C. Resulting supernatant yielded cytoplasmic scaffold- associated proteins (soluble scaffold, sS), pellets were resuspended in 300µl Hypobuffer⁺ and yielded post- nuclear membrane associated proteins (pM). Samples were kept at -80°C until used for Western Blot analysis.

4.10 Semi-quantitative determination of gene expression on transcriptional level by RNA isolation and reverse-transcription PCR

To complement data obtained by Western blot analysis, expression of specific viral- and cellular genes was analyzed on a transcriptional level. Total RNAs were extracted from treated cells using an RNeasy mini kit according to the manufacturer's instructions and were quantified spectrophotometrically. 1µg of total RNA per sample was then used as template for reverse transcription, using a Quantitect Reverse Transcription kit, following the manufacturer's protocol, which included initial degradation of viral- and cellular genomic DNA. 10% of the resulting cDNA samples served as PCR templates and were amplified by

Taq Polymerase using sets of primers, each specific for their respective cDNA fragments. PCR products were separated by electrophoresis through 2% agarose gels.

4.11 Determination of viral DNA replication by southern blot analysis

To analyze viral DNA replication in target cells, southern blot analysis was performed. Cells were seeded in 6cm petri dishes at a density of 5×10^5 cells per dish. After 24 hours, medium was removed, cells were infected with respective virus dilutions and incubated for 1 hour under gentle shaking every 10 minutes. Suspension was sucked off and 4ml DMEM⁺ were added per dish. At given time points, cells were detached by scraping with a cell lifter without taking off the medium and centrifuged at 1200g for 5 minutes. The supernatant was discarded, the pellet was resuspended in 100 μ l of TE buffer and stored at -20°C until further use. To make viral DNA accessible to southern blot analysis, 100 μ l of proteinase K- buffer and 40 μ g of proteinase K were added to the samples and digested overnight at 46°C. The next day, samples were homogenized using needle and syringe. 5x loading dye was added to the samples, the mix was loaded onto a 0.8% agarose gel and DNA was separated at 125V for 45 minutes. After electrophoresis, gels were gently shaken in 0.25M HCl for 15 minutes to partially depurinate DNA. Subsequently, DNA was denatured by 0.5M NaOH for 30 minutes to improve southern transfer efficiency. This was followed by rinsing the gels for 40 minutes with neutralization buffer. Then, DNA was blotted onto a nylon membrane overnight by neutral capillary action transfer employing 20x SSC. The next day, the DNA was cross-linked and permanently attached to the membrane by UV- irradiation. To block unspecific binding sites, the membrane was prehybridized with 50ml of hybridization buffer for 4 hours at 65°C. Meanwhile, a ³²P-NTP- labeled probe, complementary to the NS1- encoding region (nucleotides 385-1885) of the viral genome was prepared. First, 25 μ l water was mixed with 5 μ l of primer solution and 1 μ g of template. DNA was denatured at 95°C for 5 minutes. To produce radio-labeled fragments, 10 μ l of labeling buffer, 1U of Klenow Polymerase and 5 μ l of the ³²P-

dNTP mix (25 μ Ci) were added and incubated at 37°C for 45 minutes. To remove non- incorporated radioactive nucleotides, probes were mixed with 150 μ l of TE buffer and centrifuged through a sepharose coloumn at 850g for 5 minutes. The flow-through, containing ³²P- labeled fragments was denatured at 95°C for 5 minutes. 50ml of fresh hybridization buffer was mixed with the probe and added to the membranes, incubated overnight at 65°C. The next day, membranes were washed with 100ml of washing solutions 1 and -2 twice for 20 minutes each. To detect hybridized DNA, X-ray films were exposed to membranes at -80°C.

4.12 Immunoflouescence

To visualize specific proteins by the means of indirect immunofluorescent labeling, cells were seeded on spotslides at a density of 5x10³ cells per spot and were incubated for 24 hours. Depending on the experiment, cells were either first siRNA- transfected for knock-down experiments, synchronized by both isoleucine deprivation and aphidicolin- induced cell cylce arrest or were infected directly. At given timepoints, cells were fixed with 3% para-formaldehyde (30 minutes for A9, 40 minutes for MEFs, respectively), permeabilized for 10 minutes with 0.2% Triton-X100 and washed excessively with PBS. Cells were blocked for 1h with PBS+ 20% FCS. Subsequently, proteins of interest were labeled for 1 hour at room temperature with specific primary antibodies, diluted in PBS+ 2% FCS . Cells were again washed excessively with PBS and incubated with fluorophor-conjugated secondary antibodies, diluted in PBS+ 2% FCS for another hour in the dark. To stain chromatin for visualization of nuclei, 300nM DAPI was added to secondary antibody dilutions at a final concentration of 300nM. Actin was stained by tetramethylrhodamine(TRITC-)-phalloidin, which was also added to secondary antibody solutions for respective samples. Cells were washed again with PBS, covered with polyvinyl alcohol (elvanol) and sealed with a cover slip. Spot slides were put to 4°C in the dark to allow the elvanol to solidify before fluorescence microscopy. To check for the mere presence of proteins of interest,

epifluorescence microscopy was used. To analyze localization or colocalization of target proteins, confocal laser scanning microscopy was employed.

4.13 Cell cycle arrest by double synchronisation

To efficiently compare protein levels in fluorescence microscopy, cells were arrested by preventing their transition from G1- to S-phase. This was accomplished by double synchronisation, first depriving cells selectively of isoleucine, followed by inhibition of DNA synthesis by aphidicolin. Cells were seeded as shown in chapter 2.12. After 24h hours, medium was sucked off and cells were overlaid with unsupplemented DMEM without isoleucine. The lack of this essential amino acid results in an impaired ability for *de novo* protein synthesis for normal metabolism and causes cells to enter the quiescent state of interphase. Passage through one entire cell division cycle is considered to take approximately 24 hours. As for the nature of MEFs being primary cells, the time necessary for completion of one such cycle was presumed to take considerably longer. Thus, to ensure the great majority of cells would have completed mitosis and entered G0-phase, they were incubated in isoleucine-deprived DMEM for 44h. After that, media was sucked off and cells were infected at given MOIs with DMEM⁺, containing aphidicolin at a final concentration of 100µg/ml. As a selective inhibitor of DNA polymerase α , aphidicolin prevents the *de novo* synthesis of DNA for replication of the genome during S-phase. Thus, cells re-entering G1-phase after withdrawal of selective media were arrested at the G1/S border. Cells were released from G1/S- arrest 18 hours post infection by sucking off media, extensive washing with PBS and adding 70µl of DMEM⁺ to each spot. At given timepoints, cells were fixed and stained as indicated in 2.12.

5. Results

5.1 Generation of MVM virus stocks propagating in freshly prepared mouse embryonic fibroblast cells (MEF)

MVMp is a derivative of the original MVM isolate by Crawford (1968), adapted to A9 cells by serial plaque purification, picking large plaques to obtain isolates with best spreading capacity. This A9 isolate, MVM_T, was, a decade later, genetically characterized and an infectious clone DNA was prepared (Mechlinsky, 1983). During this process, MVMp lost its capacity to grow in MEFs, suggesting changes during the isolation process in A9 (Grekova et al., 2010). From the legacy of Günter Siegl, we obtained two old MVM isolates, dated back to 1968 and 1969, respectively. These isolates were used to infect freshly produced MEFs at a low multiplicity of infection (MOI) in order to amplify these viruses and to obtain virus stocks. In parallel, an MVMp stock was prepared in NBK cells for comparison. Virus was harvested upon occurrence of severe cytopathic effects, extracted by repetitive freeze- thawing and purified by CsCl- density gradient centrifugation. Only the 1968-isolate was able to kill MEFs. Thus, the characterization of only this sample obtained from G. Siegl was continued.

To analyze the stocks for their virus content, viral DNA was measured by southern blot and the infectivity was assessed by plaque assay in NBK cells in comparison to MVMp stocks. To quantify the amount of viral genomes present in viral stock solutions, titrations were performed and the amount of ssDNA, packaged into virus capsids was measured by southern blot analysis (see figure 7). Respective signal intensities of ssDNA were compared and multiplied by the corresponding dilution factor to equalize relative amounts of viral genomes in the stock solutions. Thus, the ssDNA band intensity, detected for MVMp at a dilution of 1:50 equalled that of MVM_{CR}, diluted to a concentration of 1:2.5. This results in an approximately 20-fold higher concentration of ssDNA in the MVMp

stock solution compared to that of the 1968-isolate. Interestingly, additional bands of higher molecular weight were detected in the 1968 stock. These bands migrating at 5 kb could be re-annealed positive and negative strand viral genomes packaged separately into progeny capsids. However, whether this assumption is indeed true will have to be shown using positive- and negative-strand specific probes, respectively.

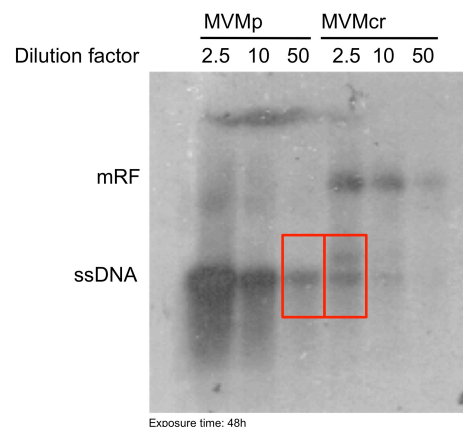


Figure 7. Titration of ssDNA in viral stocks. Serial dilutions of stock solutions were produced, DNA was isolated, separated on an agarose gel and analyzed by southern blot technique. Similar signal intensities of ssDNA- bands were compared between viruses in order to complement data, obtained from plaque assay. mRF= monomeric replicative form;

To determine infectious units of these viruses, plaque assays were performed in NBK-cells, a cell line used for titration of many rodent parvoviruses, including H-1PV, MVMp and MVMi. Therefore, this cell line was thought to be equally permissive for MVMp and the MEF 1968-isolate. NBK cells were infected with serial dilutions of the '68-isolate and of MVMp- stocks. Through multiple rounds of lytic infection, productive infection of single NBKs yielded the generation of lysis plaques, which appeared as unstained (cell- free) area after Neutralred staining (see figure 8). Titers were calculated by multiplying observed plaque numbers with respective dilution factors of the virus stocks.

For the '68-isolate, 3 plaques were counted in the dish infected with a stock-dilution factor of 10^{-7} , equalling 3 infectious units in the volume cells were infected with (200µl). Multiplication with the corresponding factor ($2,5 \times 10^7$) yielded a titer of 7.5×10^7 PFU/ml for MVM_{CR}. For MVMp, 50 plaques were

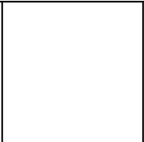

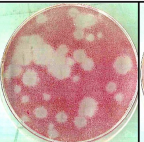
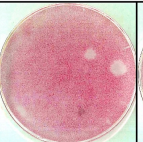
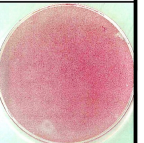
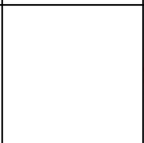




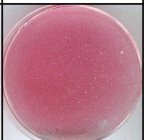

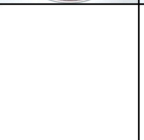


Viral dilution factor:		10 ⁻⁵	10 ⁻⁶	10 ⁻⁷	10 ⁻⁸
MVMcr					
MVMp					
uninf. control					

Figure 8. Titration of infectious particles in viral stocks. NBK cells were infected with serial dilutions of viral stocks and overlaid with semisolid media. 5d p.i., cells were stained, fixed and stock concentrations were determined from numbers of formed plaques in respective dilutions. Note that, despite showing a lower titer, MVM_{CR} resulted in markedly larger plaque sizes, as compared to MVMp.

counted in the dish infected with the same dilution factor, which resulted in a stock concentration of 1.25×10^9 PFU/ml. This shows a comparable (17-fold) ratio to that observed in the southern blot monitoring ssDNA (see above), which indicated an approximately 20- fold higher stock concentration of infectious MVMp particles, as compared to MEF-produced 1968 virus. Taken together, these results show that the 1968-isolate obviously has the ability to productively infect MEFs, as apparent from the increase of progeny particle determined by ssDNA detection in potential CsCl-gradient purified virus stocks and the production of lysis plaques after infection of NBK cells.

It should be mentioned at this place that production of a virus stock of the 1968 isolate in NBK cells produced significantly increased amounts of infectious virions. This is certainly due to the homogeneity and the significantly increased growth rate of this permissive cell population as compared to the heterogeneous MEFs. However, it is currently unclear, whether the viruses produced under these conditions retained growth capacity in MEFs. Therefore, experiments with this virus preparation were not continued.

5.2 Viral DNA amplification in A9 fibroblast cell line and freshly isolated MEFs

To determine viral DNA replication efficiency of MVMp and the 1968-isolate, A9 cells and MEFs were infected at different MOI with the previously examined virus stocks and harvested at indicated times post infection. The accumulation of viral replication intermediates (monomer (mRF) and dimer (dRF) replicative forms) and single-stranded progeny virion DNA (ssDNA) was then measured by southern blotting (see figure 9).

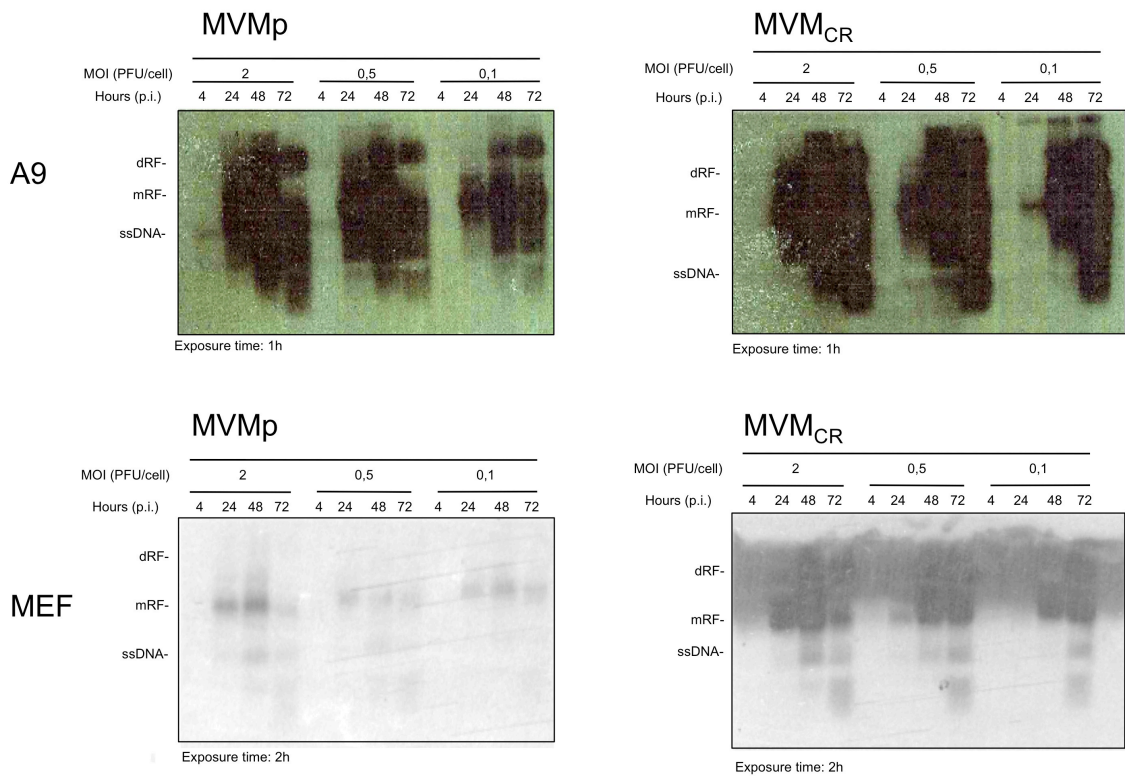


Figure 9. Replication efficiency of MVM_{CR} and MVMp. MEFs and A9 cells were infected with the indicated MOIs. Medium was changed 2h p.i. and cells were harvested after given time- points. Cells were lyzed, DNA was extracted and viral replication intermediates were detected by southern blot analysis as described in methods.

Although the viral DNA amplification of the 1968-isolate appeared somewhat slower than the prototype strain MVMp, infection of A9 cells with either virus led to a strong amplification of viral DNA including single-stranded genomes at all MOI. Starting at 24h p.i. in all cases the amounts significantly increased until

the end point of the experiment. In contrast, infection of MEFs produced a different picture. While MVMp-induced vDNA amplification was very moderate at a multiplicity of 2, it became almost unapparent at higher dilutions. This was different after infection with the 1968-isolate. Infection of MEFs with this virus produced increasing amounts of viral DNA-intermediates and ssDNA at all MOI applied, suggesting the competence for viral DNA amplification and progeny virion production. This is in agreement with previous reports of Crawford and Tattersall (Crawford, 1966), demonstrating the competence of MVM to replicate and propagate in MEFs. I therefore suggest that the 1968-isolate from G. Siegl is very similar to the original virus described by Crawford (1966) and will therefore be considered MVM_{CR}.

5.3 Viral protein synthesis

Viral DNA amplification and generation of progeny virions depends on the production of viral proteins. Therefore, I assessed expression of the non-structural proteins NS1, NS2 by immunofluorescence microscopy and measured the accumulation of these proteins together with the capsid proteins VP1, VP2 by western blotting after infection of both A9 and MEFs with the two strains MVMp and MVM_{CR}. Cells grown on spot-slides were infected or not with the respective virus strain, fixed at indicated times p.i. and stained for the presence of NS1 and NS2, respectively. As shown in figure 14, Infection of A9 cells with MVMp, produced a large proportion of NS1 positive cells already 24h p.i., while MVM_{CR} infection was only barely detectable. This is in contrast to infection of MEFs, where MVM_{CR} seemed to infect a larger proportion of the cell population than MVMp. Interestingly, after this initial production of NS1-positive cells, the detection of NS1-positive cells ceased 48 h p.i. In agreement with the DNA replication data this suggests an abortive infection leading to the elimination of primary infected cells. This is not the case for MVM_{CR}-infected MEFs, which (although to a very reduced number) showed a significant amount of NS1 positive cells at 48 h p.i. with increased staining of the viral protein in the

nucleus. This indicates persistence and/or spread through the culture of this virus. It should be mentioned that MVM_{CR}-infected MEFs appeared to exhibit an increased cytoplasmic staining of NS1 24 h p.i. as compared to MVMp-infected MEFs or infected A9 cells. However, this observation needs to be confirmed by subcellular fractionations of cell extracts (see figure 10).

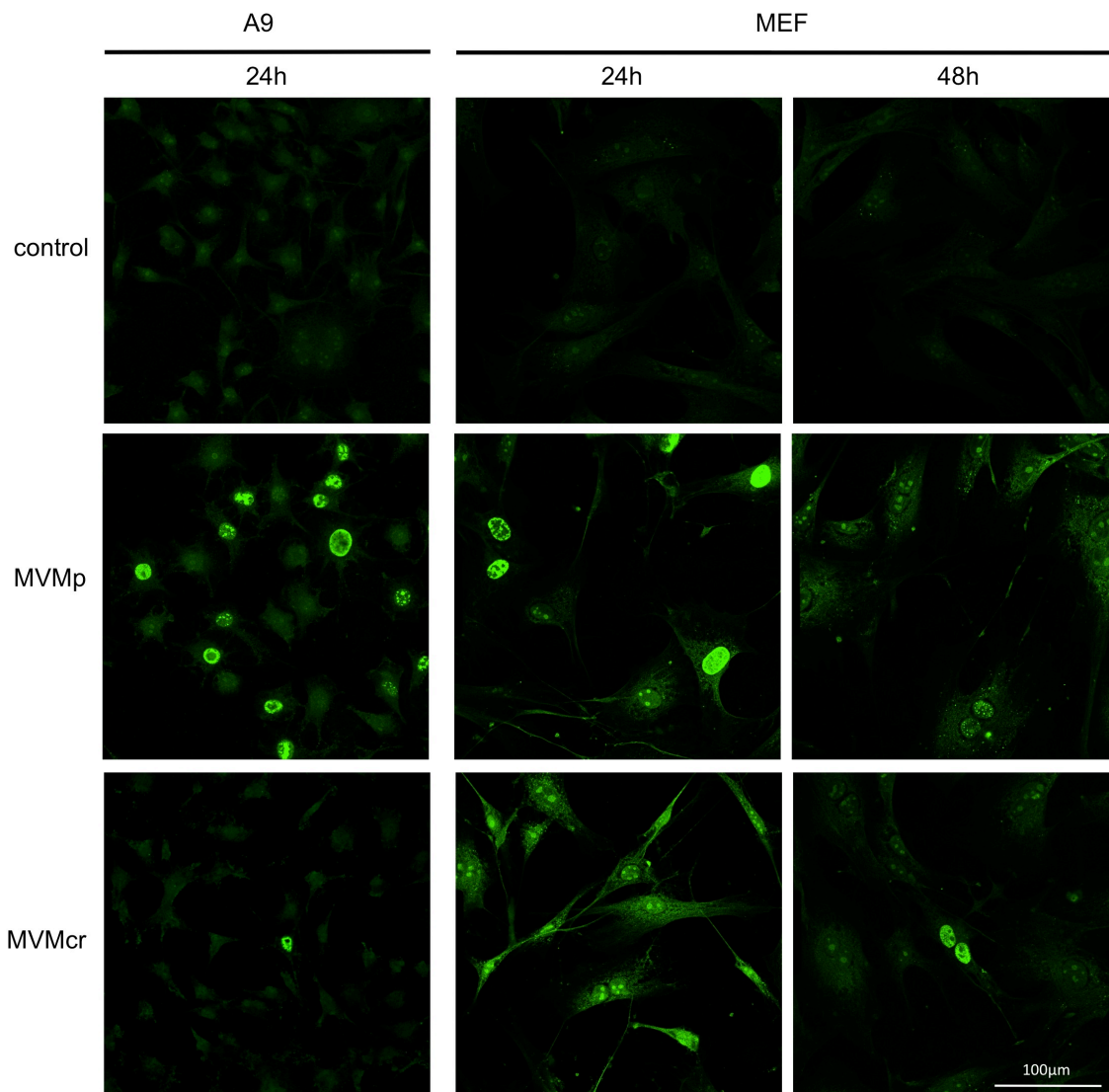


Figure 10. Analysis of NS1 expression by immunofluorescence microscopy. MEFs and A9 cells were seeded on spot slides, infected at an MOI of 10 PFU/cell and fixed after given time points. NS1 protein was detected using an anti- C- terminal NS1 primary antibody and a secondary Alexa Fluor 488 donkey anti- rabbit IgG antibody.

To further examine the intracellular distribution of NS1 and NS2 in a significant proportion of infected MEFs, synchronization experiments were performed. MEFs were arrested at the G₁/S- border by double synchronization. Cells were forced to enter G₀ by isoleucine deprivation and, following subsequent infection with either virus in parallel with an arrest at the G₁/S-border by aphidicolin, a strong inhibitor of DNA polymerases. Arrested, infected cells were released into S- phase and fixed 10h post- release (34h p.i.), NS1 could be detected in both cytoplasm and nucleus upon infection with either virus (see figure 11). Formation of subnuclear foci, however, seemed to be stronger in cells infected with MVMp. NS2 also exhibited both cytoplasmic- and nuclear localization. Major differences could neither be detected in terms of signal intensity- nor concerning distribution of the protein. Yet, subnuclear foci appeared to be larger compared to those observed for NS1.

To further evaluate the accumulation of viral proteins, infected and for control non-infected cells were harvested at indicated times p.i. and analyzed for the presence of viral proteins by western blotting (see figure 12A). In A9 cells, infection with either virus led to a steadily increasing amount of NS1 protein, which, upon infection with MVMp could first be observed 24h p.i., whereas in MVM_{CR}- infected cells it was first detectable 48h p.i.. In MVMp-infected MEFs, NS1 showed an initial increase, culminating 24h p.i. and decreasing thereafter. Upon infection of those cells with MVM_{CR}, production of detectable amounts of NS1-protein started at 24 h p.i. at a much lower level as for MVMp, however, in contrast to MVMp- infected MEFs, increased slightly over time. This is in agreement with fluorescent data, (a) presenting very low infection rate of MVM_{CR} in A9 cells 24 h p.i., (b) an abortive infection of MVMp in MEFs after at 48 h p.i., and (c) on-going infection of MVM_{CR} at 48 h p.i. at least in a small proportion of MEFs with accumulated amounts of NS1. The NS2-protein of both viruses became detectable at similar time-points as the respective NS1, however, unlike this very stable protein, the small non-structural proteins NS2 decreased significantly at the end of infection 72 h p.i. In MEFs the amount of NS2 proteins produced by either virus was under the detection limit. Viral

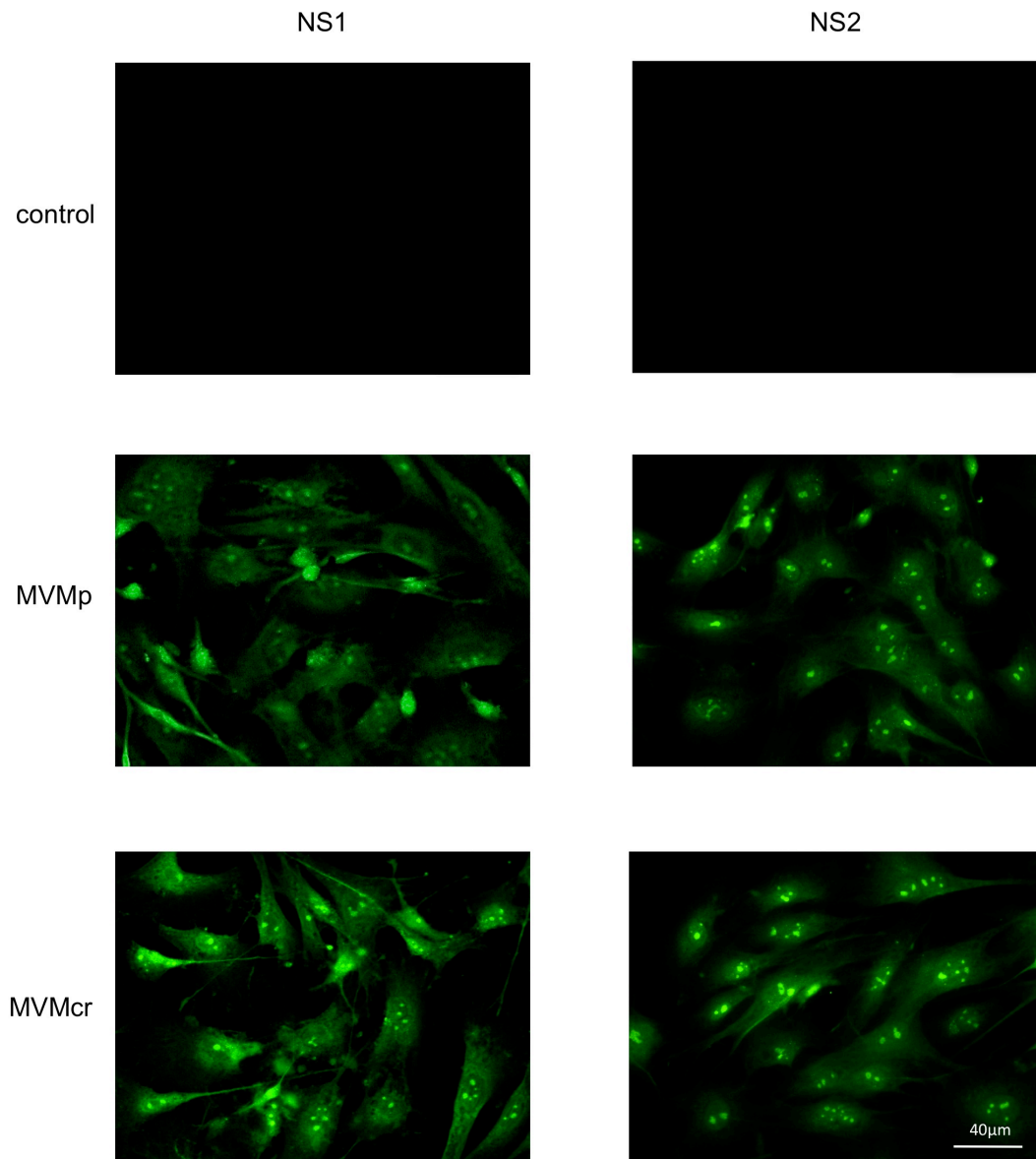


Figure 11. Analysis of viral non- structural proteins in synchronized MEFs by immunofluorescence microscopy. Preceding infection, cells were synchronized at G₀- phase by selective isoleucin deprivation. Subsequently, cells were infected at an MOI of 10 PFU/cell and released into G₁- phase in the presence of aphidicolin, in order to arrest cells at the G₁/S- border. 18h p.i., cells were released into S- phase and fixed 24h p.i.. NS1- and NS2 proteins were detected using anti- C- terminal NS1/ anti- NS2p primary antibodies and a secondary Alexa Fluor 488 donkey anti- rabbit IgG antibody. Nuclei were stained by 4',6-diamidino-2- phenylindole (DAPI).

structural proteins of both viruses followed the presence of NS1 in A9 cells. VP1 and VP2 were first detected 24h p.i. and increased in a steady and time- dependent manner. Consistently to the findings for the non- structural proteins,

in MVMP- infected MEFs, VP- protein levels culminated 24h p.i. and decreased thereafter. In MVM_{CR} infection, these proteins showed delayed accumulation, however- unlike for MVMP- they were not decreasing over time but showing virtually constant steady- state levels.

On a transcriptional level, NS1 mRNA was found to be expressed already at an early stage of infection in A9 cells with either virus and also to increase over the

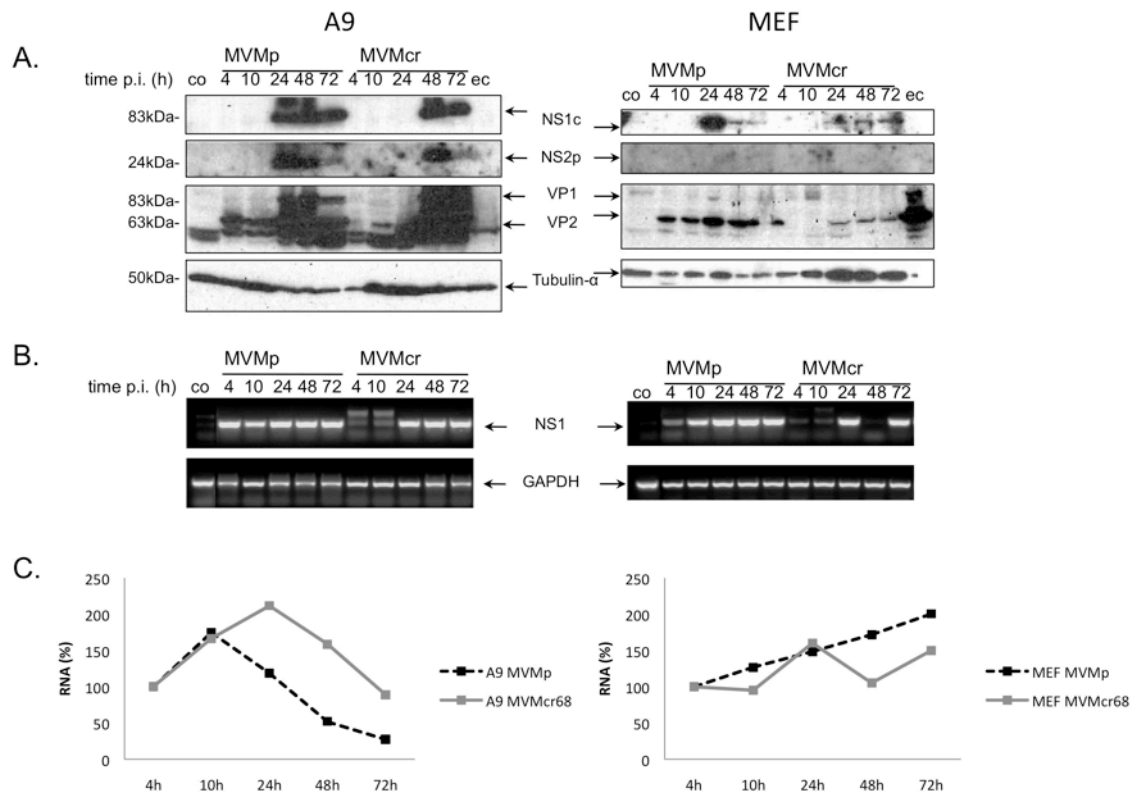


Figure 12. Kinetics of MVM_{CR} and MVMP viral protein expression in MEFs and A9 cells. Cells were infected at an MOI of 10 PFU/cell. 2h p.i., medium was changed and cells were incubated for the indicated times post-infection. (A) Proteins were extracted from lysed cells, separated by running through a 12% SDS- polyacrylamide gel and viral structural- and non- structural protein expression was analyzed by western blot as described in methods. (B) NS1- expression on a transcriptional level was determined. Total RNA was extracted from cells at given time points, 1µg of total RNA was subjected to reverse transcripton, using oligohexamer primers and reverse transcriptase. To determine NS1- transcription semiquantitatively, 10% of the resulting cDNA was used for PCR, employing NS1- specific primers. PCR products were separated and visualized by 2% agarose gel electrophoresis. GAPDH served as a loading control. (C) Total RNA amounts of harvested cells were measured spectrophotometrically. Respective amounts, detected 4h p.i. are defined as 100% and later time points depict RNA levels, relative to these respective first values.

time- course of the experiment (see figure 12B). In MEFs, NS1- mRNA of MVMP also occurred early after infection and increased over time, culminating 48h p.i. As seen on a protein level, production of NS1 in MVM_{CR}- infected MEFs showed a delayed onset also on mRNA level, but increased slightly throughout the duration of the experiment. At each time- point, total RNA- levels were measured (see figure 12C). In A9 cells, after an initial increase, levels dropped over the time- course of the experiment upon infection with either virus. As total cell numbers did not decrease significantly over the time- course of the experiment, it was excluded that this observation could be attributed to cell death, however, could be due to a virus-induced shut-off of host mRNA production (Walsh and Mohr, 2011). This marked decrease could not be observed in infected MEFs, in which RNA levels remained constant.

Taken together, these data show that the expression of both, non-structural and capsid proteins is not the limiting factor of MVMP for DNA replication and single-stranded virion DNA production in MEFs, since the levels of these proteins produced by MVM_{CR} is significantly lower than those of MVMP. However, additional experiments (e.g. examining the primary amino acid sequence, structure, and or monitoring post-translational modifications) have to be taken into consideration for the capability of MVM_{CR} but not of MVMP to propagate in MEFs. It should also be stated here that the quality of MEF preparations significantly vary in regard to MVM_{CR}-permissiveness. It is therefore essential to generate relevant data sets from several different MEF preparations.

5.4 Antiviral activities induced by MVM infections of MEFs

Normal cells are armed to sense pathogens and to react by induction of a host cell defense leading to immunity of the neighboring cells or tissue. Indeed it was shown recently that a type I interferon response was induced upon MVMP infection of MEFs possibly accounting for the shut-off of viral protein production and resistance of the cell population to the viral attack (Grekova et al., 2010).

Interestingly, when MEFs were infected at a low MOI and the cell population was monitored by phase-contrast microscopy (see figure 13), we observed a strong inhibition of cell growth upon MVMP infection, while the amount of uninfected controls or MVMP_{CR}-infected MEFs continued to increase over time. This could be due, on the one hand to a cell cycle arrest triggered by the reported Type I- interferon response in MEFs of MVMP, which, on the other

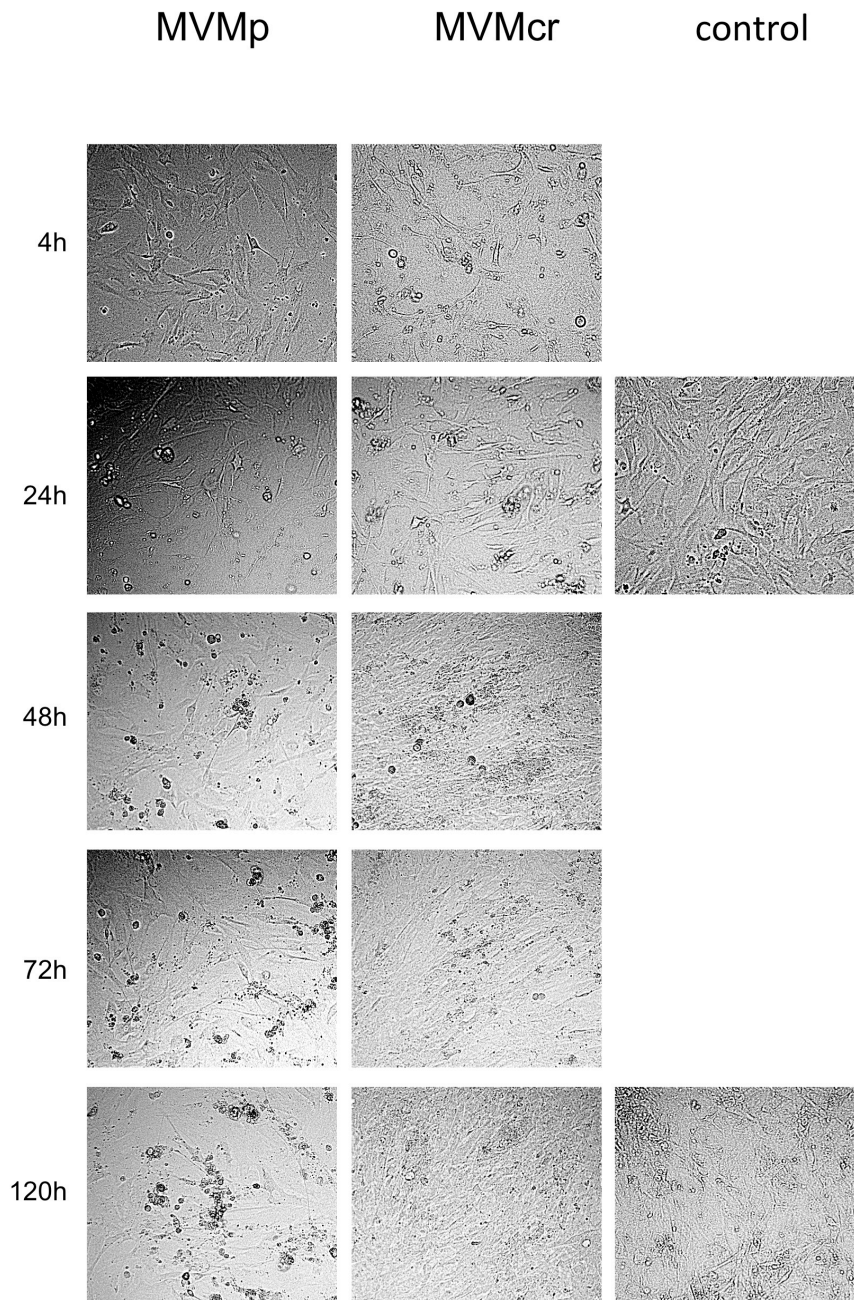


Figure 13. Growth kinetics of infected and mock- treated MEFs. Before harvest, cell density and viability of each sample was surveyed by light microscopy. 20- fold magnification was used.

hand might be counteracted by MVM_{CR}, in consequence allowing propagation of this virus strain. To investigate potential differences in antiviral responses between MVMp and MVM_{CR}, A9 cells and MEFs were infected with a low MOI and harvested at indicated times post infection. Accumulation of viral proteins and selected marker proteins (PKR, STAT1/2, phosphor-eIF2 α), previously described to be induced upon MVMp infection of MEFs was measured by western blot analysis (see figure 14). A low MOI was chosen in order to maintain a significant proportion of uninfected cells in the first round of infection, in order to obtain information about paracrine IFN- signaling pathway (STAT1/2 phosphorylation)- activation in those cells. Viral protein accumulation was comparable to the previous experiment (see figure 12A), although the time-dependent increase of NS1- protein levels in MVM_{CR}- infected MEFs was more pronounced.

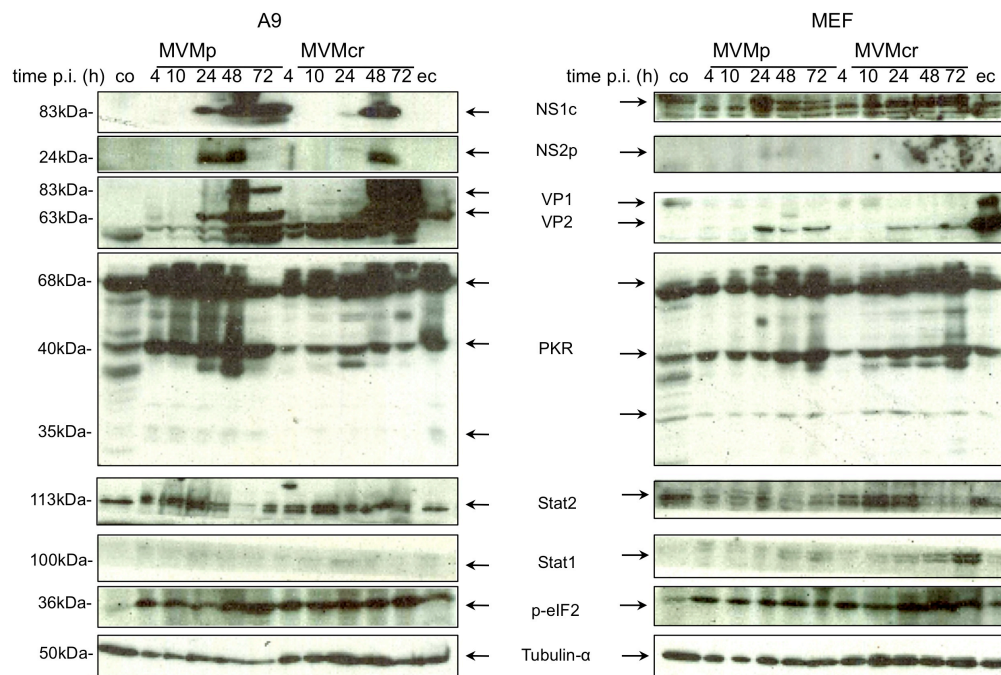


Figure 14. Dynamics of antiviral innate immune activity in MEFs and A9 cells. Stimulation of antiviral factors upon infection with MVMp or MVM_{CR} were investigated by Western blot analysis. Cells were infected at an MOI of 1 PFU/cell and harvested and lysed at indicated time points. Proteins were separated by 12% SDS-PAGE and proteins of interest were detected by blotting on a nitrocellulose membrane and specific antibodies, as described in methods. Tubulin- α was used as a loading control.

In both, A9 cells and MEFs, the amount of PKR was increased in a time-dependent manner upon infection with either virus. Similarly, phospho-eIF2 α accumulated throughout duration of the experiment in both cell entities, as compared to mock- treated cells, while there was no obvious differential pattern of eIF2 α - phosphorylation in cells, infected with MVMp or with MVM_{CR}. In A9 cells, Stat2- accumulation culminated 24h p.i. and decreased thereafter. This downward tendency after an initial increase appeared to be diminished, as Stat2 signal intensities remained largely constant after 24h p.i. In MEFs, Stat2 accumulation was stronger in cells, infected with MVM_{CR}, compared to those infected with MVMp. Upon infection with MVM_{CR}, Stat2 appeared to be upregulated very early after infection, but seemed to decrease after the time point of 24h p.i. These dynamics appeared to be less intense upon infection of MEFs with MVMp, in which Stat2 was found to be upregulated to a markedly lesser extent, also decreasing after 24h p.i. Stat1 was found not to be- or to a much lesser extent- upregulated upon infection with either virus, exhibiting a faint band 24h p.i. in A9 cells. In MEFs, the triggering of Stat1 accumulation was also faint. In contrast, infection of those cells with MVM_{CR} led to a constant increase in Stat1- protein throughout the entire time- course of 72 hours.

We then attempted to determine a potential induction of the NF κ B pathway which constitutes an early step in the cellular, antiviral innate immune response to promote type- I IFN expression. This pathway was previously shown to be induced upon transduction with recombinant AAV vectors, single-stranded linear DNA viruses similar to MVM. To analyze whether MVMp and MVM_{CR} have diverging effects on NF κ B- signaling, MEFs were infected with an MOI of 10 PFU/cell. To detect potential shifts in subcellular distribution (i.e. translocation to the nucleus) of the respective proteins of interest, which is a prerequisite for the induction of down-stream genes activated by this pathway, biochemical fractionations separating nuclei from cytoplasm were performed and proteins were detected by western blot analysis (see figure 15). Analysis of NS1 distribution showed that the protein was present in both compartments. Tubulin α served as a control for the fractionation. As seen in western blots from whole cell extracts, MVM_{CR}- NS1 signals were lower than that of MVMp, but

were increasing over the time- course. p65, one constituent of the heterodimer that forms NFκB1 upon signaling by cytoplasmic- or endosomal viral recognition receptors, was found to be slightly increased in the cytoplasmic fraction, upon infection with MVMp, whereas in the nuclear fraction levels of this protein appeared to be unaltered. In contrast, MVM_{CR} seemed to trigger an initial accumulation of p65 both in the cytoplasm and in the nucleus 24h p.i., as compared to mock- treated cells. However, after this time- point, this marked accumulation of p65 declined and dropped to a level, comparable to that of MVMp- infected cells 72h p.i. p105 is the inactive precursor of p50, the second constituent of NFκB1. p105 was found to be localized in both cytoplasmic and nuclear fractions and no major differences concerning its expression levels or localization could be observed upon infection with the two different viruses. However, a slight induction of cytoplasmic p105, compared to mock- treated cells could be detected. In contrast, a marked difference in p50 levels,

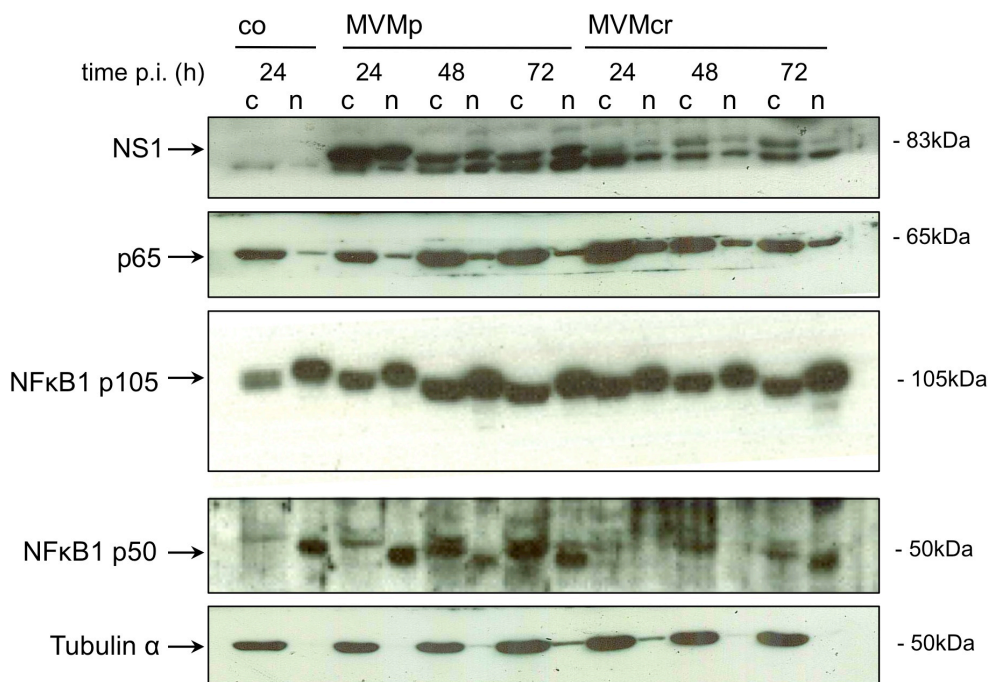


Figure 15. NFκB- activation in MEFs. To analyze nuclear accumulation of NFκB- associated signaling components, cells were infected with MVMp or MVM_{CR} and harvested after given time points. Biochemical fractionation yielded nuclear- and cytoplasmic compartments, with which SDS-PAGE and Western blot analysis was performed, in order to detect proteins of interest. Tubulin-α served as a loading control.

synonymous for the proteasomally- activated form of p105, signalling to the nucleus in conjunction with p65 could be observed. Upon infection with MVMP, cytoplasmic p50 increased steadily throughout the time- course of the experiment while showing an approximately constant presence in nuclear fractions. In MVM_{CR}- infected cells, however, cytoplasmic p50- levels were markedly lower compared to those in MVMP- infected cells, exhibiting approximately the same steady- state expression levels as compared to mock- treated cells throughout the entire time- course of the experiment. Interestingly, nuclear p50- protein in MVM_{CR}- infected cells could not be detected before 72h p.i., where signal intensity was still below that of nuclear p50 of mock- treated cells. In conclusion, these results appear very confusing and are not in agreement with previous findings. Additional experiments are therefore needed to evaluate PKR activation and Stat1/2 induction upon MVMP/MVM_{CR} infection. In particular, the commercially obtained antibodies have to be characterized for their specificity and their optimal concentrations with other known positive/negative controls. New experiments with additional preparations of MEFs have to be performed in order to obtain consistent results and to draw a conclusion.

5.5 Potential MVM sensor and counteracting targets of MEF-induced anti-viral activities

5.5.1 Host cell sensor

Previous investigations have shown a strong translocation of a cellular small glutamine-rich-tritetrapeptide containing protein, SGTA, to the nucleus of infected cells where it accumulated in replication centers (APAR-bodies) (Cziepluch et al., 1998). A function for this NS1-interacting protein for viral DNA replication, however, was not determined yet. Recently, it was shown that host cell pathogen recognition can be achieved through a family of tetrapeptide-containing proteins, IFITs which sense the triphosphate group and secondary structures of viral RNAs, which are normally not present in the cytoplasm of the host cell. This made us wonder, whether SGTA could serve as such a sensor,

recognizing the unique 3' or 5' terminal hairpin structures of parvoviral DNA. To substantiate such a hypothesis we infected MEFs with either MVMp or MVM_{CR}, respectively. Cells were harvested at indicated times p.i. and the subcellular distribution was analyzed by a combined fractionation of sedimentation and solubility towards Triton X-100 treatments. Fractions corresponding to the insoluble scaffold (iS), nuclear membrane (nM), post-nuclear membranes (pM), soluble scaffold (sS), and the soluble proteins in cytoplasm (C) were matched according to the amount of cells and analyzed for the relative protein content by western blotting. As shown in figure 16, upon infection, irrespective of the isolate under investigation and starting at 4 h p.i., SGTA became associated with membrane structures, which was maintained throughout the infection.

Interestingly, only in MVM_{CR} SGTA was also found to strongly accumulate in cytoplasmic scaffold structures, which, 72h p.i., reached approximately the same level of that observed in the nuclear- membrane fraction at the same time point. This association of SGTA to scaffolds was much reduced in MVMp infected cells, although the overall- induction of this protein appeared to be stronger upon MVMcr- infection, as compared to MVMp.

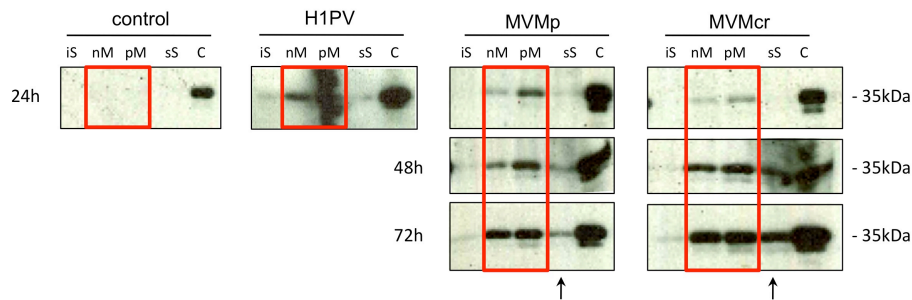


Figure 16. Induction and subcellular distribution of SGTA. MEFs were infected- or not- with MVMp and MVMcr at an MOI of 10 PFU/cell. and harvested after given time points. Insoluble nuclear scaffold- (iS), nuclear membrane- (nM), postnuclear membrane- (pM), soluble cytoplasmic scaffold- (sS) and cytoplasm- associated proteins were biochemically fractionated. SGTA- protein levels in respective compartments were detected by SDS-PAGE and Western blotting, as described in methods.

In summary, these data indicate that SGTA is induced to post nuclear membranes upon PV infection of MEFs. This was also observed after infection with H1PV, which does not replicate in these cells. Thus, it can be stated that

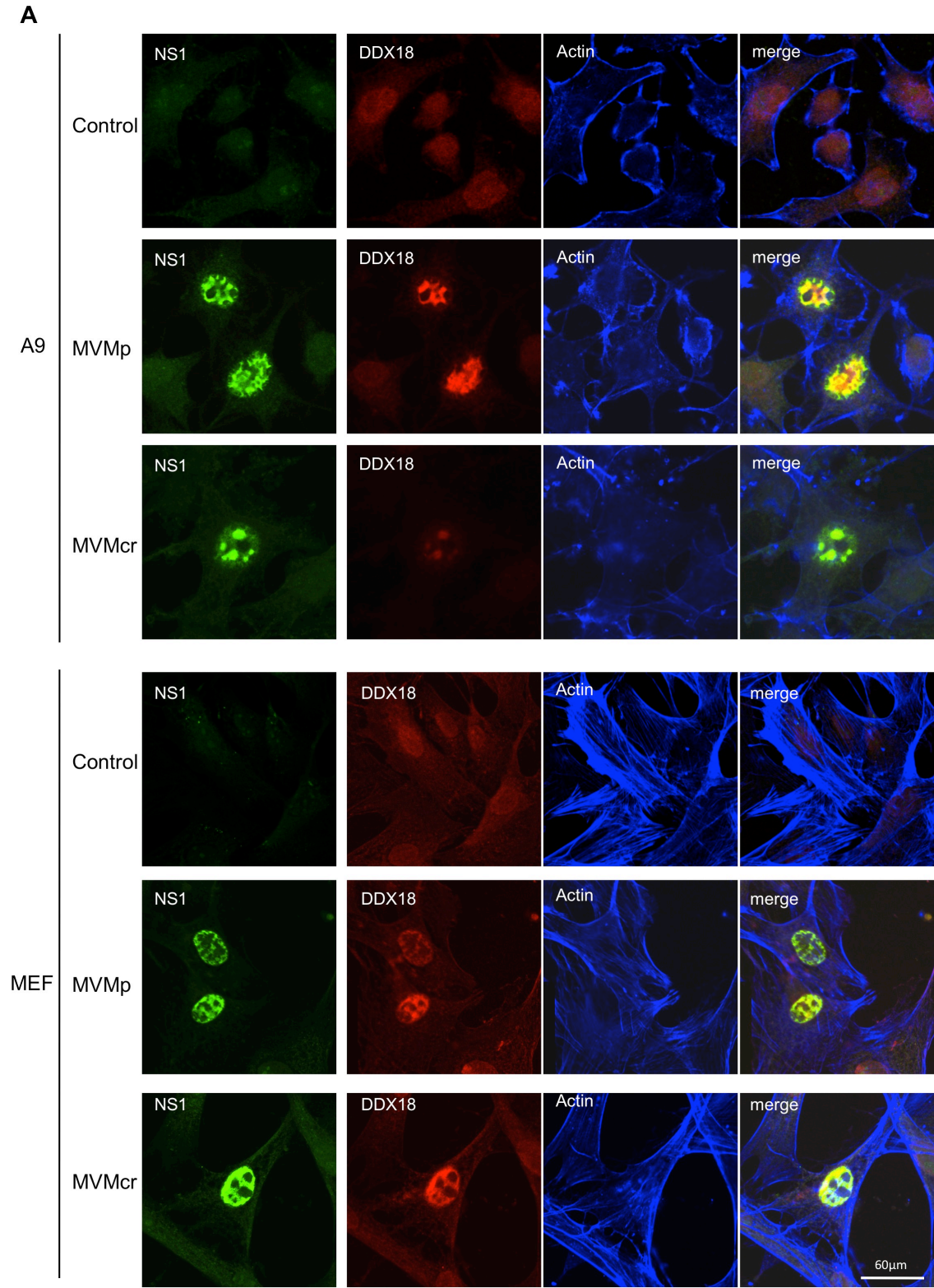
recruitment of SGTA to post nuclear membranes takes place irrespectively of whether a viral infection or viral protein expression can be established or not. This is in agreement with the sensing of the incoming viral capsids. Interestingly, PVs are recognized through a 5' end DNA tether which extrudes from the five-fold pore of the capsid (Cotmore et al., 1988). This DNA could serve as target recognition motif for IFIT and/or IFIT-like proteins in order to trigger an anti-viral response. At later stages, interaction of SGTA with NS1 and accumulation in APAR bodies could be associated with its association to scaffold structures where this complex might be essential for viral propagation in MEFs. Evidently, this is only seen after establishment of viral DNA amplification after infection of MEFs with MVM_{CR}.

5.5.2 Interference of MVM with the mRNA- processing machinery

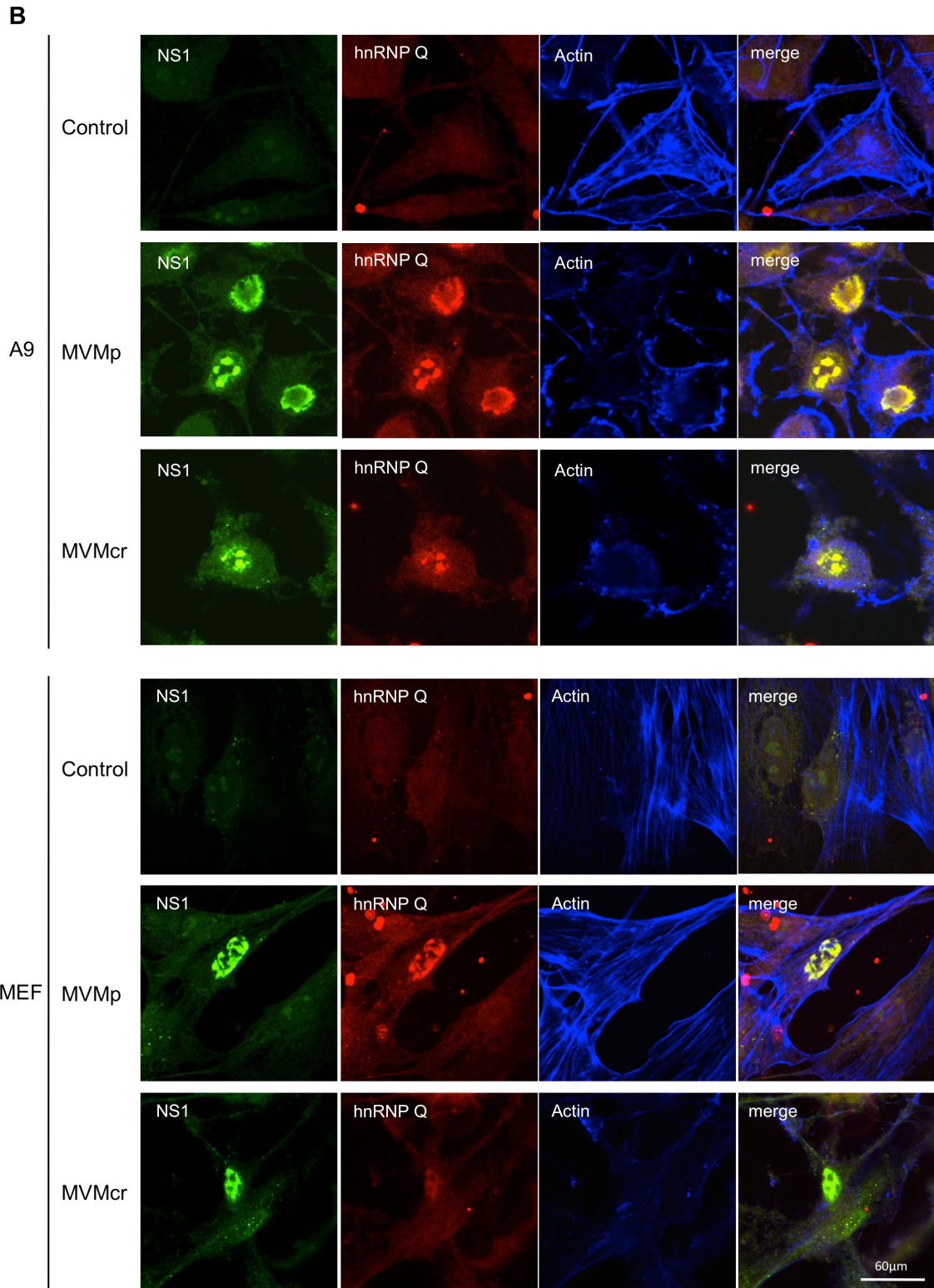
Proteomics revealed cellular mRNA processing machineries as a common denominator for the targeting through a large number of virus families to counteract anti-viral responses leading to translational shut-off (Walsh and More, 2011). Interestingly, previous investigations have found that MVM NS1 protein is able to interact with hnRNP R and Q, respectively, formerly called NSAP1 (Harris et al., 1999), DDX18, an RNA helicase, and CPSF6, an mRNA processing enzyme involved in nuclear export (Nüesch, unpublished data). A function for these interactions in MVMp infected A9 cells has not been found so far.

Therefore, we were interested to determine a potential impact of these NS1-interactions in MEFs. A first screen was attempted to identify differences in the subcellular distribution after infections with MVMp and MVM_{CR}, which could be indicative for the failure of MVMp to propagate in these cells. A9 cells and MEFs were seeded on spot slides and infected with either virus at a MOI of 10 PFU/cell. 24 hours p.i., cells were stained for NS1 and DDX18, hnRNP Q, or CPSF6, respectively. Confocal laser scanning microscopy was performed in order to reveal colocalization between these cellular proteins and the viral NS1 polypeptide. In confocal immunofluorescence microscopy, DDX18 was also found to be upregulated in the nuclear fraction upon infection of A9 cells and

MEFs with either MVMP or MVM_{CR} at 24h p.i. (see figure 17A). In both, A9 cells and MEFs, nuclear colocalization of DDX18 with NS1 upon infection with either virus was observed. This was characterized by the accumulation of DDX18 into



distinct subnuclear foci, in contrast to mock- treated cells, in which the protein was dispersed rather homogeneously in the nucleoplasm. Similar effects were observed for hnRNP-Q, which, in confocal fluorescence microscopy, was also found to be induced 24h p.i. in A9 cells and MEFs upon infection with both



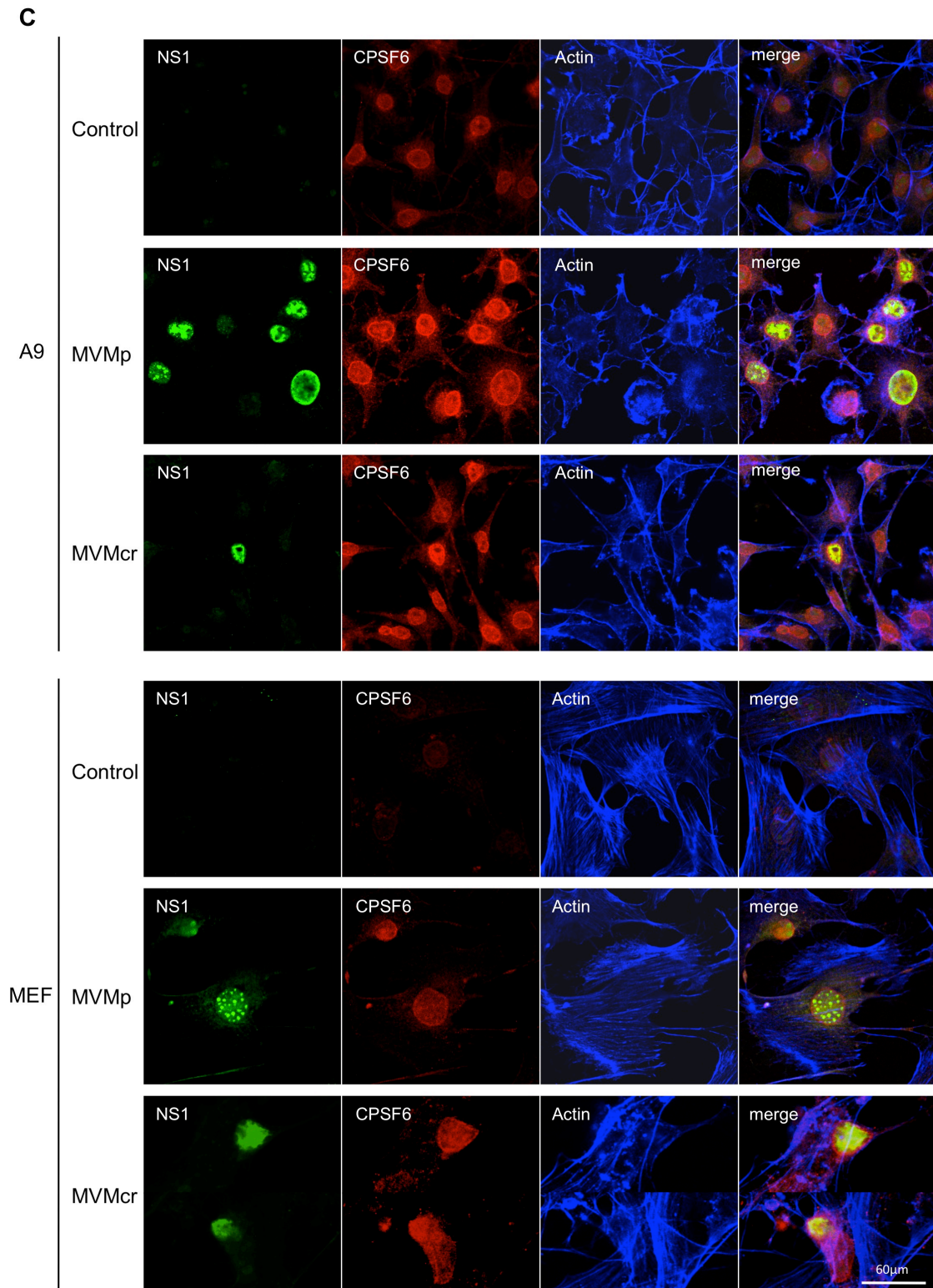


Figure 17. Analysis of upregulation and localization of RNA- processing factors in infected MEFs and A9 cells by confocal immunofluorescence microscopy. Cells were infected- or not- with MVMp and MVM_{CR} and fixed 24h p.i.. NS1 was detected using a specific C- terminal primary antibody and a donkey anti- rabbit, Alexa Fluor 488- coupled secondary antibody, actin fibers were visualized by phalloidin- rhodamine (emission wave length peak 568nm). DDX18 (A) and hnRNP Q (B) and CPSF6 (C) were detected by specific primary antibodies and Alexa Fluor

647- coupled secondary antibodies. (B, C) Colocalization of DDX18 and hnRNP Q in MEFs and in A9 cells.

viruses. In each case, the protein exhibited accumulated nuclear levels, as compared to mock- treated cells. Furthermore, colocalization of hnRNP-Q with NS1 of either virus could be observed in both, A9 cells and MEFs, in a number of NS1- positive cells (see figure 17B).

Infected MEFs showed an induction of CPSF6 over mock- treated cells 24h p.i., which was higher in cells infected with MVM_{CR}, compared to that infected with MVMp (see figure 17C). The protein showed accumulation in the nucleus but was also observed dispersed throughout the cytoplasm. At this time- point, nuclear colocalization of CPSF6 with NS1 was not obvious in MEFs infected with MVMp. In contrast, in MVM_{CR}- infected MEFs, NS1 and CPSF6 did appear to colocalize. In A9 cells, induction seemed to be less distinct. Elevated levels of nuclear CPSF6 could be observed upon infection with either virus compared to mock- treated cells; differences in presence or distribution of this protein, however, could not be detected in cells infected with either virus. Interestingly, in A9 cells, infected with either MVMp or MVM_{CR}, partial colocalization with NS1 could be observed.

To obtain further information on the dynamics of CPSF6 protein during parvovirus infection, its subcellular distribution was analyzed by a biochemical fractionation and Western Blot of treated cells. For this, MEFs were infected with either MVMp or MVM_{CR} at an MOI of 10 PFU/cell. At given time points, cells were harvested and biochemically fractionated as described in methods. This fractionation separated whole cells into nuclear scaffold- associated- (insoluble scaffold, iS), nuclear membrane- associated- (nM), cytoplasmic post- nuclear membrane- associated- (pM), cytoplasmic scaffold- associated- (soluble scaffold, sS) and freely diffusing cytosolic proteins (C). Distribution of CPSF6 in the obtained fractions was analyzed by Western Blot.

Consistently to the data obtained by confocal immunofluorescence microscopy, Western Blot analysis showed that CPSF6 was markedly induced upon infection with MVM_{CR} (see figure 18). Compared to mock- treated cells, a higher

level of this protein was observed in the cytoplasmic fraction and in the cytoplasmic scaffold at 24h p.i., exhibiting a further increase 48h- and 72h p.i.. CPSF6 was also found to localize to nuclear- and post- nuclear membranes throughout the time- course of the experiment. Additionally, a marked level of the protein was detectable associated to the nuclear scaffold 72h p.i. Importantly, upon MVMp- infection, cytoplasmic CPSF6- levels did not appear to increase as elevated as in MVM_{CR}- infected MEFs, and overall induction of this protein was found to be lower. Additionally, distribution of this protein in MEFs infected with MVMp was distinct from that in cells infected with MVM_{CR}, as association to nuclear- and post- nuclear membranes was not observed and the CPSF6 fraction associated to the cytoplasmic scaffold was markedly lower than that upon MVM_{CR}- infection.

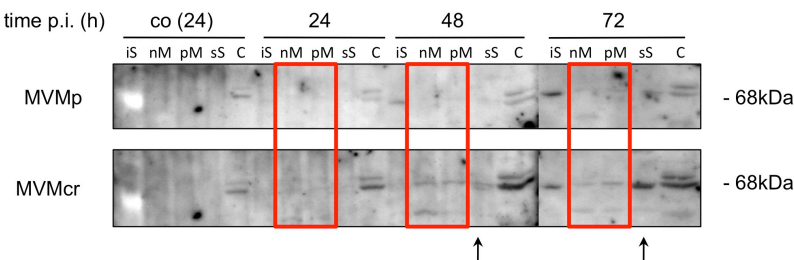


Figure 18. Induction and subcellular distribution of CPSF6. MEFs were infected- or not- with MVMp or MVM_{CR} at an MOI of 10 PFU/cell and harvested after given time points. Biochemical fractionation was performed as shown in figure 18. Detection of CPSF6 was accomplished by 10% SDS-PAGE and Western blotting.

Taken together, these experiments show that infection of MEFs with MVMp or MVM_{CR} results in differential protein dynamics of CPSF6. This suggests that specific events during RNA- processing play a role in MEF- permissibility towards MVM_{CR}. To further investigate the role CPSF6 might play in the course of parvovirus infection, it will be important to conduct additional experiments, revealing the nature of the observed induction of this protein and the consequences for (viral) protein translation.

5.6 Genetic characterization of MVM_{CR}

Evidently, MVM_{CR} retained the potential to replicate and propagate in MEFs, a feature that was lost upon adaptation to A9 cells. This made us wonder, whether the adaptation and growth on the fibroblast cell line has led to changes in the genome of these small single-stranded DNA viruses. To investigate this possibility, we purified ssDNA from a virus stock which has been produced on freshly prepared MEFs. Viral genomes were amplified by PCR in five partially overlapping fragments. Amplified fragments were isolated by agarose gel electrophoresis. Corresponding bands were extracted, ligated into pCR2.1

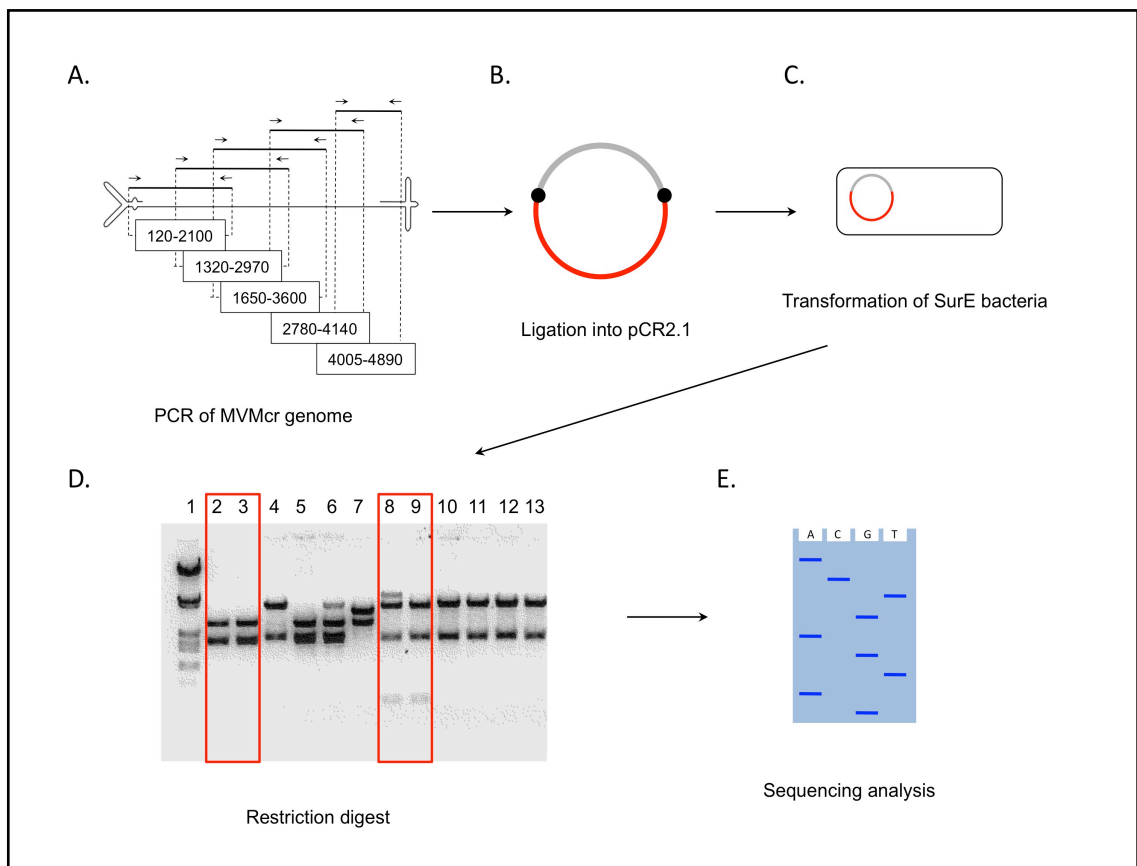


Figure 19. Genetic characterization of MVM_{CR}. Viral DNA was isolated from infectious particles and partially overlapping fragments were amplified by PCR (A). PCR products were cloned into vector pCR2.1. To amplify the generated constructs, they were introduced into *E.coli* by heat-shock transformation (B,C). Clones, picked from single colonies were checked for containing respective inserts by restriction digest (D). Clones, yielding correct band patterns, indicated by red boxes, were submitted to sequencing analysis in triplicates (E).

vector and amplified by transformation of SurE bacteria. Plasmid DNA was isolated and inserts were checked for correctness by restriction digest. Samples yielding putatively correct restriction patterns were submitted to sequencing analysis, employing DNA from three independent single colonies of respective fragments and using standard M13 primers, which anneal within the multiple cloning site of pCR2.1. Resulting nucleotide sequences were aligned with the genome of MVMp by the Pubmed Blastn-alignment computer program. In order to exclude potential sequencing errors, only base alterations, occurring in all three analyzed samples were taken into account (see figure 19).

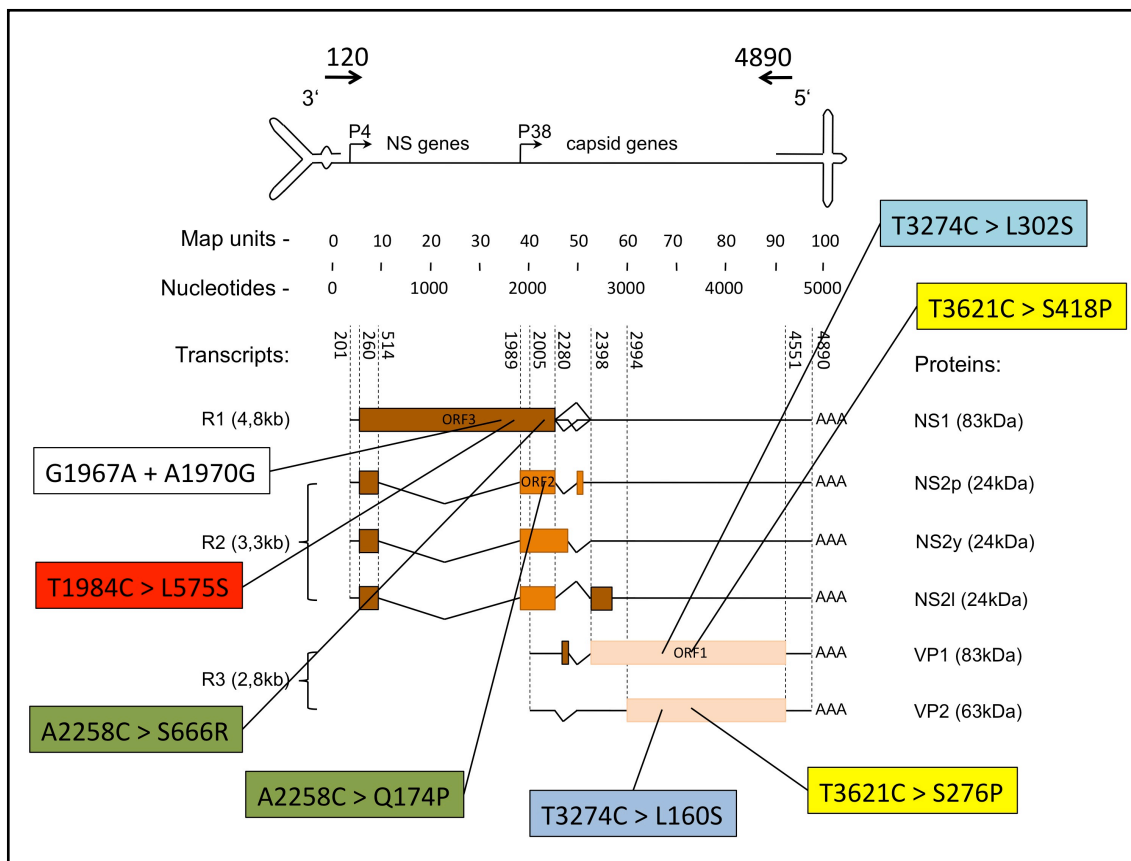


Figure 20. Localization of base alterations in MVMp in comparison to MVM_{CR}. The six identified variations map to both structural- and non- structural gene regions. Exact genomic locations of those alterations and resulting amino acid changes are indicated in coloured boxes. To minimize the probability of sequencing errors, only those alterations, occurring in all three samples of the submitted triplicates were taken into account.

Alignment of the cloned fragments of MVM_{CR} with MVMp resulted in the observation of six base alterations (see figures 20, 22). The first two variations

are located at close proximity to each other, changing a guanine (G) at residue 1967 to an adenine (A) and an A at residue 1970 to a G (see figure 21A). These two alterations are located in the NS1 coding region upstream of the NS2 specific exon, which starts at position 1989. Furthermore, these alterations lie within the 3'- acceptor of the non- structural large intron, the excision of which distinguishes R1 from R2 transcripts, and they do not result in a change of respective encoded amino acids, thus, are non- coding.

Another variation was found within the NS1- specific ORF, resulting in a Thymidine (T)- to- Cytosine (C)- change at position 1984 (see figure 21C). This alteration results in the substitution of a Leucine- for a Serine at residue 575 of the NS1 protein product.

An additional coding A- to- C base alteration within the non- structural gene region at position 2258 concerns both the NS1- ORF and the NS2- specific exon. As the excision of the large splice, which defines the generation of NS2- transcripts, accounts for a reading- frame shift, the resulting amino acid substitutions for NS1 and NS2, respectively, are distinct (see figure 21B). This yields an Arginine (R) instead of a Serine (S) at position 666 of the NS1- and a substitution of an Asparagine (N) to a Proline (P) at residue 174 of the NS2 protein product, respectively.

Besides the changes in the non- structural gene region, two coding alterations were found in the capsid- encoding part of the MVM_{CR} genome. The first is a T- to- C alteration, located at position 3274. As VP1 and VP2 share the same reading frame, the resulting L- to- S amino- acid switch is similar for both proteins. However, as VP2 is the N- terminally truncated form of VP1, respective residue numbers are distinct, yielding the alterations to be located at positions 160 and 302, respectively. This alteration concerns an amino acid of the VP proteins, that is located at the surface, close to the 5'- pore of the viral capsid. The second variation found in the capsid- encoding region is situated at genomic residue 3621. This T- to- C change accounts for a substitution of and S to a P in both VPs, being located at residues 418 for VP1- and 276 for VP2, respectively. The second altered amino acid residue does not seem to be

exposed at the particle surface, but rather appears to be buried within the interior bulk of the polypeptides, but may also be located at the inner surface of the shell, facing the DNA- filled inside of the viral particle.

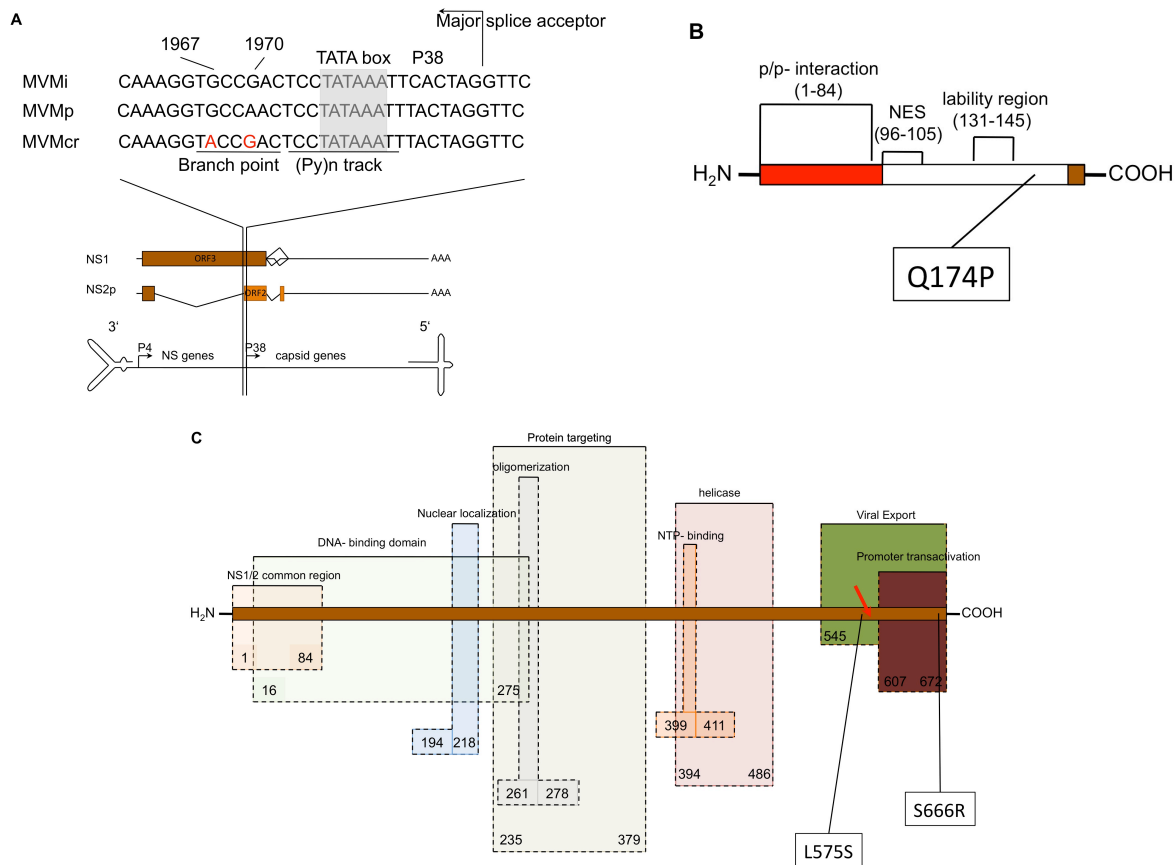


Figure 21. Alterations in the non- structural gene region. A. Nucleotide sequences of the large splice acceptor region (1960- 1993) of MVMi, MVMp and MVM_{CR} (adapted from D'Abramo, 2005). Base alterations identified in MCMcr at positions 1967 and 1970 are indicated in red. The (Py)n track indicates the polypyrimidine region of the splice site. B. Functional domains of MVMp- NS2 and the location of the amino acid alteration in MVM_{CR}. Protein- protein (p/p)- interaction region, nuclear export sequence (NES) and a lability region, which is involved in a proteasome- mediated polypeptide degradation are indicated. NS1/2 common exon is indicated in red, NS2- specific exon in white and C- terminal exon (NS2p) in brown. C. Functional domains of MVMp- NS1 and locations of amino acid alterations of MVM_{CR}. L575S is located within a region associated with viral export (Nüesch, Bär, unpublished data). The red arrow indicates the position of two phosphorylation sites near this alteration, T585 and S588 (Daeffler et al., 2003). S666R is found in the promoter transactivation domain, near the C- terminus.

G1967A + A1970G

1960	2020
CAAAGGT	G C C A A C T C C T A T A A A T T T A C T A G G T T C G G C A C G C T C A C C A T T C A C G A C A C C G A
CAAAGGT	A C C G A C T C C T A T A A A T T C A C T A G G T T C G G C A C G C T C A C C A T T C A C G A C A C C G A

T1984C

1982	2041
T T	T A C T A G G T T C G G C A C G C T C A C C A T T C A C G A C A C C G A A A A G T A C G C C T C T C A G C C A G A A
T T	C A C T A G G T T C G G C A C G C T C A C C A T T C A C G A C A C C G A A A A G T A C G C C T C T C A G C C A G A A

TPIN L LGS
 TPIN LGS
 TPIN S LGS

NS1 L575S

A2258C

2202	2261
A T C G A G G A G G A T T T G A G A G C G T G C T T C G G T G C G G A A C C G T T G A A G A A A G A C T T C	A G C G A G
A T C G A G G A G G A T T T G A G A G C G T G C T T C G G T G C G G A A C C G T T G A A G A A A G A C T T C	C G C G A G

NS1 S666R

KKDF S EPL
 KKDF EPL
 KKDF R EPL

NS2 Q174P

TVEERL Q R
 TVEERL R
 TVEERL P R

T3274C

3263	3322
A G C A A G A C T	T A G G A G G T C A A G C T A T A A A A A T A T A C A A C A A T G A C C T T A C A G C T T G C A T G A
A G C A A G A C T	C A G G A G G T C A A G C T A T A A A A A T A T A C A A C A A T G A C C T T A C A G C T T G C A T G A

TVTEQD L GGQA
 TVTEQD GGQA
 TVTEQD S GGQA

VP1 L302S / VP2 L160S

T3621C

3617	3676
A T	T C A G T T A A A C T C A C A C A C G T G G C A A A C C A A C C G T C A A C T T G G A C A G C C T C C A C T G C
A T	C A G T T A A A C T C A C A C A C G T G G C A A A C C A A C C G T C A A C T T G G A C A G C C T C C A C T G C

FDTN S VKL
 FDTN VKL
 FDTN P VKL

VP1 S418P / VP2 S276P

Figure 22. Exact genetic loci of identified base alterations and their resulting amino acid changes. Upper fragments are of MVMp, aligned lower fragments depict sequences of MVM_{CR}. Base- and amino acid variations are underlaid in yellow.

In summary, six base alterations could be identified in the MVM_{CR} genome (nucleotide numbers 120- 4890) compared to MVMp. These alterations comprise structural- and non- structural protein- encoding regions as well as non- coding variations within the acceptor region of the non- structural large splice. These findings provide the basis for future experiments, to reveal at which levels these alterations affect MVM_{CR} fitness in MEFs. It is intriguing now to analyze the impact of individual changes alone or in combination with others for their impact of MVM growth in MEFs.

5.7 MVMp recombinants

To determine which of the identified base alterations in MVM_{CR} account for the ability to replicate in primary MEFs, site- directed reverse mutagenesis was applied to introduce respective nucleotide changes into the genome of MVMp (see figure 23). Alternatively, variation- containing genome regions of MVM_{CR} were isolated by restriction endonuclease digest and inserted into corresponding regions of the expression vector pDB containing infectious clone DNA of MVMp. Generation of those recombinant MVMp clones, containing single- or combined mutations should then be assayed for infectivity in MEF cells.

Single- and combined mutant clones of MVMp were produced. Single mutants comprised the NS1- encoded Δ T1984C variation, yielding the Δ L575S alteration and Δ A2258C, accounting for the NS1/NS2 double mutation of Δ S666R and of Δ N174P, respectively. Combined mutant clones comprised the two mentioned coding variations within the non- structural gene region as well as these two variations combined with the two non- coding alterations within the 3'- large splice acceptor, yielding a quadruple mutant containing all variations observed in the non- structural gene region. Mutagenesis procedure is described in figure 21. Obtained expression vectors were submitted to sequencing analysis to verify the presence of respective desired mutation. To produce infectious particle- stocks, 293T cells were transfected with positive clones.

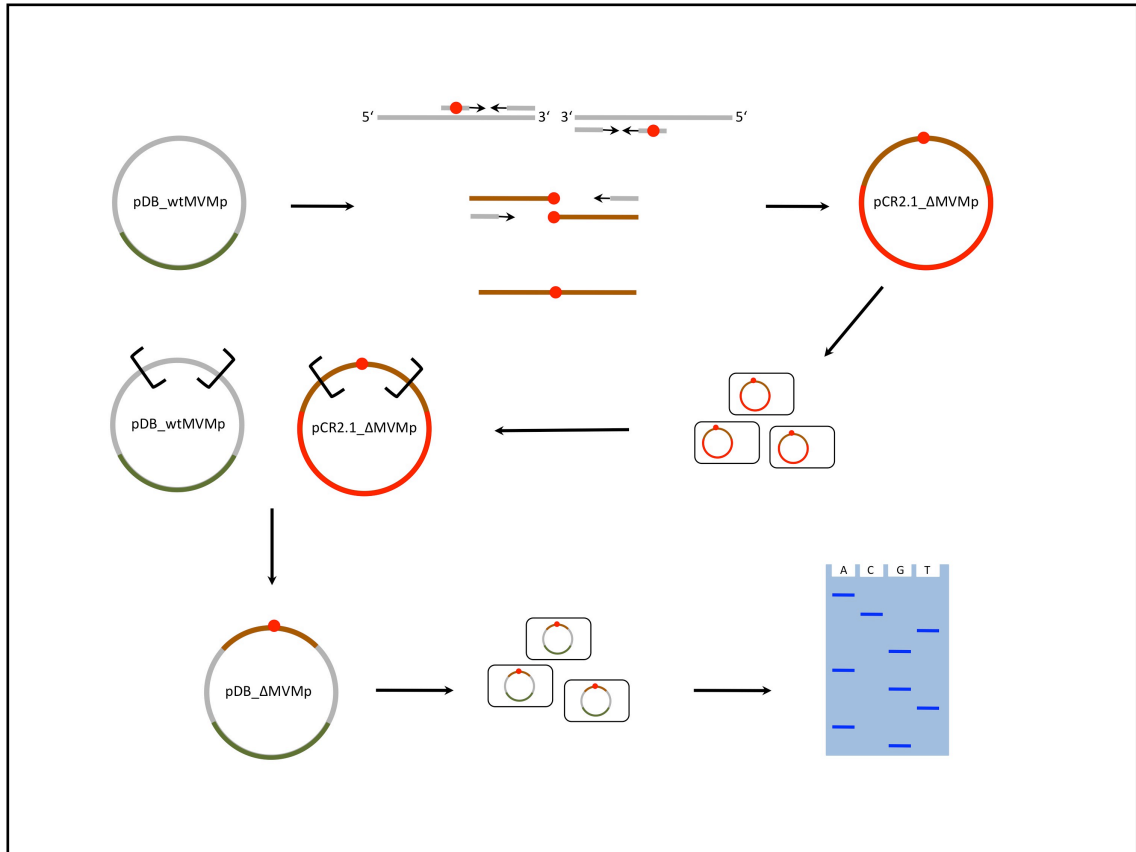
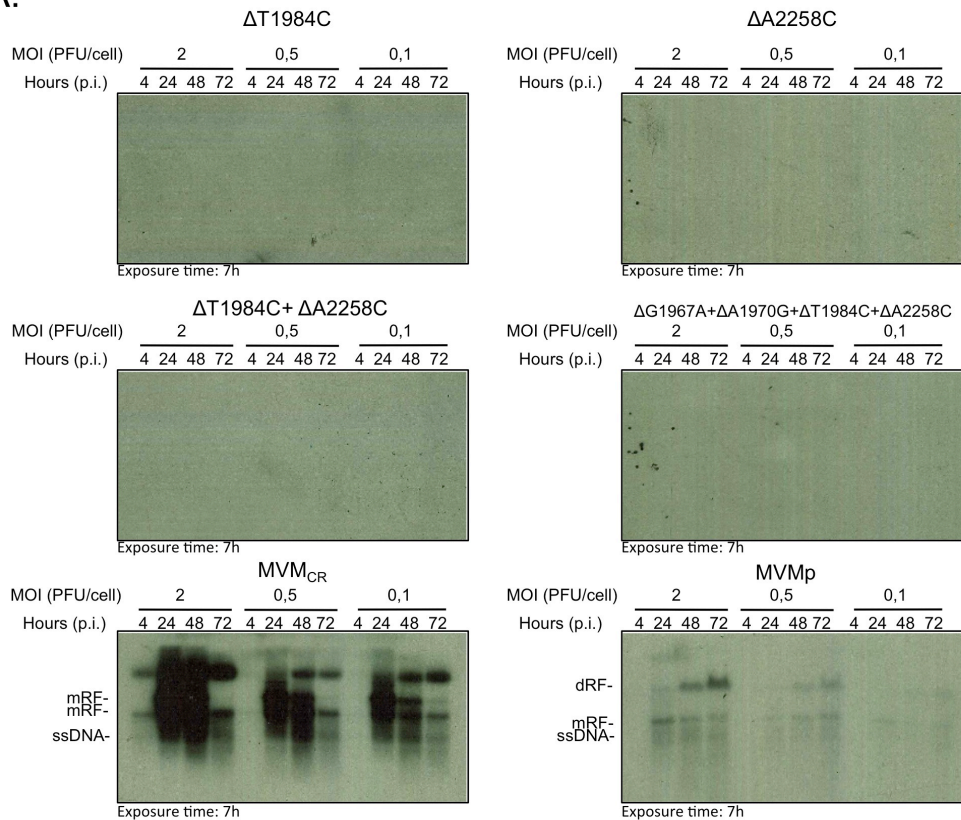


Figure 23. Site- directed mutagenesis of MVMp. By chimeric PCR, mutations were introduced into MVMp. Mutant strands were synthesized, using expression vector pDB-MVMp as a template. For each respective mutation, pairs of complementary primers were designed, which contained respective base alteration (see materials). For each mutagenesis, two separate thermal cycling reactions were carried out, one of which contained respective 3'- inward-mutant- primer and 5'- outward- primer and the other contained the 5'- inward- mutant- primer and the 3'- outward primer, respectively. PCR products were separated by agarose gel electrophoresis. A second thermal cycling reaction was performed, using the mutagenized, partially overlapping fragments and respective 5'- and 3'- outward primers. PCR products were separated by agarose gel electrophoresis, isolated and ligated into pCR2.1 vector. SurE bacteria were transformed with ligation mixtures and amplified plasmid DNA was isolated. Mutated fragments were endonuclease- digested, introduced into pDB-MVMp and sequenced.

To distinguish MVMp recombinants which had acquired the capability of productively infecting MEFs from those that had not, cells were infected and assayed for viral DNA amplification. At initial MOIs of 2-, 0.5- and 0.1 PFU/cell, respectively, no viral DNA amplification could be observed in MEFs infected with recombinant viruses (see figure 24A) over a time course of 72h. As a control, MEFs, infected with wild-type MVM_{CR} showed viral DNA replication,

A.



B.

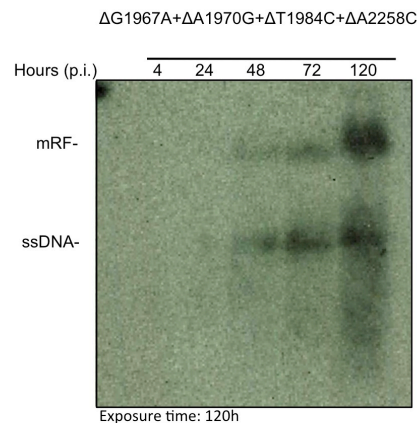


Figure 24. Replication efficiency of MVMp mutants. (A) MEFs were infected at indicated MOIs, medium was changed 2h p.i. and cells were harvested at given time points. DNA was extracted, separated on a 0,8% agarose gel and viral DNA was detected by southern blot as described in 'Methods'. (B) Repeated experiment in MEFs with the quadruple mutant at a higher MOI and an extended time course.

whereas infection of these cells with MVMp was abortive, showing a moderate signal for ssDNA production after 24h, but decreasing again after that time point in the course of the experiment. This observation was consistent with the findings in chapter , infectivity of MVMp and MVMcr'.

As a consequence, another southern blot experiment, employing higher MOIs and a prolonged time- scale was conducted, taking into account that the recombinant viruses might potentially show impaired infectivity or delayed propagation in MEFs. Over an experimentation- time of 120h at a higher MOI, only the quadruple- mutant comprising the four base variations within the non- structural gene region showed DNA replication, being detectable slightly delayed after 48h, as compared to wild-type MVM_{CR} but increasing consistently until the final time point of 120h (see figure 24B).

In summary, it can be stated that base variations concerning putative splice efficiency and non- structural proteins are essential for MVM_{CR} replication in MEFs. It remains to be shown, to which extent the capsid alterations play a role in permissibility. Due to the fact that terminal repeats and 64 bp repeat in the 3' untranslated region of viral mRNAs, which is implicated as a host range determinant (Pallier et al., 1998). could not be sequenced during this study, potential alterations in these regions (as might be present in the infectious clone DNA) might account for the delayed propagation of the quadruple mutant in those cells. Further experiments will be necessary to verify potential replication capability of all recombinant viruses (e.g. by infection of NBK) and to clearly identify, which base alterations in MVM_{CR} account for its replication- potential in MEFs.

6. Discussion

Virus- host cell interactions depict an important aspect in oncolytic virotherapy. Parvoviral oncotropism- its preferential replication in cancerous cells- is, amongst other reasons, attributed to the acquired inability of such cells to sense and counteract these invaders. In oncolytic virotherapy, the absence of a rapid immune response against the therapeutic agents is of major importance to give the virus time to replicate and spread within a tumor to promote its efficient lysis. On the other hand, at later stages of infection, an oncolytic virus should aid the triggering of a host anti- tumor immune response by an increased presentation of tumor- associated antigens. In both cases, interplay between virus and target- cell antiviral defense machinery is of great importance. Concerning parvoviruses, there is a lot to be learned about this interplay. Parvoviruses, by spontaneous genetic drift, appear to have the ability to acquire means to counteract host- antiviral immune responses, also in cells which are in principle fully functional for these responses, thus in healthy, untransformed cells, as was illustrated by the presented model in this work. This is an important safety issue, as the acquired ability for productive infection of virotherapeutic agents in healthy tissue depicts a potential threat to the treated organism. Thus, in respect to the ongoing clinical trial to treat patients suffering from glioblastoma multiforme, engaging a close relative of MVMp, H1-PV as therapeutic agent, it is of interest to fully understand the interaction of parvoviruses with its host cells on a molecular level. Deeper knowledge in this field is necessary in order to not only make parvoviral oncotherapy safer, but also to make it more efficient by using these informations to potentially modulate this interplay.

The Crawford- isolate of MVM (MVM_{CR}), the parental strain of the prototype MVM, MVMp, was originally identified as a contaminant in viral stocks produced from mouse tissue cultures. This virus was reported to productively infect primary mouse tissue (Crawford, 1966). Adaptation of MVM_{CR} to the non-primary A9- fibroblast cell line by Tattersall generated MVMp, which was a

matter of intensive studies in the subsequent years (Tattersall, 1974). During excessive passaging on A9 cells, MVMp lost the capability of replicating in MEFs, the non-transformed natural counterparts of A9. MVMp was found to trigger an innate immune response in MEFs, whereas this effect was not observed in A9 cells (Grekova et al., 2010). Due to these findings, it was hypothesized that one major reason of MEF-permissibility towards MVM_{CR} lies in the capability of this virus to counteract the mentioned innate immune response, thus making these primary cells susceptible to productive infection. Furthermore, a potential of MVM_{CR} to interfere with the host-cell RNA-processing machinery was identified throughout the course of this study, which presents another level as to how this virus might be able to replicate in natural cells.

The presented study aimed at characterizing genetic alterations of the old isolate of MVM, MVM_{CR} in comparison to MVMp, accounting for the altered phenotypes of these two viruses. Furthermore, it was attempted to identify key mechanisms of MVM_{CR} rendering it pathogenic for primary MEF cells. The presented findings should provide the basis for further studies to understand how parvoviruses potentially interact with cellular factors and how they counteract cellular-antiviral responses in order to promote their own growth.

6.1 Genetic characterization of MVM_{CR}

Sequencing analysis of MVM_{CR} revealed the presence of six base alterations in comparison to the genome of MVMp, four of which were coding, whereas the remaining two were not. Identification of these variations led to a number of hypothetical reasons, possibly accounting for MVM_{CR}'s ability to replicate in MEFs. By comprising structural-, non-structural- and non-coding changes, the potentially causative mechanisms of the observed phenotype could be found in various stages of the life cycle of MVM_{CR}, including entry-, gene expression- or replication processes. It might be the case that only one variation accounts for the altered phenotype, but bearing in mind the complex efficiency of the host

cell to eradicate viral intruders, it is also probable that some of these variations act in concert to enable MVM_{CR}- growth in MEFs.

ΔT3274C results in a Leucine- to- Serine alteration at residue 302 of VP1 and at residue 160 of VP2, respectively. This residue is located at the capsid surface near the 5- fold pore. This change, together with the downstream ΔT3621C, yielding a Proline in exchange for a Serine in the inner bulk of amino acids which build up the viral capsid, might result in structural changes of the capsid interface. Whether this might have an influence on the interaction of the virus with cellular receptors at the plasma membrane at the level of viral entry or at post-entry events such as translocation to the nucleus or uncoating remains to be shown. The possibility that structural alterations of the capsid have an impact on tropism is substantiated by works Gardiner and Tattersall and by Agbandje-McKenna, which shows that specific residues on the capsid surface determine cell tropism of allotropic MVM strains (Gardinier and Tattersall, 1988; Agbandje-McKenna, 1998). Furthermore, the presence of a Serine on the surface of MVM_{CR} instead of a Leucine adds an additional potential phosphorylation site to the viral capsid. As seen for numerous other processes during parvoviral the parvoviral life cycle, altered phosphorylation patterns of viral proteins might play an important role in pathogenicity of those viruses (Nüesch et al., 2012). However, the assumption that MVMp has an impaired ability to enter MEFs is contradictory to the findings of Grekova et al, which showed that intracellular amounts of MVMp- DNA were similar in A9 cells and MEFs, respectively, two hours after infection, a time- point at which detected viral DNA- levels can be considered to exclusively stand for entered- and not for replicated DNA (Grekova et al., 2010). It is rather conceivable that ΔT3274C near the 5- fold pore plays a role in the packaging of newly assembled capsid, as this is the site where viral DNA is inserted by the helicase function of the NS1 protein.

The genetic variations within the non- structural gene- encoding regions suggest an altered interaction pattern of the NS1 and NS2 proteins with cellular factors. The NS1/2 double- alteration, yielding an Arginine at residue amino

acid residue 666 of NS1 instead of a Serine, is located within the promoter transactivation domain of this protein. This might favour activation of MVM_{CR} promoters in MEFs, enhancing gene expression, whereas MVMp- NS1 might be discriminated against in this respect. Arguing against this hypothesis is the finding, presented in this work that initial expression of both non- structural and structural proteins of MVMp could be detected and that this expression showed to be at least as efficient as that of MVM_{CR}.

ΔL575S of the NS1 protein might also have an effect on how this protein is able to modulate cellular interactions to enable growth of MVM_{CR} in MEFs. Differential phosphorylation of NS1 is an important feature throughout the viral life cycle, which also contributes to the direct cytotoxicity of this protein. Protein kinase C (PKC)- family members, for example, are known to phosphorylate the NS1- C- terminal region (Lachmann et al., 2008). The fact that the identified change at NS1- position 575 also yields a residue that is potentially prone to phosphorylation raises the possibility that modification at this residue results in an altered function of the protein. It potentially makes possible the interaction of NS1 with another cellular protein, which it was not able to interact with if MVMp's Leucine is present on this position. In fact, mutational analyses of Daeffler and coworkers revealed that changing two PKC- phosphorylation sites, T585 and S588, respectively, to an Alanine interfered with cytotoxicity (Daeffler et al., 2003). In this study, the former mutation impaired host- cell killing, whereas the latter led to an increased viral cytotoxicity. However, the assumption that altered NS1 function, exerting direct cytotoxicity in MEFs, could be the major cause of these cells to be permissive for MVM_{CR} seems rather questionable, since in infection experiments with MEFs, cytopathic effects were equally low for MVM_{CR} as compared than with MVMp. Bearing in mind that MVM_{CR} shows replicative activity in those cells, it is rather conceivable that NS1 exerts an altered function in viral replication processes. Furthermore, the region within which ΔL575S is located is involved in egress mechanisms. By Daeffler and coworkers, it could be shown that mutations of the adjacent phosphorylation sites T585 and S588 affect the cytotoxic potential of MVMp (Daeffler et al., 2003).

The two non- coding alterations are located in the acceptor region of the large intron, which defines splicing of NS1 primary transcripts to generate NS2- pre-mRNA. This suggests that excision of this intron of MVM_{CR}- DNA in MEFs is distinct to that of MVMp. This might lead to a balance- shift between NS1 and NS2 in favour of one of these proteins, which, in turn, might account for the productive infection of MVM_{CR} in MEFs. In western blot experiments of total cell lysates of infected MEFs, NS2 protein could be detected neither for MVM_{CR}, nor for MVMp. This might be attributed to two reasons, first being the relatively slow proliferation of MEFs and second being the high turn- over rate of this protein (Cotmore and Tattersall, 1990). It might be conceivable that enhanced excision of the large splice leads to the favoured generation of NS2, the function of which might be required for MVM_{CR} to replicate in MEFs. This hypothesis is substantiated by the observation of D'Abramo and coworkers that changes in the large splice acceptor of the lymphotropic strain of MVMi led to increased fitness of this virus in fibroblasts, which was attributed to an accumulation of NS2. These mutations caused a shift of tissue tropism, as besides the acquired ability to replicate in fibroblasts, MVMi had lost infectivity in lymphocytes (D'Abramo et al., 2005). Importantly, the two mutations observed in this study are located exactly at the same positions as those identified for MVM_{CR} in this work. These include base alterations at genome positions 1967 and 1970, respectively. D'Abramo found a substitution of a Guanine at position 1970 for an Adenine, present in MVMp. In this work, the opposite was observed. In MVM_{CR}, the Adenine, found in MVMp was substituted for a Guanine. Inversely, in MVM_{CR}, Guanine of nucleotide 1967 was found to be similarly changed to an Adenine as was observed for MVMi upon selection in fibroblasts. In the case of MVMi adapted to fibroblasts, it is apparent that these base alterations lead to an enhanced recognition of this regulatory site by the splice machinery in this cell type. MVM_{CR} has the ability to replicate in MEFs, primary fibroblasts, while MVMp is only able to infect transformed A9 cells. This, however, does not include a shift of tissue- tropism, but only a switch of onco- tropism, in which, in a transformation- dependent manner, MVMp has lost the capability of infecting natural cells. Thus, it remains to be determined whether an altered splice

pattern actually accounts for this advantage of MVM_{CR} to infect primary fibroblasts. Importantly, the ΔG1970A mutation was also observed by Choi and Coworkers, when passaging MVMI in fibroblasts. In this study, an accumulation of NS2 could also be observed (Choi et al., 2005). NS2 was shown to interact with the nuclear export factor Crm1 (Bodendorf et al., 1995). Despite the fact that there is no evidence of neither NS2, nor Crm1 to bind to assembled capsids, mutational disruption of this NS2-Crm1- interaction resulted in retention of progeny virions of MVMp in the nucleus (Miller and Pintel, 2002). Still, it is possible that enhanced interaction of those two proteins mediate a more efficient export of newly produced MVM_{CR} in MEFs, as compared to MVMp. The coding mutation of NS2, found in the present study to generate a Proline at residue 174 in MVM_{CR} in exchange for a Glutamine in MVMp might provide an additional advantage. However, in the light of the observation that export of newly generated virions does not seem to be the limiting factor for MVMp in MEFs, as its infection seems to be aborted already at earlier stages of the infectious cycle, it appears that the potential effect of enhanced NS2 function is probably not the only decisive factor for MVM_{CR} replication in those cells. This is presumable upon the finding that MVMp replication in MEFs seems to be abortive already at earlier steps, since DNA amplification and ssDNA production in MEFs is greatly reduced in comparison to that of MVM_{CR}. Additionally, differential phosphorylation patterns of NS2 proteins of MVM_{CR} and MVMp, respectively, were found in *in vivo* metabolic labeling experiments upon MEF infection (Nüesch, unpublished data) (see figure 25). This suggests that the coding base alteration of this protein- despite not yielding a new amino acid, prone to phosphorylation- gives rise to an alternate phospho- peptide variant, which is not observed for MVMp. This might be due to slight steric alterations of NS2 by the inserted Proline in exchange for Glutamine, adding flexibility to the adjacent polypeptide chain which potentially exposes serine- or threonine residues in proximity of this modification. One such epitope might be a Threonine residue, located only six amino acids upstream of the generated Proline.

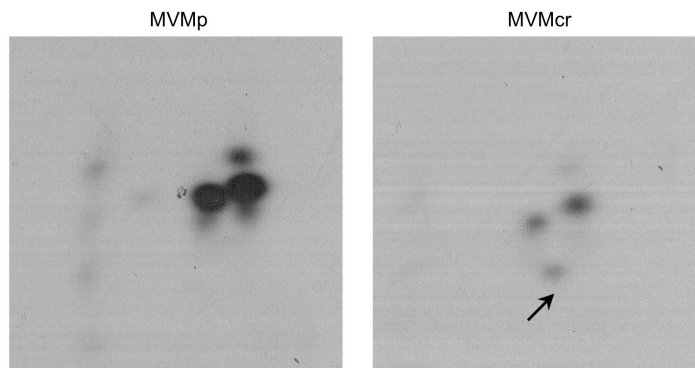


Figure 25. *In vivo* phosphorylation of NS2 in MVMp- and in MVM_{CR}- infected MEFs. Cells were infected with MVMp or MVM_{CR}. *De novo* phosphorylation of NS2 was analyzed by metabolic labeling with ³²P-ATP. NS2 was purified by immunoprecipitation and SDS-PAGE. Phosphorylation of individual NS2- polypeptides was determined by tryptic digest and two-dimensional thin layer electrophoresis and chromatography. Phosphopeptides were revealed by autoradiography. The arrow shows a phosphopeptide that was induced upon MVM_{CR} infection.

6.2 Infectivity of MVMp and MVM_{CR} in MEFs

Southern blot experiments, analyzing viral DNA replication efficiency revealed a clear deficiency of MVMp to do so in MEFs. While ssDNA production in MVM_{CR}-infected cells was observed in all applied MOIs, MVMp infection caused comparably low DNA amplification during the time- course of the experiment which eventually decreased to an almost undetectable level of ssDNA in the lower applied MOIs. In contrast, as expected, in A9 cells both viruses were capable of efficiently replicating DNA and a clear correlation between the different applied MOIs could be observed, meaning that the onset of *de novo* synthesis could be detected at a strongest level in cells, infected with the highest MOI of 2 PFU/ml.

On a protein level, MVMp gene products could be observed. This finding, which appears counterintuitive, has to be interpreted in conjunction with the fact that after an initial increase of both structural- and non- structural proteins, their level drops again to an almost undetectable level, as seen for NS1 in MEFs 72h p.i. at an MOI of 10 PFU/ml. This could be explained in a way that delivery of

MVMp- DNA to nuclei of MEFs is generally intact and that unpackaging and conversion of the negative strand genome to a positive sense- transcription template is also not suppressed in those cells, so that initial transcription can take place. In A9 cells, MVMp infection resulted in detectable NS1 protein 24h p.i. which increased until the endpoint of the experiment. The fact that in MEFs, MVMp- NS1 dropped markedly 24h p.i. thus suggests that inhibition of the viral replication cycle is triggered at a point later than the stage of viral translocation to the nucleus and initiation of protein expression. Possibly, viral patterns, produced during this process are recognized by antiviral sensors, which mediate the shut-off of any further DNA- and protein synthesis, an effect which MVM_{CR} might possibly be able to counteract.

Despite the fact that MVM_{CR} showed productive infection of MEFs, as shown by southern blot analysis of viral DNA replication, onset of protein production appeared to be delayed in comparison to MVMp. This might be attributed to the fact that MVM_{CR}, utilized to test replication efficiency derived from a stock, distinct from that used for analyses on protein production. This second stock, produced on MEFs (see results) had possibly yielded a lower titer than presumed by the calculations of the plaque assay, performed for this virus. Initially, another MVM_{CR}- stock had also been produced through infection of NBK cells, yielding a titer which was higher by an approximate factor of 10^3 than that obtained by infected MEFs. This was attributed to the substantially slower proliferation rate of the primary cells. However, the MVM_{CR}- stock produced on NBK cells was not applied for further study, since infection of MEFs led to the observation of an altered phenotype of this virus compared that produced in MEFs. In terms of dynamics of viral protein production, this phenotype resembled that observed for MVMp in MEFs and it showed an initial increase in NS1 production, which eventually dropped again radically (data not shown). This suggests that MVM_{CR} particles of this stock acquired genetic changes which result during the production process, which rendered them incapable of infecting MEFs. This, in turn, might be attributable to a decreased selective pressure in NBK cells, enabling the emergence of MVM_{CR} particles which lack the genetic integrity, critical for productive infection of MEFs. Another reason of

the apparently delayed propagation of MVM_{CR} in MEFs might be that stocks were not produced from infectious clones of that virus, but from a solution of infectious particles. This raises the probability that a more- or- less heterogeneous mixture of coexisting quasispecies is present in the viral stocks, of which each might show different infectivity towards those cells. Additionally, the method applied for isolation of MEFs from pregnant mice bore the chance for a certain heterogeneity within the obtained cell entity, including cell types that were not susceptible to MVM_{CR} infection. This seems conceivable, since in immunofluorescence microscopic analysis of infected MEFs, a relatively low proportion of NS1- positive cells in the whole population was observed despite administration of an MOI of 10 PFU/ml.

Another observation of an obviously reduced cell- death rate in MVM_{CR}- compared to mock- infected- as well as to MVMp- infected MEFs, was made. In infection experiments those cells infected with MVM_{CR} grew at a faster rate and at the final time- point, these cells had reached higher confluency as compared to mock- treated cells. This interesting observation might be an effect of MVM_{CR} interfering with cellular mechanisms counteracting viral infection. In case MVM_{CR} is able to counteract antiviral responses, this might cause the cells to maintain their proliferative state by not shutting off protein synthesis, for example.

6.3 Susceptibility of MEFs towards MVM_{CR}

The presented study clearly suggests that productive MVM_{CR} infection of MEFs lies in the intrinsic ability of this virus to counteract antiviral responses in these cells. Decreased levels of p65 and p50, the peptides forming the NFκB1 signaling complex which signal to the nucleus to induce type- I IFN expression, could be detected upon infection with MVM_{CR}, as compared to MVMp. As mentioned earlier, NFκB1- activation is, amongst others, mediated by intracellular recognition of viral patterns, either in the endosome or in the cytoplasm. For AAV, the engagement of endosomal TLR9 receptor was

suggested by Jayandharan and coworkers to be the factor to sense parvoviral DNA upon entry into the target cell (Jayandharan et al., 2011; Zhu et al., 2009). Additionally, work by Grekova and coworkers showed an MVMP- dependent upregulation of TLR3 in MEFs (Grekova et al., 2010). The fact that parvoviruses are ssDNA- viruses and that TLR3 is considered to be a sensor of dsRNA, appears intriguing to this argument, but it can not be excluded that viral transcription intermediates, forming secondary structures might, through autophagy, stimulate TLR3 activation in endosomes. The observed reduction of NF κ B1- forming factors in MEFs suggests that MVM_{CR} in some way evades or suppresses this antiviral signaling cascade. Since cellular pattern recognition receptors against viruses are considered to target majorly their nucleic acid components, it seems rather unlikely that the identified capsid modifications account for an altered recognition of the MVM_{CR} particle compared to MVMP.

PKR induction was observed upon infection of MEFs with both, MVMP and MVM_{CR}. By phosphorylation of the translation- initiation factor eIF2 α , PKR mediates a shut- off of macromolecular synthesis to impair viral growth. Ventoso and coworkers showed that PKR activation in MEFs upon infection with MVMP is critical, since inhibition of this kinase led to an increased production of viral proteins. In this study, apart from an induction of PKR by MVM_{CR}, increased amounts of phosphorylated eIF2 α was also found (Ventoso et al., 2010). However, since despite these observations, levels of NS1 protein were found to clearly increase irrespective of a potential translation inhibition, it is conceivable that PKR induction is not a potent inhibitor of MVM_{CR} infection in MEFs.

This study hypothesized that MVMP inhibits the cellular type I IFN response at a certain point. Recognition of a virus in a cell leads to IFN- β induction, which signals in an autocrine and paracrine-, Jak-Stat- mediated manner to trigger an antiviral state of surrounding cells. According to this, MVM_{CR} was expected to suppress this signaling cascade at one- or possibly various stages. In fact, it could be shown that, after an initial induction for up to 24h p.i. with MVM_{CR} in MEFs, Stat1- levels were decreasing to an almost undetectable level. This is

another observation, which suggests that antiviral signaling in these cells cannot be properly exerted upon infection with MVM_{CR}. Surprisingly, an inverse effect was observed for Stat1. While Stat2 was decreasing, Stat1 showed a time- dependent induction. One reason for this might be that induction of Stat1 might in this case not be sufficient for efficient antiviral signaling and that the missing Stat2 depicts the absence of a binding partner needed by Stat1 to activate interferon- stimulated genes. In this respect, it would be important to determine levels of phosphorylated forms of Stats, in order to find whether not only altered induction of these proteins, but also their reduced activation leads to an advantage of MVM_{CR} to grow in MEFs. The relatively low levels of MVMp- induced Stats can be interpreted in a way that viral life cycle is aborted already at earlier stages in infected cells and that they do not necessarily need an IFN- β - mediated Stat- activation. This must also be seen in the light of the fact that the used MOI of 1 PFU/ml was relatively low. Employing an MOI of 10 PFU/ml, a time- course dependent accumulation- and also phosphorylation of Stats could be detected in MEFs upon infection with MVMp by Grekova and coworkers, suggesting that the number of MVMp particles, present per cell have an influence on how fast this virus can be eradicated by MEFs (Grekova et al., 2010).

Induction of SGTA in MEFs was a very interesting feature of MVM_{CR} infection. This protein was formerly identified by Cziepluch and coworkers as an interaction partner of NS1, showing accumulation in APAR bodies during parvoviral replication, which suggested a specific role of SGTA in the parvoviral life cycle (Cziepluch et al., 1998). In this study, SGTA was found to be both upregulated and differentially distributed upon MVM_{CR}- infection, compared to MVMp. In MVM_{CR}- infected MEFs, a marked amount of this protein was found to relocate to the cytoplasm and to cytoplasmic membranes. This is somewhat surprising, since former studies on SGTA dynamics during MVM infection showed that it colocalizes with NS1- and to be present to a large extent in the nucleus. IFIT proteins have been shown to bind viral 3'- triphosphate RNA and to be strongly upregulated upon IFN- signaling and viral infection (Guo et al., 2000). This specificity towards triphosphate- RNA has been attributed to the

TPR- regions of these proteins (Pichlmair et al., 2011). Specifically, crystallographic imaging of IFIT proteins revealed the presence of positively charged pockets, which probably account for the RNA- binding (Yang et al., 2012). Since SGTA shares these TPR- motifs with IFIT- proteins, it is possible that this protein also has a specific role in the sensing of viral nucleic acids, thus depicting a novel pattern recognition receptor. However, in case SGTA is able to recognize viral nucleic acids, in the specific case of MVM_{CR}, it is improbable that it accounts for an altered recognition of this virus in comparison to MVMp, as gene transcripts of these two viruses are not expected to show differences in terms of their 3'-/5' termini or their secondary structures. Bearing in mind that 3'-termini of parvoviral mRNAs probably do not account for recognition in a cell, it is conceivable that structural motifs of these parvoviral RNAs, as well as of respective genomes are recognized by cellular recognition factors. This is supported by the findings of Pichlmair and coworkers that MDA5 activation also requires the presence of abnormal RNA structures (Pichlmair et al., 2009). Additionally, RNA- secondary structures contribute to RIG-I activation (Saito et al., 2007). SGTA only disposes of three TPR- motifs, whereas IFITs contain more of these, IFIT2, for example contains nine TPR- repeats. Thus partially self- complementary mRNA of parvoviruses or the terminal hairpins of their respective genomes are probably too big to fit into a potential binding pocket of monomeric SGTA. However, as TPR- motifs are capable for homooligomerization, it is possible that SGTA forms a complex multiple monomers, which is able to sense parvoviral structures (Lamb et al., 1995). In MEFs, the recruitment of SGTA to cytoplasmic scaffold- and to post- nuclear membrane- structures upon MVM_{CR}- infection might suggest that there is a certain interaction of the virus with this protein in those compartments. It is imaginable that the role of SGTA in susceptibility of MEFs towards MVM_{CR} lies in binding of this protein to viral DNA, shielding it from recognition by cellular pattern recognition receptors such as TLR9 or DAI. This would preclude that there exist structural differences between MVM_{CR} and MVMp. These differences are most likely to be found in the hairpins of their respective ITR- regions. Therefore, it would be important to determine, whether adaptation of

MVMp to A9 fibroblasts caused alterations within these regions. This hypothesis would be consistent with the finding that NFκB1 activation seems to be decreased in MVM_{CR}- infected MEFs, as this signaling complex is an effector of both endosomal- and cytoplasmic pattern recognition receptors. This would mean that MVM_{CR} is able to evade antiviral counteraction in MEFs at an early stage of infection, whereas MVMp is recognized in those cells and is subsequently aborted.

During this study, another interesting observation was made. In immunofluorescent microscopy, the RNA- processing- associated protein CPSF6, formerly shown to be an interaction partner of parvoviral NS1, appeared to be upregulated markedly stronger upon MVM_{CR}- than upon MVMp infection. Also, this protein colocalized with MVM_{CR} NS1 in the nucleus, whereas this was not obvious for MVMp NS1. CPSF6 also appeared to be redistributed into the cytoplasm in cells, infected with MVM_{CR}. Furthermore, immunofluorescent microscopic analysis of infected MEFs suggested an upregulation of DDX18 and hnRNP-Q and also a nuclear colocalization of these proteins with NS1 in infected cells. However, in this case, effects did not seem to differ between the two viruses. As mentioned earlier, these proteins are associated with mRNA metabolism. This suggests that NS1 could potentially redirect these RNA- editing factors towards viral gene transcripts to favour maturation of viral RNAs over cellular ones and to enhance viral protein expression, while cellular RNA translation would be impaired. This scheme goes well together with the notion that NS1 expression mediates arrest in S- or S/G2- stages of the cell cycle, respectively (Anouja et al., 1997). During S-phase, cellular DNA amplification is shut- down due to the recruitment of replication factors, such as DNA- polymerase (POL) α, to APAR bodies. A parallel hijacking of the post- transcriptional RNA- processing machinery by NS1 would add an additional component to parvovirus- induced deregulation of cellular processes, complementing the disturbances seen on the level of replication. This scheme would not be the first of this kind to be observed, since other cases of viral perturbations of the cellular RNA- processing machinery are known. For instance, NS1 of influenza A virus interacts with the poly(A) binding

protein nuclear 1 (PABPN1). This protein is necessary for proper polyadenylation and interference of influenza A with this mechanism has been shown to reduce host cell mRNA maturation and –export (Chen and Krug, 2000; Chen et al., 1999). Importantly, PABPN1 forms a complex with CPSF6, possibly providing a link to the potential strategy of MVM_{CR} to prevail in MEFs. Additionally, a redistribution of transcription- associated proteins has recently been observed upon infection with CPV (Ihalainen et al., 2012). In this study, a nuclear reorganization of proteins, associated with transcription (such as TATA-binding protein and transcription factor II α), RNA- processing (PABPN1) and - export (Tap protein) has been identified. Also, the mRNA- transport factor CRM1 is essential for the nuclear export of influenza A- mRNA (Sandri-Goldin, 2004). As mentioned earlier, CRM1 was also shown to interact with parvoviral NS2. This depicts a potential link to MEF- permissiveness for MVM_{CR}, since the alteration in the NS2 amino acid sequence in comparison to MVMp obviously lead to an altered phosphorylation pattern of this protein in those cells. This might enable MVM_{CR}- NS2 to enhance viral mRNA- export, possibly via an increased binding- affinity towards CRM1.

The fact that hnRNPs are important in viral infection was shown by Pichlmair and coworkers, which stated that hnRNP U depicts a critical node, targeted by multiple distinct viruses (Pichlmair et al., 2012). In a work by Harris and coworkers, parvoviral NS1 was observed to interact with a formerly unknown protein, called NS1- associated protein 1 (NSAP1) (Astell et al., 1998). This protein shows an 80%- sequence homology with the heterogeneous ribonucleoprotein hnRNP R. The observation of the present study that, in MEFs, hnRNP Q seems to be upregulated and also to be colocalizing with NS1 upon infection with MVM adds another clear hint that parvoviruses are able to interfere with the host- cellular RNA- processing machinery.

Taken together, this study provided clear hints that the observed genetic alterations, identified in MVM_{CR}, compared to MVMp, lead to a modulation of the antiviral machinery in MEFs. Also, it seems probable that, by modified functions of the NS1- or NS2 proteins or by accumulation of the latter, this virus

is able to utilize the cellular RNA- metabolism machinery to its own advantage in order to efficiently replicate in those primary cells. However, further studies will need to be conducted in order to provide an indepth view of the exact molecular mechanisms behind the presented obervations in order to pinpoint the actual factors that account for MVM_{CR} permissibility in MEFs. Therefore, a detailed analysis of the type-I IFN response will be necessary. To learn, which base alterations in the MVMp genome account for infectiousness in MEFs, single- and combined mutant variants will have to be assayed for replication potential in those cells. From a virologic point of view, this will be important to potentially identify novel interaction points at which viruses interfere with cell integrity. In respect to oncolytic therapy, these findings will help to define critical safety points in parvoviral anticancer treatment, in order to decrease the danger of a potential host- range switch in patients from cancerous- to healthy tissue. This knowledge could furthermore add to the attempt to fight viral infections, as other viral species might share similar mechanisms to modulate cellular antiviral responses.

7. Summary

Although significant improvements have been achieved during the last decades there are still a large number of cancers (e.g. glioma, PDAC, malignant melanoma) with only limited treatment potential and poor prognosis. Therefore, new therapies are desperately needed. Oncolytic virotherapy is an emerging field in cancer research and among the agents under consideration, rodent parvoviruses (PV) are promising candidates due to their natural oncotropism, their specific killing potential for neoplastically transformed cells, and their oncosuppressive potential combined with their low pathogenicity for humans.

A key issue for a successful virotherapy of cancer with self-propagating agents resides in the specific attack of tumor cells, while normal tissue remains unaffected. This is often achieved due to the interplay between the virus and the host innate immune system, which is altered/defective upon transformation and therefore allows the agent to propagate under these conditions, while healthy tissues, effecting an intact anti-viral response, are protected. Parvovirus MVMp was recently shown to be able to induce an interferon β -mediated anti-viral response in normal mouse embryonic fibroblast cells (MEFs) leading to an abortive infection, while transformed A9 cells, proficient for virus propagation did not. However, on a molecular level, very little is known about the interaction of parvoviruses with the host cell- innate immune system. Gaining deeper insight in these mechanisms will not only help us to better evaluate the safety of administration of this potential therapeutic agent, but also teach us the potential use of an innate immune-response to initiate a potential immune response directed towards (infected) tumor cells.

The current study aimed to investigate the MVM interplay with the antiviral activity executed in MEFs comparing the prototype strain MVMp with MVM_{CR}. While the former variant was shown to induce an effective antiviral response leading to an abortive infection in these host cells, the latter strain was thought to sustain propagating being able to counteract this host defense mechanism.

To this end, an old isolate, dated back to 1968 was amplified in MEFs and compared to MVMP for its replication capacity, genetic differences and induction of antiviral responses. The latter investigations aimed at the identification of potential cellular sensors as well as targets for the virus to counteract the host responses. The genetic differences should reveal the plasticity of the agent to adopt growth in a restrictive environment generated by the host innate immune response.

From two old isolates obtained by Günter Siegl, I was able to amplify one, the 1968 isolate in MEFs. This virus isolate revealed six genetic differences to the well characterized MVMP strain, of which four affected the properties of the non-structural proteins NS1/NS2 and two were associated with the viral capsid. The four changes in the non-structural gene region placed into MVMP back-bone were sufficient to allow viral DNA amplification and progeny virus particles production in MEFs, although at very low efficiency. Even though, I was not able to reproduce previously published MEF-induced antiviral activities, comparison of MVMP versus MVM_{CR} infection of MEFs revealed interesting findings in regard to the search of host cell sensors and targets for a virus-induced counteracting activity: (i) SGTA, a tetratricopeptide-containing protein was induced by MVMP and MVM_{CR} to associate to (post-nuclear) membrane structures, which could resemble endosomes as early as 4 h post-infection. In analogy to the recently described tritetratricopeptide-containing IFIT-proteins, sensing unique viral 5'-RNA-structures this NS1-interacting protein could be a host cell sensor for PV genomic DNA. The 5'end, being able to form a secondary structure extrudes from the five-fold pore of infecting capsids. (ii) A common feature of virus targets to counteract host antiviral responses was identified in complexes of viral proteins with host mRNA processing factors. Among three NS1-interacting mRNA modifying enzymes, DDX18, hnRNP-Q, CPSF6, only the latter product was specifically targeted by MVM_{CR} but not MVMP. It seems feasible to further investigate the targeting of this mRNA-processing/polyadenylation/export factor as a target for PV-induced counteracting activity of the host cell innate immune response.

In summary, this study provided the basis for the characterization of the virus host cell interplay with the innate immune system. The identification of genetic alterations will allow either alone or in combination to determine their impact on virus growth, antiviral activities, and counteracting activities in MEFs. Thereby SGTA seems to be an attractive potential target for further investigation as a viral sensor. On the other hand the interaction of NS1 with the mRNA processing enzymes, particularly CPSF6, deserves particular consideration as (a) viral target(s) to counteract the host antiviral response.

8. Zusammenfassung

Wenngleich signifikante Verbesserungen über die vergangenen Jahrzehnte erzielt werden konnten, besteht weiterhin eine große Anzahl an Krebsarten (wie zum Beispiel Gliom, Pankreaskarzinom, malignes Melanom) mit nur limitiertem Behandlungspotential und schlechter Prognose. Aus diesem Grund sind neue Therapieansätze dringend notwendig. Onkolytische Virotherapie ist ein aufstrebender Bereich der Krebsforschung. Unter den viralen Agenzien, die in diesem Belang in Betracht gezogen werden sind Nager- Parvoviren vielversprechende Kandidaten aufgrund ihres natürlichen Onkotropismus, deren Potential, neoplastisch transformierte Zellen spezifisch zu töten sowie aufgrund ihrer onkosuppressiven Effekte kombiniert mit einer vergleichsweise geringen Pathogenizität im Menschen.

Ein Schlüsselprinzip einer erfolgreichen Virotherapie gegen Krebs mit Propagierungs- kompetenten Agenzien liegt in der spezifischen Attackierung von Tumorzellen, während normales Gewebe von dieser unberührt bleibt. Dies ist oft bedingt durch das Zusammenspiel des Virus mit dem angeborenen Immunsystem der Wirtszelle. Dieses ist oft Transformations- bedingt beeinträchtigt oder defekt, was unter diesen Umständen eine Propagierung des viralen Agens zulässt, während gesunde Gewebe über eine intakte antivirale Antwort verfügen und somit geschützt sind. Es wurde vor Kurzem gezeigt, dass das Parvovirus MVMp eine Interferon- β - medierte, antivirale Antwort in normalen embryonalen Mäusefibroblasten (MEFs) induziert, was zu einer abortiven Infektion führt, während dieser Effekt in transformierten A9 Fibroblasten, welche permissiv für dieses Virus sind nicht beobachtet werden konnte. Auf molekularer Ebene ist jedoch sehr wenig über die Interaktionen von Parvoviren mit dem angeborenen Immunsystem ihrer Wirtszellen bekannt. Einen tieferen Einblick in diese Mechanismen zu bekommen wird nicht nur dabei helfen, die sichere Anwendung dieser potentiellen Therapeutika besser zu evaluieren, sondern auch eine potentielle Benutzung des angeborenen Immunsystems anzudenken, welche gegen (infizierte) Tumorzellen gerichtet ist.

Die vorliegende Studie hatte zum Ziel, das Zusammenspiel von MVM mit der antiviralen Aktivität in MEFs zu untersuchen, wobei der Prototyp- Stamm MVMp mit MVM_{CR} verglichen wurde. Während für ersteres Virus eine effective antivirale Antwort gezeigt werden konnte, welche zu einer abortiven Infektion in diesen Zellen führt, konnte letzterer Stamm propagieren, was seiner angenommenen Fähigkeit zugesprochen wird, diesen zellulären Abwehrmechanismus zu bekämpfen. Zu diesem Zweck wurde ein altes Isolat (1968) in MEFs amplifiziert und mit MVMp auf dessen Replikationskapazität, genetische Differenzen sowie Induktion antiviraler Antworten untersucht. Letztere Untersuchungen zielten darauf ab, potentielle zelluläre Sensoren sowie Zielpunkte viraler Bekämpfung der Wirts- Immunantwort zu identifizieren. Die genetischen Unterschiede sollten die Dynamik dieser Agenzien aufdecken, Wachstumsfähigkeit in einer restriktiven Umgebung, bedingt durch eine angeborene Immunantwort des Wirts, wiederzuerlangen.

Von zwei Isolaten, welche von Günter Siegl bezogen wurden, war es möglich, eines- das 1968- Isolat- in MEFs zu amplifizieren. Dieses Virusisolat zeigte sechs genetische Differenzen gegenüber dem gut charakterisierten MVMp- Stamm, von welchen vier die Eigenschaften der Nicht- Strukturproteine betraf und zwei mit einer Veränderung des viralen Kapsid assoziiert waren. Platzierung der vier Alterierungen der nicht- strukturellen Genregion in das MVMp Genom waren ausreichend, virale DNA Amplifikation sowie Produktion neuer Viruspartikel in MEFs zu erlauben, wenngleich mit niedriger Effizienz. Obwohl es nicht möglich war, die zuvorgehend publizierten MEF- induzierten antiviralen Aktivitäten zu reproduzieren, zeigte der Vergleich zwischen MVMp gegenüber MVM_{CR} Infektion in MEFs interessante Befunde hinsichtlich der Suche nach Wirtszell- Sensoren und nach Angriffspunkten einer viralen Bekämpfungsstrategie: (i) SGTA, ein Tetratricopeptid- beinhaltendes Protein, wurde durch MVMp und MVM_{CR} bereits 4h nach Infektion induziert und assoziierte mit post- nukleären Membranstrukturen, welche Endosomen darstellen könnten. In Analogie zu den kürzlich beschriebenen Tetratricopeptid- beinhaltenden IFIT- Proteinen, welche an einzigartige virale 5'- RNA Strukturen binden, könnte obiges NS1- bindende Protein als Wirtszell- Sensor für

genomische DNA von Parvoviren fungieren. Das 5'-Ende, welches in der Lage ist, Sekundärstrukturen auszubilden, ist durch die 5-fach Pore des infizierenden Kapsids nach Außen exponiert. (ii) Ein gemeinsamer Mechanismus von Viren, intrazelluläre antivirale Antworten zu unterdrücken liegt in der Identifizierung von Komplexen viraler Proteine mit Wirts-mRNA-Prozessierungsfaktoren. Unter drei NS1-interagierenden-, mRNA-modifizierenden Enzymen, DDX18, hnRNP-Q und CPSF6, wurde nur Letzteres ein spezifisches Ziel von MVM_{CR}, jedoch nicht von MVMP zu sein. Es erscheint naheliegend, diesen mRNA-Prozessierungsfaktor als Ziel für parvovirale Bekämpfung zellulärer Immunantworten zu untersuchen.

Zusammenfassend lieferte diese Studie die Basis für die Charakterisierung der Interaktion des Virus mit dem angeborenen Immunsystem der Wirtszelle. Die Identifikation der genetischen Alterierungen wird es erlauben, deren Auswirkungen auf virales Wachstum, antivirale Aktivitäten sowie etwaiger Bekämpfungsmechanismen in MEFs, entweder einzeln, oder kombiniert zu bestimmen. Diesbezüglich scheint SGTA als viraler Sensor einen attraktiven, potentiellen Ausgangspunkt für weitere Untersuchungen darzustellen. Auf der anderen Seite verdient die Interaktion von NS1 mit mRNA-Prozessierungs-Proteinen, im Speziellen CPSF6, besondere Aufmerksamkeit als viraler Angriffspunkt, eine antivirale Antwort der Wirtszelle zu bekämpfen.

9. References

- Agbandje-McKenna, M., Llamas-Saiz, A.L., Wang, F., Tattersall, P. and Rossmann, M.G. 1998. Functional implications of the structure of the murine parvovirus, minute virus of mice. *Structure*. 6(11):1369-81.
- Allaume, X., El-Andaloussi, N., Leuchs, B., et al. 2012. Retargeting of rat parvovirus H-1PV to cancer cells through genetic engineering of the viral capsid. *J Virol*. 86(7):3452-65.
- Anouja, F., Wattiez, R., Mousset, S., Caillet-Fauquet, P. 1997. The cytotoxicity of the parvovirus minute virus of mice nonstructural protein NS1 is related to changes in the synthesis and phosphorylation of cell proteins. *J Virol*. 71(6):4671-8.
- Bashir, T., Horlein, R., Rommelaere, J. and Willwand, K. Cyclin A activates the DNA polymerase delta -dependent elongation machinery in vitro: A parvovirus DNA replication model. 2000. *Proc Natl Acad Sci U S A*. 97(10):5522-7.
- Bär, S., Daeffler, L., Rommelaere, J. and Nüesch, J.P. 2008. Vesicular egress of non-enveloped lytic parvoviruses depends on gelsolin functioning. *PLoS Pathog*. 4(8):e1000126.
- Berg, J.M., Tymoczko, J.L. and Stryer, L. (2007) *Biochemistry* (6 ed.), New York: WH Freeman & Co.
- Bodendorf, U., Cziepluch, C., Jauniaux, J.C., Rommelaere, J. and Salomé, N. 1999. Nuclear export factor CRM1 interacts with nonstructural proteins NS2 from parvovirus minute virus of mice. *J Virol*. 73(9):7769-79.
- Carter, B. J. 2006. Clinical development with adeno-associated virus vectors. *Parvoviruses*. Kerr, J.R., Cotmore, S.F., Bloom, M., Linden, R. and Parrish, C.R.; London, Hodder Arnold; 499-510.
- Cattaneo, R., Miest, T., Shashkova, E.V. and Barry, M.A. 2008. Reprogrammed viruses as cancer therapeutics: targeted, armed and shielded. *Nat Rev Microbiol*. (7):529-40.
- Chapman, M. S., Agbandje-McKenna, M. 2006. Atomic structure of viral particles. *Parvoviruses*. Kerr, J.R., Cotmore, S.F., Bloom, M., Linden, R. and Parrish, C.R.; London, Hodder Arnold; 125-140.
- Chen, Z. and Krug, R.M. 2000. Selective nuclear export of viral mRNAs in influenza-virus-infected cells. *Trends Microbiol*. 8(8):376-83.
- Chen, Z., Li, Y. and Krug RM. 1999. Influenza A virus NS1 protein targets poly(A)-binding protein II of the cellular 3'-end processing machinery. *EMBO J*. 18(8):2273-83.
- Choi, E.Y., Newman, A.E., Burger, L. and Pintel, D. 2005. Replication of minute virus of mice DNA is critically dependent on accumulated levels of NS2. *J Virol*. 79(19):12375-81.
- Corbau, R., Salomé, N., Rommelaere, J. and Nüesch, J.P. 1999. Phosphorylation of the viral nonstructural protein NS1 during MVMp infection of A9 cells. *Virology*. 259(2):402-15.
- Cornelis, J. J., Deleu, L., Koch, U. and Rommelaere, J. (2006). Parvovirus oncosuppression. *Parvoviruses*. Kerr, J.R., Cotmore, S.F., Bloom, M., Linden, R. and Parrish, C.R.; London, Hodder Arnold; 365-376.

- Cotmore, S. F. and Tattersall, P. 1988. NS-1 polypeptide of minute virus of mice is covalently attached to the 5' termini of duplex replicative-form DNA and progeny single strands. *J Virol.* 62:851-60.
- Cotmore, S.F. and Tattersall, P. 1990. Alternate splicing in a parvoviral nonstructural gene links a common amino-terminal sequence to downstream domains which confer radically different localization and turnover characteristics.
- Cotmore, S. F., Tattersall, P. 2006. Structure and organization of the viral genome. *Parvoviruses*. Kerr, J.R., Cotmore, S.F., Bloom, M., Linden, R. and Parrish, C. Cotmore, S.F. and Tattersall, P. 2007. Parvoviral host range and cell entry mechanisms. *Adv Virus C.R.*; London, Hodder Arnold; 73-94.
- Crawford, L.V. 1966. A minute virus of mice. *Virology* 29: 605-612
- Cziepluch, C., Kordes, E., Poirey, R., Grewenig, A., Rommelaere, J. and Jauniaux, J.C. 1998. Identification of a novel cellular TPR-containing protein, SGT, that interacts with the nonstructural protein NS1 of parvovirus H-1. *J Virol.* 72(5):4149-56.
- Cziepluch. C., Lampel, S., Grewenig, A., Grund, C., Lichter, P. and Rommelaere J. 2000. H-1 parvovirus-associated replication bodies: a distinct virus-induced nuclear structure. *J Virol.* 74(10):4807-15.
- D'Abramo, A.M., Ali, A.A., Wang, F., Cotmore, S.F. and Tattersall P. 2005. Host range mutants of Minute Virus of Mice with a single VP2 amino acid change require additional silent mutations that regulate NS2 accumulation. *Virology.* 340(1):143-54.
- Daeffler, L., Hörlein, R., Rommelaere, J. and Nüesch, J.P. 2003. Modulation of minute virus of mice cytotoxic activities through site-directed mutagenesis within the NS coding region. *J Virol.* 77(23):12466-78.
- Dettwiler, S., Aringhieri, C., Cardinale, S., Keller, W. and Barabino, S.M. 2004. Distinct sequence motifs within the 68-kDa subunit of cleavage factor Im mediate RNA binding, protein-protein interactions, and subcellular localization. *J Biol Chem.* 279(34):35788-97.
- Dubaele, S., Chène, P. 2007. Cellular studies of MrDb (DDX18). *Oncol Res.* 16(12):549-56.
- Dupressoir, T., Vanacker, J.-M., Cornelis, J.J., Duponchel, N. and Rommelaere, J. 1989. Inhibition by Parvovirus H-1 of the Formation of Tumors in Nude Mice and Colonies in Vitro by Transformed Human Mammary Epithelial Cells. *Cancer Res* 49:3203-3208
- Eichwald, V., Daeffler, L., Klein, M., Rommelaere, J. and Salomé, N. 2002. The NS2 proteins of parvovirus minute virus of mice are required for efficient nuclear egress of progeny virions in mouse cells. *J Virol.* 76(20):10307-19.
- Faisst, S., Guittard, D., Benner, A., Cesbron, J.Y., Schlehofer, J.R., Rommelaere, J. and Dupressoir, T. 1998. Dose-dependent regression of HeLa cell-derived tumours in SCID mice after parvovirus H-1 infection. *Int J Cancer.* 75(4):584-9.
- Finkelstein, S.E. and Fishman, M. 2012. Clinical opportunities in combining immunotherapy with radiation therapy. *Front Oncol.* 2012; 2: 169.
- Fuertes, M.B., Woo, S.R., Burnett, B., Fu, Y.-X. and Gajewski, T.F. 2012. Type I

- interferon response and innate immune sensing of cancer. *Trends in Immunology*. 1471-4906
- Gardiner, E.M. and Tattersall P. 1988. Mapping of the fibrotropic and lymphotropic host range determinants of the parvovirus minute virus of mice. *J Virol*. 62(8):2605-13.
- Geletneky, K., Huesing, J., Rommelaere, J. et al. Cancer. 2012. Phase I/IIa study of intratumoral/intracerebral or intravenous/intracerebral administration of Parvovirus H-1 (ParvOryx) in patients with progressive primary or recurrent glioblastoma multiforme: ParvOryx01 protocol. 12: 99.
- Geletneky, K., Kiprianova, I., Ayache, A., Koch, R., Herrero Y Calle, M., Deleu, L., Sommer, C., Thomas, N., Rommelaere, J. and Schlehofer, J.R. 2010. Regression of advanced rat and human gliomas by local or systemic treatment with oncolytic parvovirus H-1 in rat models. *Neuro Oncol*. 2010 Aug;12(8):804-14.
- Grekova, S., Zawatzky, R., Hörlein, R., Cziepluch, C., Minckberg, M., Davis, C., Rommelaere, J. and Daeflfer, L. 2010. Activation of an Antiviral Response in Normal but Not Transformed Mouse Cells: a New Determinant of Minute Virus of Mice Oncotropism. *J Virol*. 84(1): 516–531.
- Guo, J., Hui, D.J., Merrick, W.C. and Sen, G.C. 2000. A new pathway of translational regulation mediated by eukaryotic initiation factor 3. *EMBO J*. 19(24):6891-9.
- Haller, O., Kochs, G. and Weber, F. 2006. The interferon response circuit: induction and suppression by pathogenic viruses. *Virology*. 344(1):119-30.
- Harris, C.E., Boden, R.A. and Astell, C.R. 1999. A novel heterogeneous nuclear ribonucleoprotein-like protein interacts with NS1 of the minute virus of mice. *J Virol*. 73(1):72-80.
- Harris, R. E., Coleman, P. H. and Morahan, P.S. 1974. Erythrocyte association and interferon production by minute virus of mice. *Proc Soc Exp Biol Med* 145, 1288-1292.
- Hueffer, K. and Parrish, C.R. 2003. Parvovirus host range, cell tropism and evolution. *Curr Opin Microbiol*. 6(4):392-8.
- Ihalainen, T.O., Willman, S.F., Niskanen, E.A., Paloheimo, O., Smolander, H., Laurila, J.P., Kaikkonen, M.U. and Vihinen-Ranta, M. 2012. Distribution and Dynamics of Transcription-Associated Proteins during Parvovirus Infection. *J Virol*. 86(24):13779-84.
- Jayandharan, G.R., Aslanidi, G., Martino, A.T., Jahn, S.C., Perrin, G.Q., Herzog, R.W. and Srivastava A. 2011. Activation of the NF-kappaB pathway by adeno- associated virus (AAV) vectors and its implications in immune response and gene therapy. *Proc Natl Acad Sci U S A*. 108(9):3743-8.
- Kabat, J.L., Barberan-Soler, S. and Zahler, A.M. 2009. HRP-2, the *Caenorhabditis elegans* homolog of mammalian heterogeneous nuclear ribonucleoproteins Q and R, is an alternative splicing factor that binds to UCUAUC splicing regulatory elements. *J Biol Chem*. 284(42):28490-7.
- Kaufmann, J.K. and Nettelbeck, D.M. 2012. Virus chimeras for gene therapy,

- vaccination, and oncolysis: adenoviruses and beyond. *Trends Mol Med*.18(7):365-76.
- Lachmann, S., Bär, S., Rommelaere, J. and Nüesch, J.P. 2008. Parvovirus interference with intracellular signalling: mechanism of PKC ϵ activation in MVM-infected A9 fibroblasts. *Cell Microbiol.* (3):755-69.
- Lamb, J.R., Tugendreich, S. and Hieter, P. 1995. Tetrahedral peptide repeat interactions: to TPR or not to TPR? *Trends Biochem Sci.* 20(7):257-9.
- López-Bueno, A., Rubio, M.P., Bryant, N., McKenna, R., Agbandje-McKenna, M. and Almendral, J.M. 2006. Host-selected amino acid changes at the sialic acid binding pocket of the parvovirus capsid modulate cell binding affinity and determine virulence. *J Virol.* 80(3):1563-73.
- Malathi, K., Saito, T., Crochet, N., Barton, D.J., Gale, M. Jr and Silverman, R.H. 2010. RNase L releases a small RNA from HCV RNA that refolds into a potent PAMP. *RNA.* 16(11):2108-19.
- Miller, C.L. and Pintel, D.J. 2002. Interaction between parvovirus NS2 protein and nuclear export factor Crm1 is important for viral egress from the nucleus of murine cells. *J Virol.* 76(7):3257-66.
- Naeger, L.K., Salomé, N. and Pintel, D.J. 1993. NS2 is required for efficient translation of viral mRNA in minute virus of mice-infected murine cells. *J Virol.* 67(2):1034-43.
- Naik S, Nace R, Federspiel MJ, Barber GN, Peng KW and Russell SJ. 2012. Curative one-shot systemic virotherapy in murine myeloma. *Leukemia.* (8):1870-8.
- Naik, S. and Russell, S.J. 2009. Engineering oncolytic viruses to exploit tumor specific defects in innate immune signaling pathways. *Expert Opinion on Biological Therapy* 9:9, 1163-1176
- Nettelbeck, D.M. 2008. Cellular genetic tools to control oncolytic adenoviruses for virotherapy of cancer. *J Mol Med (Berl).* 86(4):363-77.
- Nüesch, J.P. Regulation of non-structural protein functions by differential synthesis, modification and trafficking. 2006. *Parvoviruses.* Kerr, J.R., Cotmore, S.F., Bloom, M., Linden, R. and Parrish, C.R.; London, Hodder Arnold; 275-290.
- Nüesch, J.P., Bär, S. and Rommelaere, J. Viral proteins killing tumor cells: new weapons in the fight against cancer. 2008. *Cancer Biol Ther.* Sep;7(9):1374- 6.
- Nüesch, J.P., Corbau, R., Tattersall, P. and Rommelaere, J. 1998. Biochemical activities of minute virus of mice nonstructural protein NS1 are modulated In vitro by the phosphorylation state of the polypeptide. *J Virol.* 72(10):8002-12.
- Nüesch, J.P., Lacroix, J., Marchini, A. and Rommelaere J. 2012. Molecular pathways: rodent parvoviruses mechanisms of oncolysis and prospects for clinical cancer treatment. *Clin Cancer Res.* 18(13):3516-23.
- Nüesch, J.P. and Rommelaere, J. 2006. NS1 interaction with CKII α : novel protein complex mediating parvovirus-induced cytotoxicity.
- Nüesch, J.P. and Rommelaere, J. 2007. A viral adapter protein modulating casein kinase II activity induces cytopathic effects in permissive cells. *Proc Natl Acad Sci U S A*; 104(30):12482-7
- Pallier, C., Greco, A., Le Junter, J., Saib, A., Vassias, I. and Morinet, F. 1998.

- The 3' untranslated region of the B19 parvovirus capsid protein mRNAs inhibits its own mRNA translation in nonpermissive cells. *J Virol.* 71(12):9482-9.
- Pichlmair, A., Lassnig, C., Eberle, C.A. et al. 2011. IFIT1 is an antiviral protein that recognizes 5'-triphosphate RNA. *Nat Immunol.* 5;12(7):624-30.
- Pichlmair, A. and Reis e Sousa, C. 2007. Innate recognition of viruses. *Immunity.* 27(3):370-83.
- Pichlmair, A., Schulz, O., Tan, C.P., Rehwinkel, J., Kato, H., Takeuchi, O., Akira, S., Way, M., Schiavo, G. and Reis e Sousa C. 2009. Activation of MDA5 requires higher-order RNA structures generated during virus infection.
- Pitha, P.M. 2000. Introduction: interferon's connection to cancer. *Semin Cancer Biol.* (2):69-72.
- Qiu, J., Yoto, Y., Tullis, G. and Pintel, D.J. 2006. Parvovirus RNA processing strategies. *Parvoviruses.* Kerr, J.R., Cotmore, S.F., Bloom, M., Linden, R. and Parrish, C.R.; London, Hodder Arnold; 253-274.
- Rommelaere, J. and Cornelis, J. J. 1991. Antineoplastic activity of parvoviruses. *Journal of Virology Methods* 33: 233-51.
- Rommelaere, J., Geletneky, K., Angelova, A.L., Daeffler, L., Dinsart, C., Kiprianova, I., Schlehofer, J.R. and Raykov, Z. 2010. Oncolytic parvoviruses as cancer therapeutics. *Cytokine Growth Factor Rev.* 21(2-3):185-95.
- Raykov, Z., Balboni, G., Aprahamian, M. and Rommelaere J. 2004. Carrier cell-mediated delivery of oncolytic parvoviruses for targeting metastases. *Int J Cancer.* 109(5):742-9.
- Rehwinkel, J., Tan, C.P., Goubau, D., Schulz, O., Pichlmair, A., Bier, K., Robb, N., Vreede, F., Barclay, W., Fodor, E. and Reis e Sousa C. 2010. RIG-I detects viral genomic RNA during negative-strand RNA virus infection. *Cell.* 140(3):397-408.
- Rogers, G.L., Martino, A.T., Aslanidi, G.V., Jayandharan, S., Srivastava, A. and Herzog, R.W. 2011. Innate Immune Responses to AAV Vectors. *Front Microbiol.* 2:194.
- Russell, R.J. and Peng, K.-W. 2007. Viruses as anticancer drugs. *Trends Pharmacol Sci.* (7): 326–333.
- Russell, S.J., Peng, K.W. and Bell, J.C. 2012. Oncolytic virotherapy. *Nat Biotechnol.*;30(7):658-70.
- Sandri-Goldin, R.M. 2004. Viral regulation of mRNA export. *J Virol.* 78(9):4389-96.
- Schmid, S.R. and Linder, P. 1992. D-E-A-D protein family of putative RNA helicases. *Mol Microbiol.* 6(3):283-91.
- Siegl, G. 1984. Biology and pathogenicity of autonomous parvoviruses. K. Bern. *The Parvoviruses.* New York: Plenum Press, 297-362.
- Tattersall, P. 1972. Replication of the parvovirus MVM. I. Dependence of virus multiplication and plaque formation on cell growth. *J Virol.* (4):586-90.
- Tattersall, P. 2006. The evolution of parvovirus taxonomy. *Parvovirus oncosuppression.* *Parvoviruses.* Kerr, J.R., Cotmore, S.F., Bloom, M., Linden, R. and Parrish, C.R.; London, Hodder Arnold; 5-14. *J Virol.* 80(10):4729-39.
- Toolan, H. 1990. The rodent parvoviruses. P. Tijssen. *Handbook of Parvoviruses, Volume II.* Boca Raton: CRC Press, 159-176.

- Valdivieso, M., Kujawa, A.M., Jones, T. and Baker, L.H. 2012. Cancer Survivors in the United States: A Review of the Literature and a Call to Action *Int J Med Sci.* 2012; 9(2): 163–173.
- Venkataraman, T., Valdes, M., Elsby, R., Kakuta, S., Caceres, G., Saijo, S., Iwakura, Y. and Barber, G.N. 2007. Loss of DExD/H box RNA helicase LGP2 manifests disparate antiviral responses. *J Immunol.* 178(10):6444-55.
- Ventoso, I., Berlanga, J.J. and Almendral JM. 2010. Translation control by protein kinase R restricts minute virus of mice infection: role in parvovirus oncolysis. *J Virol.* 84(10):5043-51.
- Walsh, D. and Mohr, I. 2011. Viral subversion of the host protein synthesis machinery. *Nat Rev Microbiol.* 9(12):860-75.
- Weitzman, M.D. 2006. The parvovirus life cycle: an introduction to molecular interactions important for infection. *Parvoviruses.* Kerr, J.R., Cotmore, S.F., Bloom, M., Linden, R. and Parrish, C.R.; London, Hodder Arnold; 143-156.
- Yang, Z., Liang, H., Zhou, Q., Li, Y., Chen, H., Ye, W., Chen, D., Fleming, J., Shu, H. and Liu, Y. 2012. Crystal structure of ISG54 reveals a novel RNA binding structure and potential functional mechanisms. *Cell Res.* 22(9):1328-38.
- Zhu, J., Huang, X. and Yang, Y. 2009. The TLR9-MyD88 pathway is critical for adaptive immune responses to adeno-associated virus gene therapy vectors in mice. *J Clin Invest.* 119(8):2388-98.
- Zhukov, N. V. and Tjulandin, S. A. 2008. Targeted Therapy in the Treatment of Solid Tumors: Practice Contradicts Theory. *Biochemistry (Moscow)*, Vol. 73, No. 5, pp. 605-618.

Curriculum Vitae

Personal Details:

Name: Bernhard Englinger
Citizenship: Austrian

Education

09/1998- 06/2006: Secondary school: Goethe- Gymnasium Astgasse (modern languages), 1140 Vienna

Studies:

10/2007-07/2010: Bachelor's degree in Nutritional Sciences, University of Vienna
10/2008-02/2009: Participation at the anatomical dissection course „Organmorphologie II“ at Medical University of Vienna
10/2009-05/2010: Bachelor thesis at the Institute of Medical Chemistry and Pathobiochemistry; Topic: „Effect of carbamylated low-density lipoprotein on protein expression of ATP- binding cassette- transporter A1 and G1 in THP-1 macrophages“
SS 2010+ WS 2010/11: Tutorial contract at University of Vienna for the course „Biochemisches Praktikum für Ernährungswissenschaftler“ at the Institute of Medical Chemistry and Pathobiochemistry
WS 2010/11: Tutorial contract at Medical University of Vienna for the course „BL13- Ernährung und Verdauung“ at the Institute of Medical Chemistry and Pathobiochemistry
Since 10/2010: Master's study of Molecular Biology; focus: cell biology and molecular medicine, University of Vienna
10/2011-01/2012: Internship at the Institute of Cancer Research Vienna, research unit: Development of Experimental Cancer Therapies, Group Walter Berger
02/2012-01/2013: Master Thesis at German Cancer Research Center (DKFZ) Heidelberg, research unit: F010 Applied Tumor Virology; Topic: Autonomous Parvovirus Interaction with the Innate Immune System. P.I.: Dr. Jürg P.F. Nüesch
03/2013-05/2013: Internship at Yale University School of Medicine, Department of Laboratory Medicine; P.I.: Prof. Peter J. Tattersall PhD

Publications:

Englinger, B., Miklos, W., Heffeter, P., Jungwirth, U., Ferk, F., Knasmüller, S., Lötsch, D., Grusch, M. and Berger, W. Selection for Trabectedin Resistance Induces Stable and p53-independent Hypersensitivity Against Cisplatin in Human Colon Cancer Cells. *European Journal of Cancer* vol. 48 July, 2012. p. S256-S257 (scientific abstract)

S. Schreier, M. Hollaus, E. Pemberger, S. Fruhwürth, C. Röhrli, F. Liebscher, B. Englinger, J. Becker, A. Schmidt, H. Scharnagl, C. Aufricht, H. Stangl, W. Strobl. Effect of chronic renal failure on serum and HDL cholesterol efflux capacity and macrophage ABCA1/ABCG1 expression. 2011; *Atherosclerosis Suppl* 12 (1) 45-4 (scientific abstract)